



## Durham E-Theses

---

### *A seismic refraction study of the earth's crust beneath S. W. Britain*

Holder, Andrew Peter

#### How to cite:

---

Holder, Andrew Peter (1969) *A seismic refraction study of the earth's crust beneath S. W. Britain*, Durham theses, Durham University. Available at Durham E-Theses Online: <http://etheses.dur.ac.uk/9239/>

#### Use policy

---

The full-text may be used and/or reproduced, and given to third parties in any format or medium, without prior permission or charge, for personal research or study, educational, or not-for-profit purposes provided that:

- a full bibliographic reference is made to the original source
- a [link](#) is made to the metadata record in Durham E-Theses
- the full-text is not changed in any way

The full-text must not be sold in any format or medium without the formal permission of the copyright holders.

Please consult the [full Durham E-Theses policy](#) for further details.

A SEISMIC REFRACTION STUDY OF THE EARTH'S

CRUST BENEATH S. W. BRITAIN

A thesis submitted for the Degree of

Doctor of Philosophy

in the

University of Durham

by

Andrew Peter Holder

Hatfield College



September 1969

## ABSTRACT

This thesis describes a seismic refraction project undertaken in south west Britain in November 1966, designed to investigate crustal structure associated with a granite batholith. The results and interpretation of the data collected are presented in the form of crustal structure sections along the three lines of shots. These results are then compared with those obtained in other areas of the British Isles and the geological implications are discussed. Suggestions for the design of future crustal structure experiments based upon the experience gained in south west England are also included.

Several methods of analysis have been employed. Least squares straight lines have been fitted to first arrival travel time data and time term analyses have been applied to the major phases thus identified. Amplitude and velocity filtering measurements have been made of both first and secondary arrivals. The importance of a large amplitude secondary arrival, identified as a supercritical reflection from the Moho, is emphasised and an explanation of its amplitude characteristics is provided in terms of a lower crust exhibiting a gradual increase of velocity with depth.

The average crustal velocity along the line of the south west England peninsula and between Land's End and Brittany

is about 6.1 km/sec with an upper crustal velocity of about 5.8 km/sec. The crust is about 27 to 28 km thick with an almost horizontal Moho and a sub-Moho  $P_n$  velocity of about 8.07 km/sec. The granite batholith of south west England extends to a depth of about 11 km beneath which the lower crust exhibits a gradual increase of velocity with depth. For the region between Land's End and Ireland there is some evidence for a higher  $P_n$  velocity and average crustal velocity with a dipping Moho such that the thickness of the crust beneath southern Ireland may be about 30 km.

## ACKNOWLEDGMENTS

I wish to thank Professors K.C. Dunham and G.M. Brown for the privilege of being able to work in the Durham University Geology Department. I am especially indebted to Professor M.H.P. Bott for his help and direction during the whole period of this research. My thanks are due to Dr. R.E. Long and to many staff, research students and technical staff members of the Department in whose company it has been a pleasure to work. I am also most grateful to several members of the computing staff at both the Durham and Newcastle University computing centres, especially Mr. R. Oddy and Mrs. A. Roberts (née Beeckmans), whose help has been invaluable. In addition, I wish to express my thanks to Dr. H.I.S. Thirlaway for the use of the facilities at the UKAEA seismology unit and to the other members of Blacknest whose help and advice are always so freely given.

The south west England experiment was sponsored in part by NERC and also by the Air Force office of scientific research through the European office of aerospace research, OAR, United States air force under contract AF61(052)-733 as part of ARPA's project vela uniform. I am most grateful to the Standing Committee for Research Awards at Durham for personal financial support during the 3 years of this research.

## CONTENTS

	Page
CHAPTER 1.	
1.1 Introduction	1.1
1.2 Geology of the south western peninsula	1.1
1.3 Geophysical investigation along the peninsula	1.4
1.4 Aims of the 1966 experiment	1.8
1.5 Previous work in the area	1.10
CHAPTER 2.	
2.1 Experimental details	2.1
2.2 Data preparation	2.18
CHAPTER 3.	
3.1 The classical method	3.1
3.2 Adjustments for upper crustal variation	3.5
3.3 First arrival travel time graphs	3.7
3.3.1 Line 1 travel time graphs	3.9
3.3.2 Interpretation of line 1 travel time data	3.11
3.3.3 Line 2 travel time graphs	3.17
3.3.4 Interpretation of line 2 travel time data	3.18
3.3.5 Line 3 travel time graphs	3.25
3.3.6 Interpretation of line 3 travel time data	3.26
3.4 Time terms	3.30
CHAPTER 4.	
4.1 Stacked records	4.2
4.2 Amplitude measurements	4.4
4.3 Velocity filtering	4.5
4.4 The analysis and interpretation of all the data	4.9
4.4.1 Analysis of $P_g$ and $P_n$ arrivals	4.10
4.4.2 Analysis of later arrivals	4.11
4.4.3 The nature and use of the large amplitude secondary arrival	4.12
4.4.4 Line 1, final interpretation	4.23
4.4.5 Line 2, results and interpretation	4.27
4.4.6 Line 3, results and interpretation	4.30
4.5 Conclusion	4.34

	Page
CHAPTER 5.	
5.1 Comparative crustal structure around the British Isles	5.1
5.2 Geological interpretation of the results from the south west England experiment	5.7
5.3 Suggestions for the design of future crustal structure experiments	5.13
APPENDIX A. South west England experiment - shot data	A.1
APPENDIX B. First arrival travel time data for all stations from the south west England experiment	A.4
APPENDIX C. Paper tape data input programme	A.14
APPENDIX D. Least squares straight line programme	A.22
APPENDIX E. Time term analysis programme	A.24
APPENDIX F. Velocity filtering programme and results	A.29
APPENDIX G. Plot of velocity filtered records (programme)	A.44
APPENDIX H. The theory behind the use of the critical distance ( $C_1$ ) and the grazing incidence distance ( $C_2$ ) in the evaluation of the depth at which a linear increase of velocity with depth begins	A.47
BIBLIOGRAPHY	

## FIGURES

	Page following
Fig.1. The geology of the south west England peninsula	1.2
Fig.2. Bouguer anomaly map of south west England (after Bott and Scott 1964)	1.4
Fig.3. Bouguer anomaly profile over Bodmin Moor between A and A <sup>1</sup> on fig.2 (after Bott and Scott 1964)	1.6
Fig.4. Seismic station positions in the south west Britain area including the three lines of shots of the south west England experiment	1.10
Fig.5. The geology of the sea areas around south west Britain (after Whittard 1962 and Donovan 1968)	1.14
Fig.6. The shot-receiving station configuration for the south west England experiment	2.1
Fig.7. Block diagram of the F.M. recording apparatus at four of the stations along the south west England peninsula (after Long 1968)	2.6
Fig.8. Sketch maps of the Dartmoor (above) and Bodmin Moor (below) array stations	2.7
Fig.9. Sketch map of the Land's End array station	2.8
Fig.10. Schematic diagrams of seismic data processing system (after Lucas 1966). 1 - Array field recording system	2.8
Fig.11. Schematic diagrams of seismic data processing system (after Lucas 1966). 2 - Array field replay system	2.10
Fig.12. Schematic diagrams of seismic data processing system (after Lucas 1966). 3 - Laboratory replay system	2.11



- Fig.13. U/V recorder trace of shot 11 of the south west England experiment as received by 5 of the geophones at the Land's End station 2.13
- Fig.14. Schematic diagrams of seismic data processing system (after Lucas 1966). 4 - Punch replay system 2.13
- Fig.15. Histogram of the least squares residuals from the first arrival travel time data of the south west England experiment. The calculated normal curve is also included 3.4
- Fig.16. Bouguer anomaly profile along lines 2 and 3 3.5
- Fig.17. First arrival travel time graphs for the Dartmoor station (above) and the Bodmin Moor station (below) 3.10
- Fig.18. First arrival travel time graphs for the Carnmenellis station (above) and the Land's End station for the line 1 shots (below) 3.10
- Fig.19. First arrival travel time graphs for the Scilly Isles station (above) and the Eskdalemuir station (below) 3.10
- Fig.20. The extent of line 1 giving a truly reversed  $P_n$  velocity 3.13
- Fig.21. First arrival travel time graphs for the Waterford station (above) and the Land's End station for the line 2 shots (below) 3.18
- Fig.22. Residual data and an interpretation of the Bouguer anomaly profile along the northern part of line 2 3.19
- Fig.23. Suggested structure in the upper crust along the southern half of line 2 3.22
- Fig.24. First arrival travel time graphs for the line 3 shots (above) and the French stations (below) 3.25
- Fig.25. Residual data from line 3 3.28

Fig.26.	The standard deviation of the solution versus the refractor velocity for the P <sub>n</sub> (2nd solution) and P <sub>g</sub> time term solutions	3.35
Fig.27.	The stacked record of the line 1 shots at the Land's End station	4.2
Fig.28.	Frequency responses of the recording systems at the Scilly Isles station (above) and at the Carnmenellis and Bodmin Moor stations (below)	4.4
Fig.29.	Amplitude - distance graphs for various phases at the Bodmin Moor, Carnmenellis and Scilly Isles stations	4.4
Fig.30.	A crustal model and calculated reduced travel time graphs for the P-waves travelling through it	4.20
Fig.31.	The stacked record of the line 1 shots at the Scilly Isles station	4.24
Fig.32.	The stacked record of the line 1 shots at the Carnmenellis station	4.24
Fig.33.	The stacked record of the line 1 shots at the Bodmin Moor station	4.24
Fig.34.	The crustal models for lines 1 (above), 2 (middle) and 3 (below) of the south west England experiment	4.27
Fig.35.	The stacked record of the line 2 shots at the Waterford station	4.28
Fig.36.	The stacked record of the line 2 shots at the Land's End station	4.28
Fig.37.	The stacked record of the line 3 shots at the Land's End station	4.30
Fig.38.	The stacked record of the line 3 shots at the French stations	4.30

following page

- Fig.39. The geological interpretation of  
the crustal model along line 1 5.13
- Fig.40. Paper tape format A.14
- Fig.41. Smoothed and correlator outputs for an  
arrival travelling across the Land's  
End array at a velocity of 5 km/sec. A.30

## TABLES

Page following

Table 1. Sedimentary delay times for the line 1 shots.	3.5
Table 2. Results of the least squares process of fitting straight lines to the travel time data of the south west England experiment.	3.8
Table 3. Minimum depths to the Moho for stations along line 1.	3.16
Table 4. $P_g$ time terms.	3.34
Table 5. $P_n$ time terms, first solution.	3.35
Table 6. $P_n$ time terms, second solution.	3.35
Table 7. Estimates of crustal thickness and average crustal velocity for the stations recording the line 1 shots.	4.17
Table 8. Estimates of depths to the top of the lower crustal layer including the data used in their evaluation.	4.23

## CHAPTER 1

1.1 Introduction

A specialised seismic refraction project, designed to investigate crustal structure associated with a granite batholith, was undertaken in south west Britain during the early part of the November 1966. The project was organised by members of the Department of Geology, University of Durham in collaboration with the Hydrographic Department of the Royal Navy and other scientific establishments. The design of the experiment was based on the seismic refraction technique which has been used in many parts of the world to elucidate deep structures otherwise unseen by surface methods.

This chapter describes the general geology of the south west England area and in particular the nature of the granite batholith as revealed by various geological and geophysical studies. It includes a summary of the previous work undertaken in the area covered by the experiment and discusses the scientific background and aims of the seismic refraction experiment as carried out in November 1966.

1.2 Geology of the south western peninsula

South west Britain was selected as being a particularly interesting area because of the occurrence of

large granite intrusions along the south west England peninsula. The geology of the area is shown in fig.1. The peninsula is characterised by a series of highly contorted Palaeozoic sediments which have been affected by low grade metamorphism. The general structure of the area is a broad trough, known as the Culm synclinorium, with its axis aligned east-west through central Devonshire. The central part of the trough is composed of Carboniferous sediments, consisting of massively bedded shales, a bed of agglomerates and tuffs and a series of lenticular limestones. The axis of the synclinorium is occupied by the finger-like Crediton trough composed mostly of New Red Sandstone, resting unconformably on the Carboniferous.

Towards the north Devonian rocks outcrop. These are predominantly marine rocks but three intercalations of continental Old Red Sandstone do occur. Towards the south of the synclinorium, outcrops of lower, middle and upper Devonian rocks of marine facies are present consisting of slates, mudstones and limestones. In the extreme south west the rocks are of indeterminate age, possibly lower Devonian. These are the Mylor beds or 'killas' of south west Cornwall. There are two areas of possible Precambrian rocks, one in the Start Point area consisting of low grade schists (Tilley 1923) and the other comprising the igneous complex of the Lizard (Flett and Hill 1946). However, radioactive age dates on

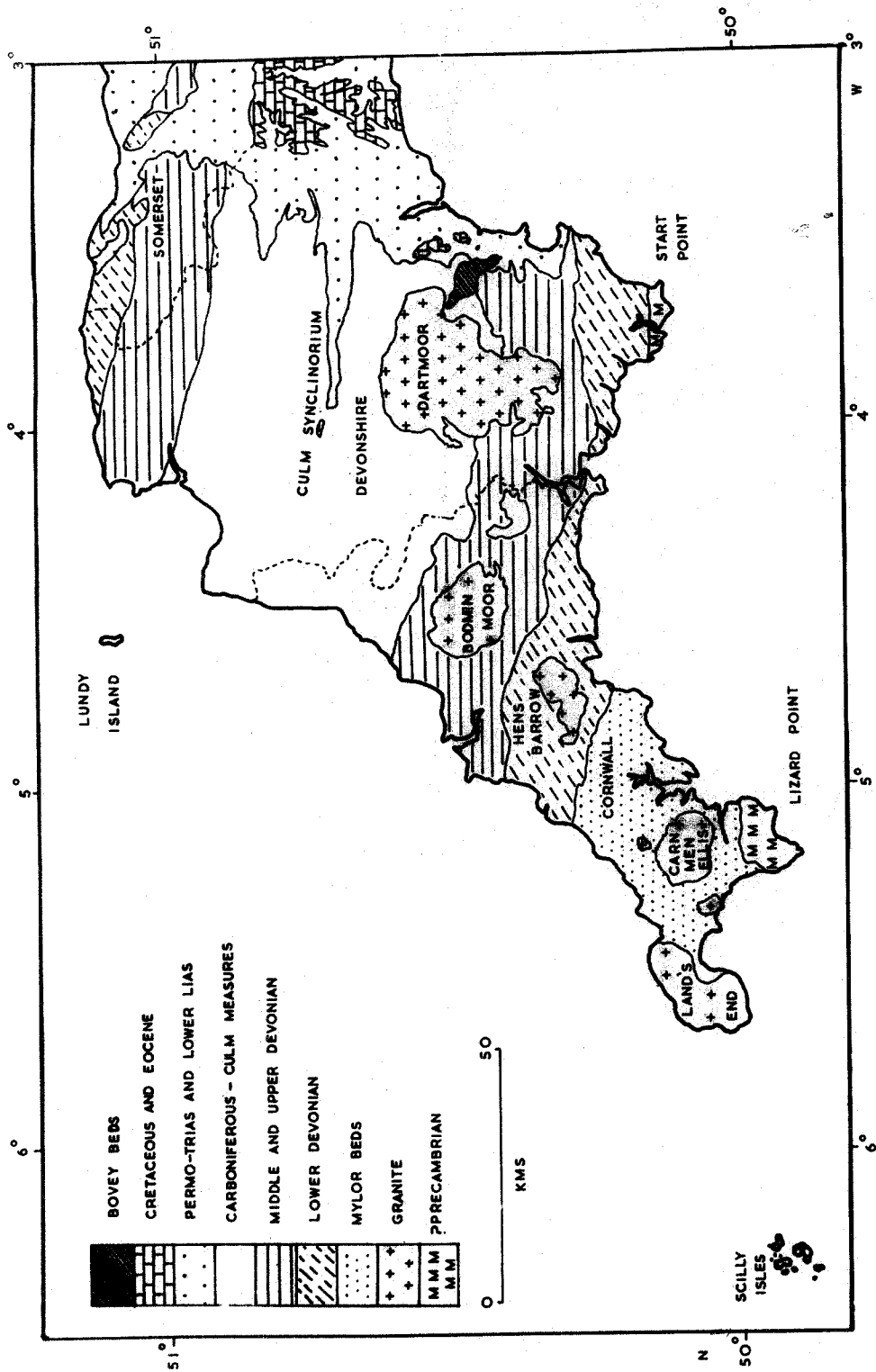


Fig.1. The geology of the south west England peninsula

the Lizard rocks indicate that they may be younger (Miller and Green 1961a and 1961b, Dodson 1961). The whole of the area was metamorphosed by the marginal effect of the earth movements which built up the eastern part of the Variscan fold belt. The main effect is that of the imposition of slaty cleavage on the finer grained sediments.

Cutting across these Palaeozoic sediments, and also causing considerable doming, is a series of alkali granites of Armorican age. Radioactive age dating on some specimens gives ages of  $280 \pm 10$  million years (Long 1962, Miller and Mohr 1964, Sabine and Snelling 1969). The main masses are those of Dartmoor, Bodmin Moor, Hensbarrow, Carnmenellis and Land's End. The Scilly Isles are also formed of granite and other smaller outcrops are seen in several areas. The bulk of the rock forming these intrusions is a coarse, porphyritic, biotite granite (Exley and Stone 1964). It consists of large phenocrysts of potash felspar up to 5cm in length, plagioclase felspar, quartz and biotite set in a coarse matrix of more than 3mm average grain size. Accessory minerals include zircon, apatite and ores. Other granite types include a finer porphyritic biotite granite, a basic microgranite and single occurrences of lithionite granite, so called because of the presence of lithionite mica, and a fluorite granite. Elvans also occur in moderate numbers throughout the peninsula,



being composed of granite porphyries and having a dyke- or sill-like form.

Each of the outcropping granite masses is surrounded by a metamorphic aureole. Thermal spotting occurs and it is estimated that the usual thickness of alteration averages about 1000 metres at right angles to the granite surface. The granite contacts are sharp with very little permeation of material into the country rocks. They may be described, in fact, as typical examples of 'plutons', the highest level in the granite series described by Read (1957).

For a full description of the geology and structure the Regional Guide (Dewey 1948) should be consulted.

### 1.3 Geophysical investigations along the peninsula

A geophysical study described by Bott, Day and Masson-Smith (1958) reveals the subsurface shape and extent of the granites. They undertook a gravity and magnetic survey of the whole of the south western peninsula, the Bouguer anomalies of which are presented in fig.2. The main gravity features brought out by the survey are that :-

(i) A belt of large negative Bouguer anomalies of up to -50mgals follows the granite belt, the minimum values corresponding to outcrops of granite.

(ii) The Bouguer anomaly falls in a NNE direction across Exmoor by about 20mgals.

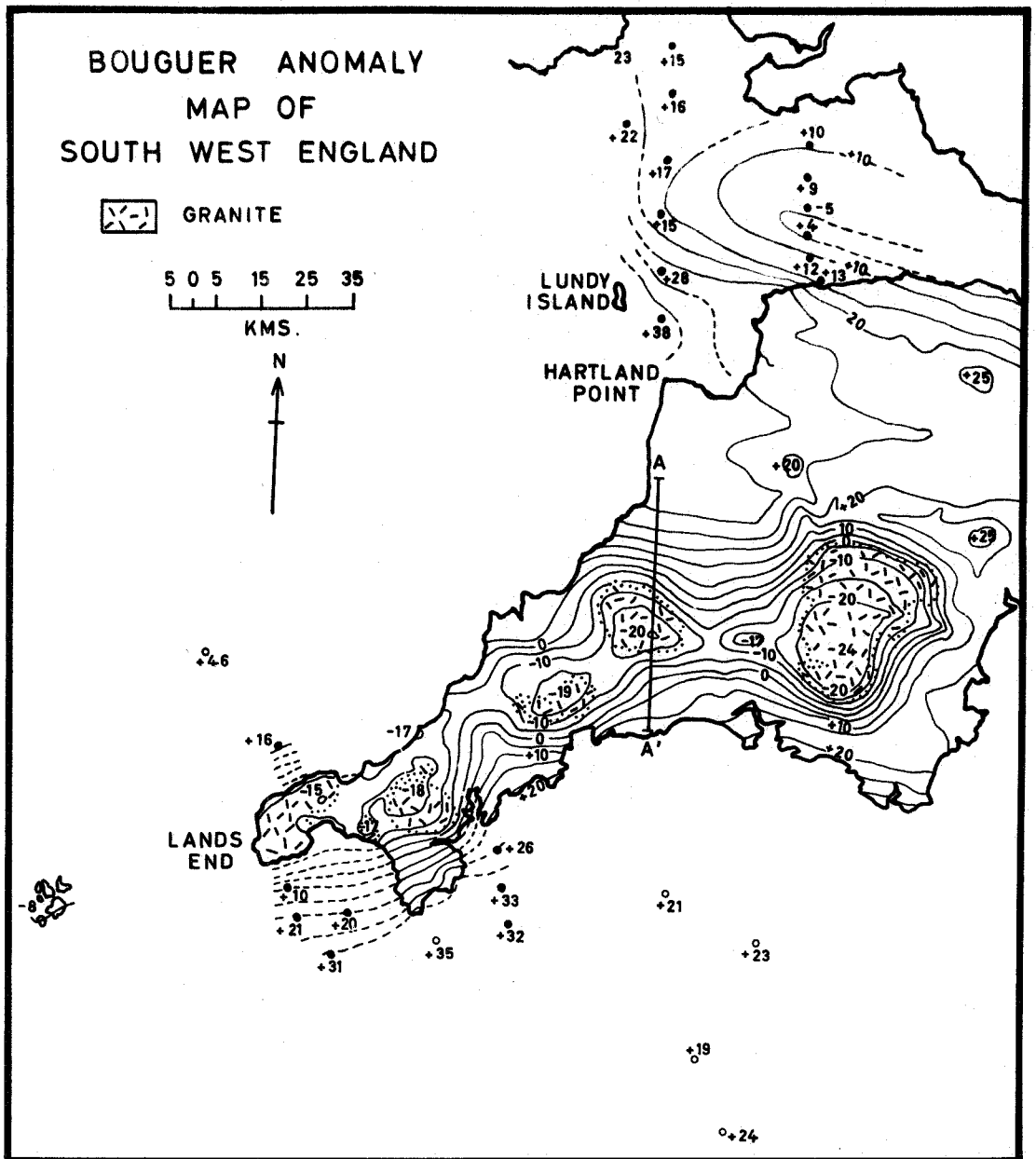


Fig.2. Bouguer anomaly map of south west England (after Bott and Scott, 1964).

(iii) The Bouguer anomaly rises southwards by about 10-15mgals along the Start and Lizard peninsulas.

(iv) The regional Bouguer level is relatively high and rises gradually in a westerly direction.

Subsequent unpublished gravity surveys at sea along a line crossing the extreme west of the peninsula from north to south confirm the high regional characteristics and the low Bouguer anomalies corresponding to the granite belt.

The full interpretation of these anomalies is given by Bott, Day and Masson-Smith (1958), and Bott and Scott (1964), but is summarised here. The negative Bouguer anomalies along the peninsula are attributed to the low density of the granite masses in relation to the country rocks because :-

(i) The high value of the gravity gradient and second derivative require a very shallow density contrast.

(ii) Samples of granite give densities of 2.58-2.64gm/cc while the Devonian rocks of South Devon give values of 2.61-2.86gm/cc (Bott, Day and Masson-Smith 1958). Samples of the killas give  $2.71 \pm .05$ gm/cc (Scott, unpublished).

A density contrast of  $-0.16 \pm .03$ gm/cc was used to give quantitative estimates of granite thicknesses. The continuity of the anomalies suggest that the exposed granites form cupolas on a large batholith of considerable

extent, an idea which has been postulated before, e.g. Rastall (1931). In regions between the granite outcrops, the roof is not more than 2 to 3km beneath the ground surface. In some areas it is noticeable that the metamorphic aureole extends several kilometers away from the visible granite contact, indicating that the roof is not far below ground. On the basis of the shape of the gravity anomalies it can be seen that the batholith has a relatively flat roof region with steeply sloping walls generally inclined outwards. An example of a typical two dimensional Bouguer anomaly profile with its geological interpretation is shown in fig.3. The interpretation of this Bodmin Moor profile shows an intrusive body of granite with a negative density contrast extending to a depth of 12km with steeply dipping sides and a more dense northern section. Another interpretation which could be applied is that of an intrusive body of granite with a uniform density contrast but extending to greater depths in the south. The fit of the calculated anomaly for this model to the observed anomaly is not as good as that for the former model. This interpretation is typical for most of the granite outcrops along the peninsula. Thus the gravity survey reveals the presence of an elongated granite batholith with steeply dipping sides and extending to a depth of about 12km with a denser northern region.

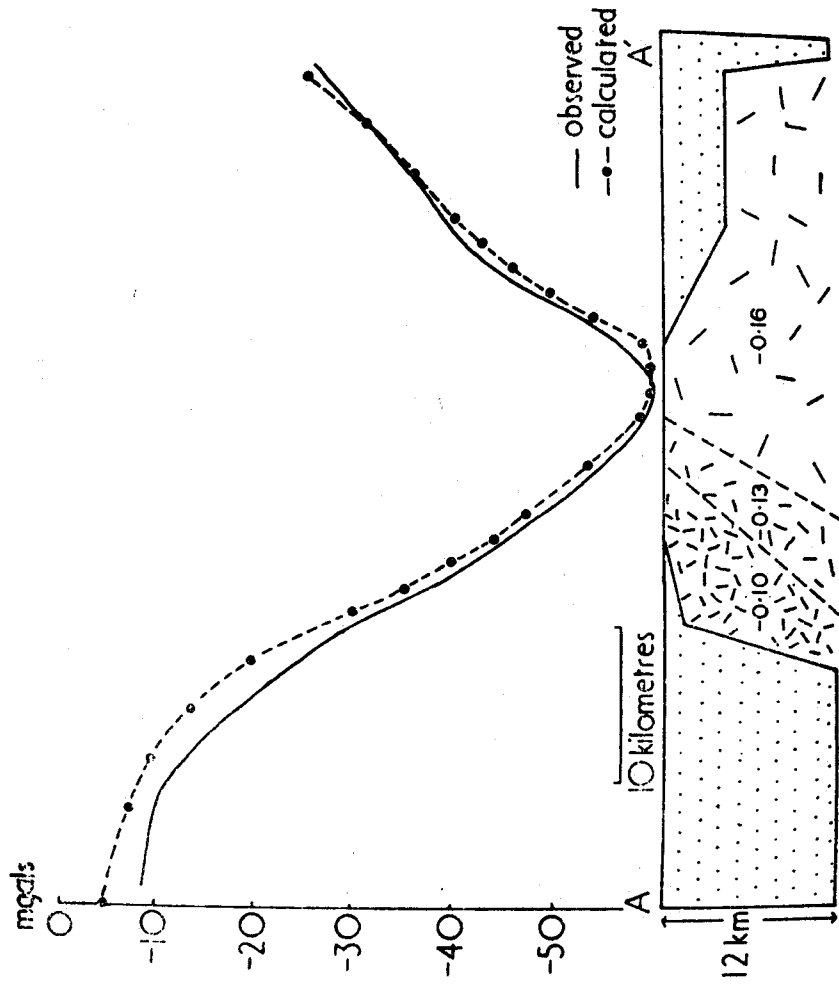


Fig.3. Bouguer anomaly profile over Bodmin Moor between A and A' on fig.2.  
 (after Bott and Scott 1964).

The western extent of the batholith is unknown. Midford (1966) describes a gravity low between Land's End and the Isles of Scilly which is interpreted as a granite extending to a depth of at least 10km below sea level. The Scilly Isles are formed of granites of the same type as those found in the mainland belt but no quantitative estimate of the depth to which the granite extends is possible with the data as it is at the moment. Whitmarsh (1967) gives a gravity profile along a NW - SE trending line some 60km west of the Scilly Isles. This shows a gravity low over the Haig Fras granite in the north west and another low with a steep sided high on its southern margin towards the south eastern end of the traverse. He proposes that this southern low is a manifestation of another granite with its top 450 metres below sea level (the water depth in this region is 150 metres) thus extending the chain of the granites at least to this position some 60km WSW of the Scilly Isles.

Shallow seismic refraction profiles (see below) indicate the presence of thin sediments covering basement rocks out to a further 60km west south westwards from the granite postulated by Whitmarsh. Magnetic evidence (see below) also indicates the presence of a shallow basement in this area extending west south westwards but plunging steeply towards the south south east.

Bott and Scott (1964) suggest that an isostatic mechanism could be the cause of the high ground associated with the granite belt. The basement ridge, extending the line of the south western peninsula, could well be a manifestation of the same mechanism operating in this area suggesting that granites extend well to the west of the Scilly Isles.

#### 1.4 Aims of the 1966 experiment

The vertical extent of the granite batholith as revealed by its gravity anomaly raises a considerable problem regarding its origin. This problem is part of the general problem related to the origin of granites which has been hotly debated for many years (Read 1956, Reynolds 1947). In the present case the granites were emplaced after folding and metamorphism of country rocks and, whatever the emplacement mechanism, it must have involved the removal of a large volume of country rocks. This problem has been studied by Bott (1956) who concluded that most of the country rocks descended to replace the uprising granitic material. Whatever the interpretation, the crust underlying the granite batholith must have been disturbed. Thus the problem of granite batholiths cannot be isolated from a study of the crust as a whole.

Two principal hypotheses have been put forward concerning the shape of the granite batholiths in relation to the crust. The first suggests that batholiths are surrounded

on all sides and below by rocks denser than themselves. The second suggests that batholiths merge at a depth of 10km into a layer which has a granitic composition. Gravity methods provide no means of testing between these two hypotheses. The seismic refraction method provides a tool which may be able to distinguish between them. It has been shown that the granite batholith in this region extends at least from Dartmoor to the Scilly Isles, a distance of about 200km and possibly even further. The width of the granite belt is of the order of 30-50km. Lengthwise it is thus large enough to accommodate most of a seismic refraction line which would sample seismic velocities throughout the whole thickness of the crust down to the Mohorovicic discontinuity.

One of the main aims of this project was, therefore, to determine the crustal structure and topmost mantle velocities along the length of the granite batholith. It was decided to set up a seismic refraction line of shots extending west south westwards from Land's End with detectors placed at suitable sites along the peninsula. In order to supplement this information it was also decided to determine the crustal structure and topmost mantle velocities along two lines at right angles to the batholith. These lines extend from Land's End to southern Ireland and from Land's End to north western France respectively. (see fig.4). A study of the previous work in the areas covered by these three refraction lines is therefore necessary and a



summary of this work is given below.

### 1.5 Previous work in the area

Work in the sea areas surrounding the south west England peninsula and extending to southern Ireland and to north western France has been of a rather limited nature. A number of seismic refraction stations have been occupied and individual gravity and magnetic traverses cross the area but no systematic geophysical survey has been attempted in the region covered by the large scale seismic refraction project of 1966. Most of the work seems to have been concentrated towards the west and south of the peninsula. Only recently have gravity profiles been completed in the eastern Celtic sea.

Some of the earliest seismic work is reported by Bullard and Gaskell (1941). Several sea stations were set up at points along an extensive line running roughly west south westwards from the Lizard and short refraction lines were shot at each station (see fig.4). It was found that the basement underlying sediments on the continental shelf slopes gently downwards on receding from the land in a WSW direction out to the position of their station 6 (AR 6 in fig.4). Thereafter the basement slopes more steeply to reach a depth of 2.5km at the 100 fathom line. The seismic velocities given for the basement rocks vary from 4.6 - 7.3km/sec

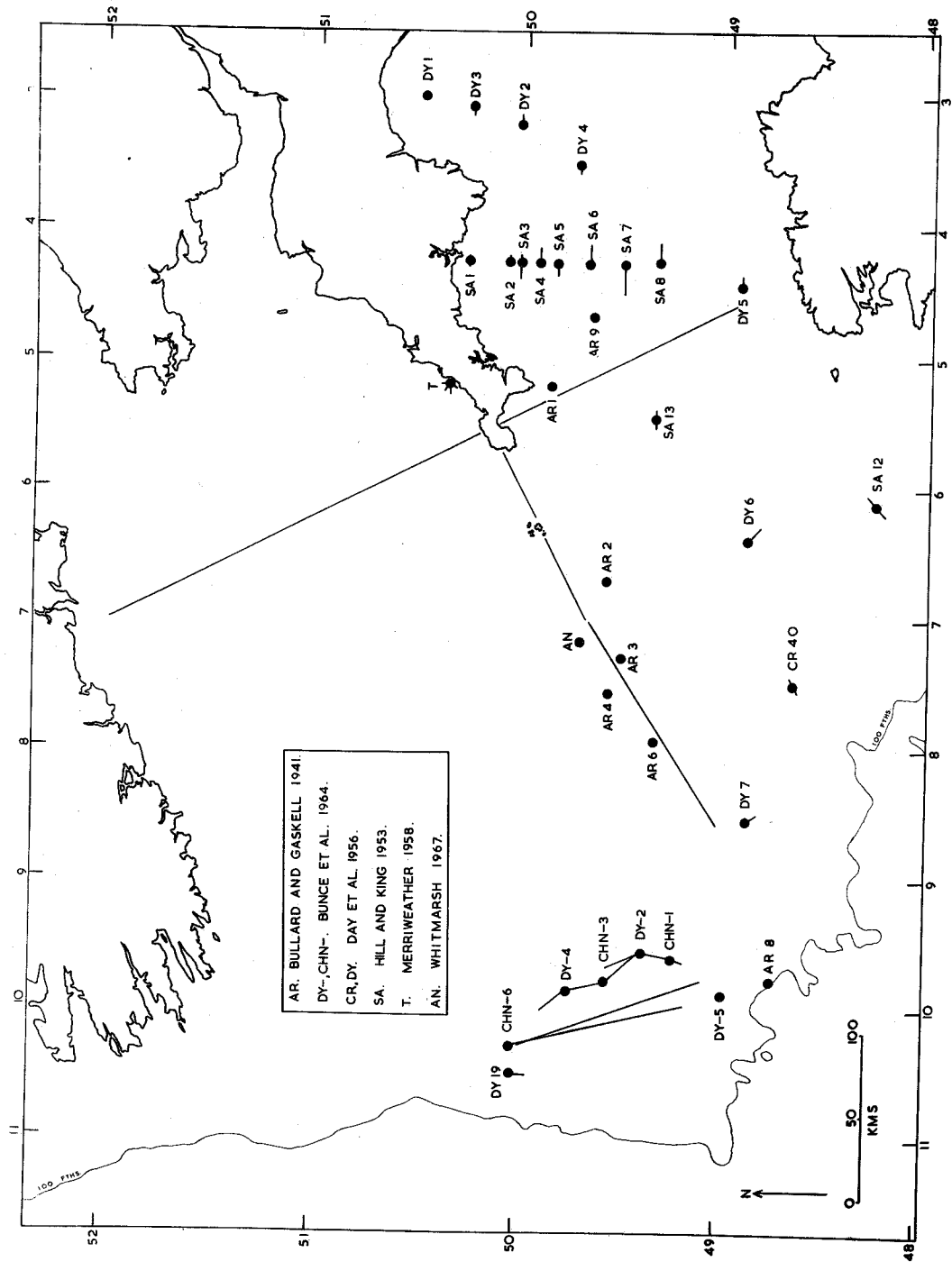


Fig. 4. Seismic station positions in the south west Britain area including the three lines of shots of the south west England experiment.

while those for the sediments above range from 1.8 - 2.9km/sec.

Several similar stations were set up by Hill and Laughton (1954) in the approaches to the English channel towards the south of the stations occupied by Bullard and Gaskell (see fig.4). These give seismic velocities within the basement rocks of 6.10 - 6.34km/sec and depths to the basement of up to 4.27km with a general dip of this basement towards the west. Three other layers above the basement were recognised with velocities ranging from 4.85km/sec near the bottom of the 'consolidated sediments' to 1.96km/sec near the top of the 'unconsolidated sediments'. However, many of these refraction lines were not reversed thus making an assumption of horizontal layering necessary for the above values of velocity and thickness to be true.

Day, Hill, Laughton and Swallow (1956), on the basis of short refraction lines shot at locations along a line extending southwards from Plymouth (see fig.4), recognised four classes of seismic velocity thus :-

1.7 - 2.5km/sec	Mesozoic
2.7 - 3.6km/sec	Permo Triassic
3.65- 4.85km/sec	Palaeozoic
5.2 - 7.0km/sec	Metamorphics and Igneous (Basement)

Structure contours drawn by Day et al on the basement give a picture of an elongated trough running northwestwards

along the centre of the western approaches to the English channel reaching a depth of at least 3km and rising to zero depth near the French coast.

More recently, Bunce et al (1964) shot profiles near the edge of the continental margin some 350km due west of Lands' End. They shot three short profiles (28km each) and one long profile (125km), the latter in a north-south direction. The highest velocity attained in the short profiles was 5.5km/sec while, in the long profile, a 6.10km/sec layer underlain by a medium having a velocity of 7.7km/sec was found. A dip of what was presumed to be the Moho towards the south was tentatively postulated on scanty data.

The area between the south western peninsula and Ireland is devoid of published seismic profiles, except for several short unreversed profiles shot by Merriweather (1958) near Perranporth in Cornwall. He found the basement to be at a depth of 400 metres with an unreversed velocity of 5.8km/sec overlain by Devonian schists having a velocity of 4.4km/sec. Whitmarsh (1967) gives the results of a short unreversed line of twelve shots exploded along a 25km length of the gravity profile mentioned earlier in this chapter. Unfortunately no arrivals from the basement were received although they are to be expected in a profile of this length. Two layers were found, an upper 1.6km/sec layer and a lower 1.9km/sec layer identified as the Cretaceous with its top lying 200 metres

below sea level. He proposes that seismic waves hitting the walls of the postulated granite, interpreted from the gravity data, would be reflected and scattered thus accounting for the non-existence of arrivals from the basement during his refraction survey. The steep-sided gravity high on the southern margin of the proposed granite (see earlier discussion on gravity measurements), he says, represents a protrusion of the basement into the Cretaceous.

A gravity survey conducted by Brown and Cooper (1952) in the eastern parts of the south western approaches to the English channel shows a high Bouguer anomaly running east-west along the centre of the Channel. Close to the French coast a low was found probably owing its existence to the granitic nature of the rocks outcropping in the vicinity. More recently, unpublished gravity profiles running from Land's End and the Scilly Isles to north west France confirm the high Bouguer anomaly in the northern and central parts of the south western approaches and the low towards the French coast. It would seem that the thickening pile of sediments revealed by the seismic survey of Day et al has no apparent effect on the gravity values. The westerly gravity profiles and another one extending between Ireland and Land's End will be discussed in a later chapter.

A magnetic survey by Hill and Vine (1965) in the south western approaches reveals a marked ENE - WSW lineation

of the anomalies. This is considered by them to reflect the relief of the metamorphic basement, which in turn delineates an Hercynian structural trend. Broad magnetic features extending along the direction given above suggest a series of ridges and troughs in the basement surface.

Thus gravity, magnetic and seismic work indicate a trough or series of troughs in the western approaches to the English channel, with the low velocity sedimentary material thinning northwards against the westward extension of the Cornubian batholith area. Coring and dredging work has given additional evidence of surface geology within the region which is summarised in fig.5.

The only systematic gravity results from the Celtic sea region are those of Blundell, Davey and Graves (1968). Their survey covered the southern part of the Irish Sea and the north eastern part of the Celtic sea. The anomalies show a similar trend direction to that found further south with a broad, but steep sided, gravity low running west south westwards from the southern Irish Sea eventually bifurcating in the north eastern area of the Celtic sea. Seismic measurements indicate that there are two seismic layers :-

2.2km/sec	1km thick
3.5km/sec	2km thick

thus showing that sediment depths of 3km are found in this area also.

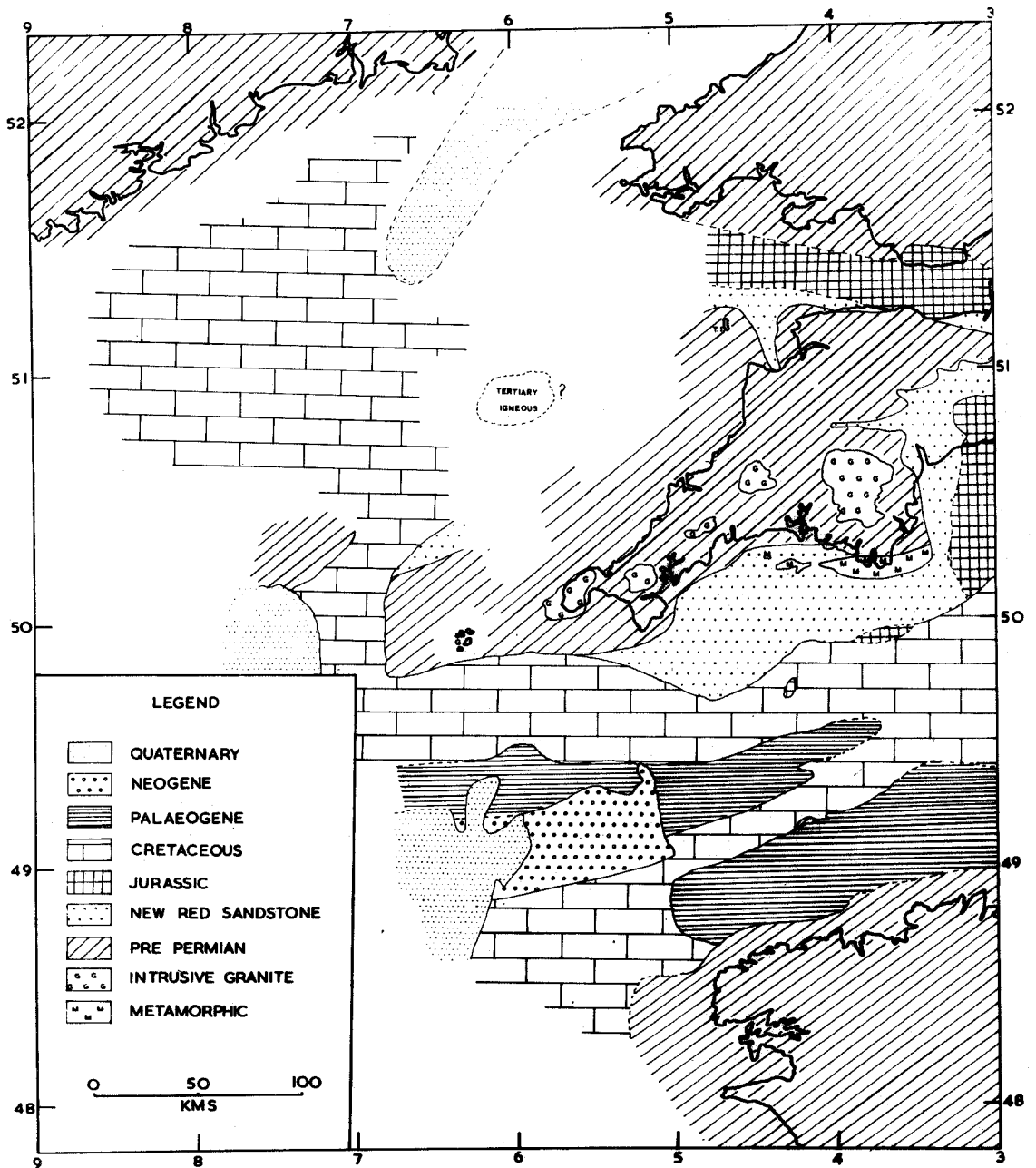


Fig.5. The geology of the sea areas around south west Britain (after Whittard 1962, and Donovan 1968).

A gravity traverse by Midford (1966) from St. David's Head to Land's End gives high gravity values southwards from St. David's to approximately  $51^{\circ}20'N$ . Thereafter a break in the profile marks the position of a gravity low with a steep southern gradient in the region of  $51^{\circ}N$ . The rest of the traverse shows high gravity values immediately to the north of the Land's End area. The northern part of the traverse runs along the eastward margin of the basin described by Blundell et al. Coring and dredging work has been carried out in the Celtic sea and this is summarised in fig.5.

It is apparent from the foregoing that, in general, the uppermost layers of the Earth's crust beneath the area covered by the 1966 refraction experiment exhibit a marked ENE-WSW structural trend. There is an irregular cover of sedimentary material with seismic velocities ranging from 1.7 to 4.85km/sec. Crystalline basement velocities seem to be in the range 5.2 to 7.0km/sec. However, large parts of the area are still relatively unknown and the problems posed by the lack of observational data will become apparent in later chapters of this thesis.



## CHAPTER 2

This chapter deals with the experimental details of the southwest England project. Each individual receiving station is described and summaries of two contrasting types of recording apparatus are included. Some of the problems encountered during the project are mentioned and the general quality of the data collected is assessed. The determination of shot instants and the preparation of the raw data ready for processing are also described in this chapter.

### 2.1 Experimental details

The shot-receiving station configuration is shown in fig.6. Lines 1 and 2 extend approximately 250km west south westwards and northwards respectively from Land's End and line 3 extends some 150km southwards from Land's End to the coast of north west France. Forty-five, time fused, 136kg depth charges were detonated by H.M.S. Hecla during the period 4th - 8th November 1966. They were all detonated approximately 15km apart on the sea bottom and there were no failures. The shot firing sequence went almost exactly to plan with very few delays for near vicinity shipping and in a relatively quiet weather period. Line 2 was shot first with H.M.S. Hecla firing shots 42-25 during the evening of the 4th November. Line 2 was continued during the morning

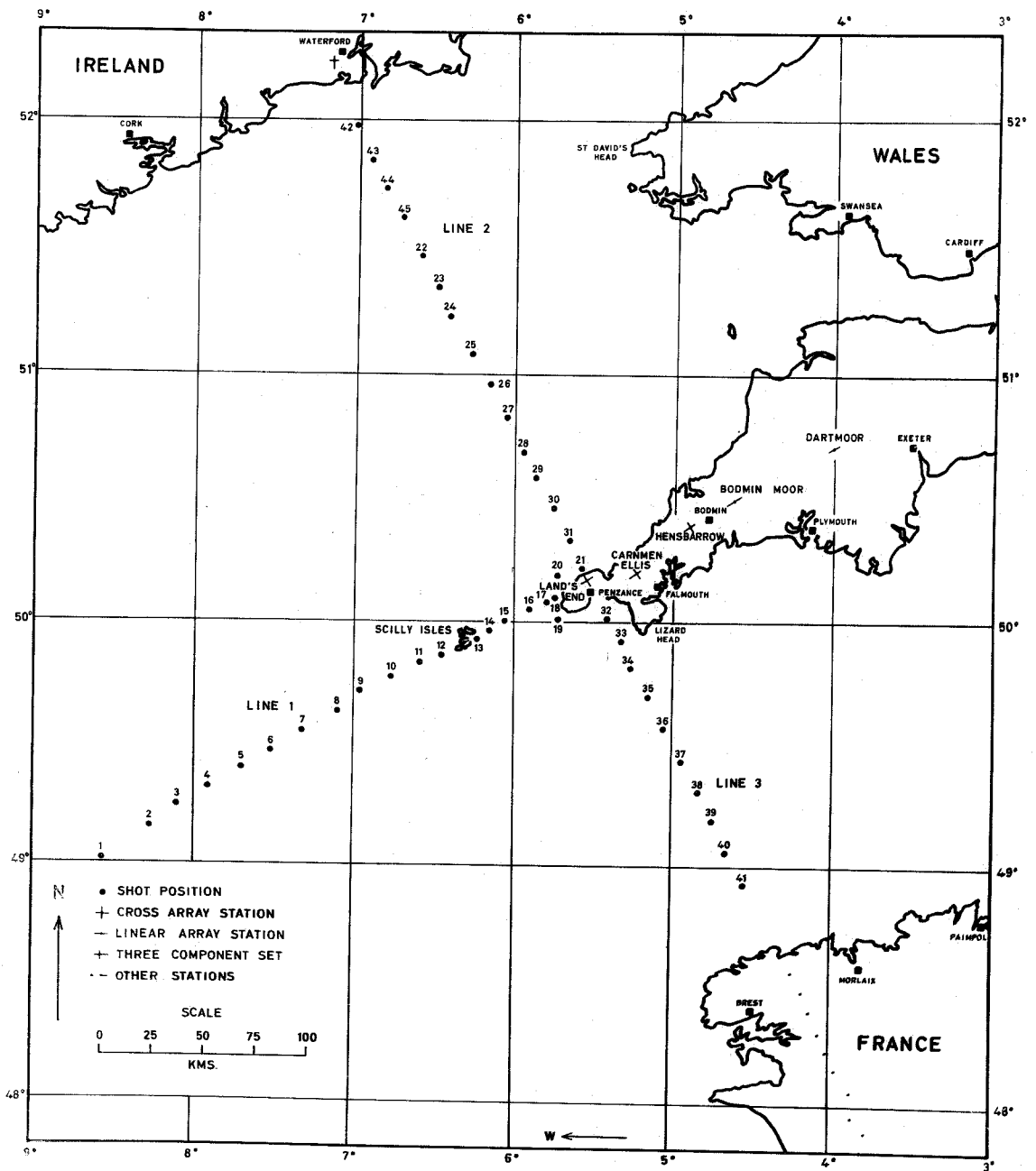


Fig.6. The shot-receiving station configuration for the south west England experiment.

of the 5th November and line 3 was completed towards the end of that afternoon. H.M.S. Hecla then returned to Devonport to take on more depth charges and then steamed westwards dropping shot 19 on the afternoon of the 7th. Line 1 was completed during the morning and afternoon of the 8th. The shot positions were fixed using the Decca navigation chain. These positions together with their associated errors are given in Appendix A.

The shot instant was recorded on board H.M.S. Hecla as follows. Near the time of firing the output of a geophone, together with the outputs of a time encoder, the B.B.C. Light programme and a standard radio time frequency (WWV) were played out on an ultra violet recording oscillograph and also recorded on magnetic tape. The time interval between the splash time and the advent of the water-wave arrival seen on the recorder was measured by a stop-watch and the ship's speed was noted. Thus the distance from shot point to ship could be determined. The time taken for the water wave to travel to the ship was calculated assuming a water-wave velocity of 1.5km/sec and this time was subtracted from the arrival time seen on the recorder to give the absolute shot instant. The time encoder was periodically recorded against WWV to check for drift so that when WWV was not available an accurate shot instant could still be determined. The only problem with this system was

that of identifying the first water-wave arrival. These shot instants were read to the nearest 0.01 second and they are given together with their associated errors in Appendix A.

As the time for each shot approached, H.M.S. Hecla broadcast messages two minutes before splash, one minute before splash and at the splash time. The output of the P.D.R. was then broadcast until it was ascertained on board ship that the shot had been fired. A last message indicating the success of the firing and the expected time of the next shot was then sent out.

Each receiving station recorded a standard radio frequency (in most cases MSF which is accurate compared to WWV to a few microseconds) in addition to the output of a time encoder. Thus the absolute shot instant could be related easily to each individual system time encoder. Reception of MSF during the period 1000-1600hrs was difficult but most stations recorded enough to correct for time-encoder drift. Some of the stations were recording continuously while others, receiving the broadcast messages from H.M.S. Hecla, recorded during the shot periods only.

Land receiving stations were set up as follows :-

A. Eire : Nr. Waterford ( $52^{\circ}13.6'N$ ,  $7^{\circ}09.7'W$ )

A three component set of Willmore Mark II (1c/s) seismometers consisting of one vertical and two horizontals,

one aligned north-south and the other aligned east-west was placed on a rocky outcrop. Frequency modulated magnetic tape recordings were taken of the shot periods only. Most of the shots from line 2 were recorded and some from line 1. This station was operated by Professor T. Murphy and Mr. B. Jacob of the Dublin Institute of Advanced Studies, School of Cosmic Studies, Dublin.

- B. Dartmoor : Okehampton camp ( $50^{\circ}43.0'N.$ ,  $4^{\circ}00.0'W$ )
- C. Bodmin Moor ( $50^{\circ}30.2'N.$ ,  $4^{\circ}37.5'W$ )
- D. Hensbarrow ( $50^{\circ}23.6'N.$ ,  $4^{\circ}39.2'W$ )
- E. Carnmenellis ( $50^{\circ}11.5'N.$ ,  $5^{\circ}13.9'W$ )

These four frequency modulated magnetic recording stations were set up by members of the Durham University Geological Department under the supervision of Dr. R. E. Long. It was hoped that all stations would record continuously during the whole period over which the shots would be fired. There were, however, some difficulties and except for the Bodmin Moor station which did record continuously over the period, the stations only recorded the period during which line 1 was shot.

Long (1968) describes in detail the type of apparatus that was used at these stations. It was modified for a later experiment in Iceland but basically it remains the same. The seismometer outputs are amplified, filtered and frequency modulated by a seismometer package located close to each

seismometer in the field. The amplifiers were powered by twelve 1.5 volt HP2 batteries which were changed halfway through the experiment. The modified version is now powered from a single group of accumulators at the central recording station. The total bandwidth of the amplifier is from 0-10kc/s so that the frequency response of the system is controlled entirely by the filter. The signal is normally recorded at as wide a frequency range as possible but frequencies well outside the seismic band of interest are attenuated to reduce noise levels and thus increase the dynamic range of the system. There was no remote facility for automatic gain control or calibration for the south west England experiment although this is now incorporated in the modified system.

The F.M. signals are transmitted by ordinary field telephone cable to the central recording station where they are fed by the line terminating transformers via another set of amplifiers to the recording heads of a magnetic tape recorder. The tape recorder uses 14 inch reels of 1 inch magnetic tape with up to 24 channels of information. A tape recording speed of 15/64 inch/sec was used in this project. Each station records a standard radio time frequency and the output of a system time encoder which has second, ten second and minute markers. A code following each minute marker gives the hour and minute and, on the modified system, the day according to

a time code used by the United Kingdom Atomic Energy Authority. The recording stations were powered by batteries which were re-charged by mains battery chargers. The tape deck motors were driven by mains electricity. The dynamic range of the system as used in south west England is estimated to be about 55db's but as Long (1968) points out, this can be considerably improved in the modified system. Fig.7 shows a schematic diagram of the recording system as it was used for the south west England project.

The magnetic tapes are replayed in Durham at four times real time, the output of each channel being demodulated and fed to either a twenty four channel oscilloscope or an eight channel pen recorder. Krohn-Hite frequency filters are available for filtering individual channels.

The Dartmoor and Bodmin Moor stations consisted of 2 linear arrays each comprising 5 vertical Willmore Mark I (1c/s) seismometers. These were set approximately half a kilometre apart along the direction of line 1. Two horizontal seismometers of the same design, one radial and one transverse to the direction of line 1, were set up alongside one of the vertical seismometers in each array thus forming 3 component sets. The Dartmoor station was at the greatest distance from the shots of line 1 but it was found that signal to noise levels were good and most of the shots were picked up. However, the

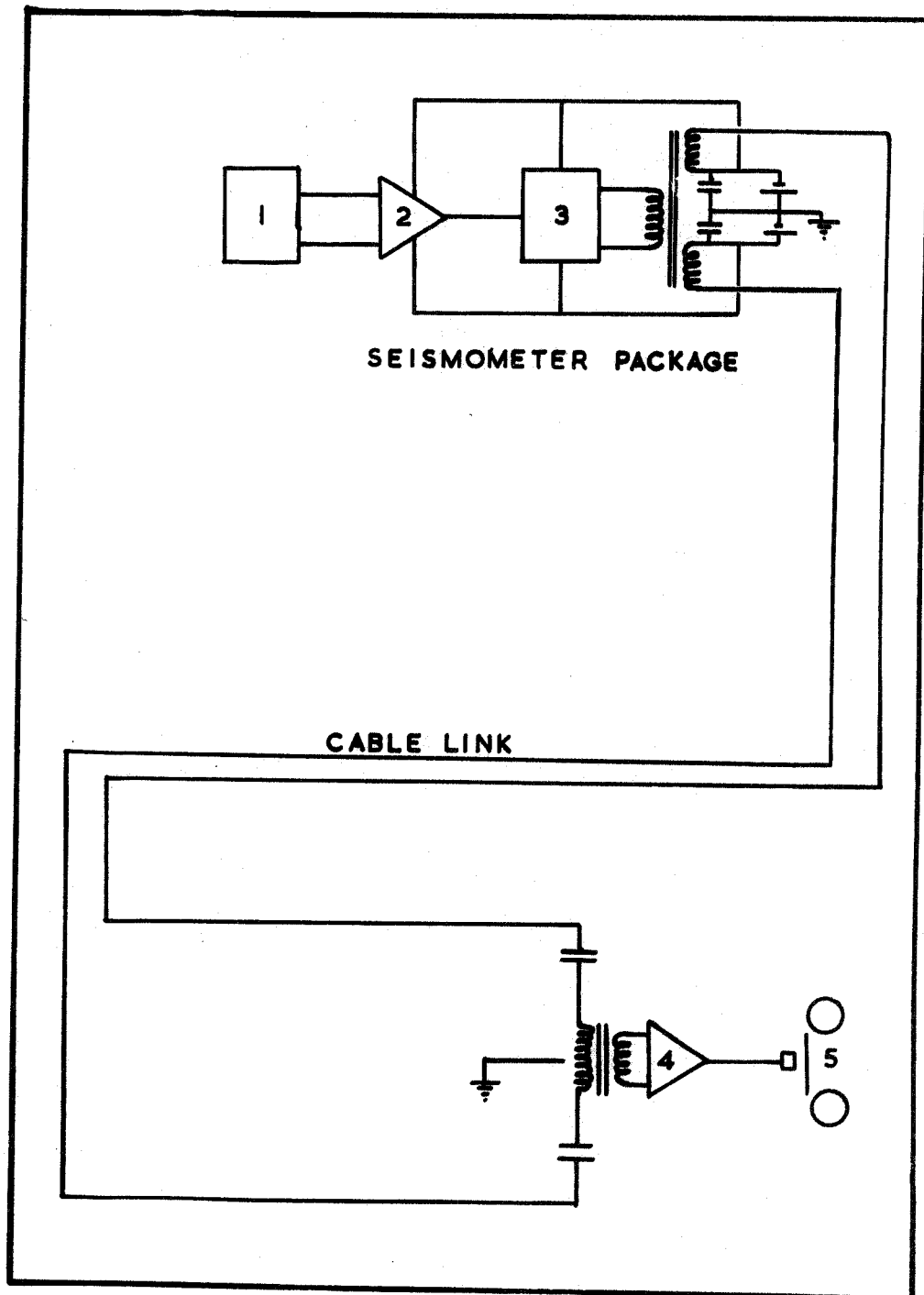


Fig.7. Block diagram of the F.M. recording apparatus at four of the stations along the south west England peninsula (after Long 1968). Key : 1, seismometer; 2, pre-amplifier and frequency filter; 3, frequency modulator; 4, limiting amplifier; 5, magnetic tape recorder.



coherence of arrivals across the array was poor because of poor individual sites, poor matching of seismometers and a preponderance of water.

The Bodmin Moor station recorded all the shots, and signal to noise levels were good even for the most distant shots. Signal coherence across the array was also good. The time encoders at both stations registered a drift of approximately 0.01 second per day and no difficulty was encountered with the timing of onsets. Fig.8 shows diagrams of the Bodmin Moor and Dartmoor sites.

The Hensbarrow and Carnmenellis sites both consisted of 3 component sets of Willmore Mark I (1c/s) seismometers each with one vertical and two horizontals, one radial and the other transverse to the direction of line 1. F.M. recording of the shots of line 1 only was possible at both stations and the horizontals at the Hensbarrow site were later found to be non-functional. It was also found later that the time encoder at Hensbarrow was faulty thus rendering the data from this station unusable. All three channels at the Carnmenellis station, on the other hand, worked well and good records of all the line 1 shots were obtained. The time encoder registered a similar drift to those at the Dartmoor and Bodmin Moor stations.

F. Land's End : Lady Down's Farm ( $50^{\circ}10.0'N.$ ,  $5^{\circ}33.0'W$ )

This station acted as the communications centre for

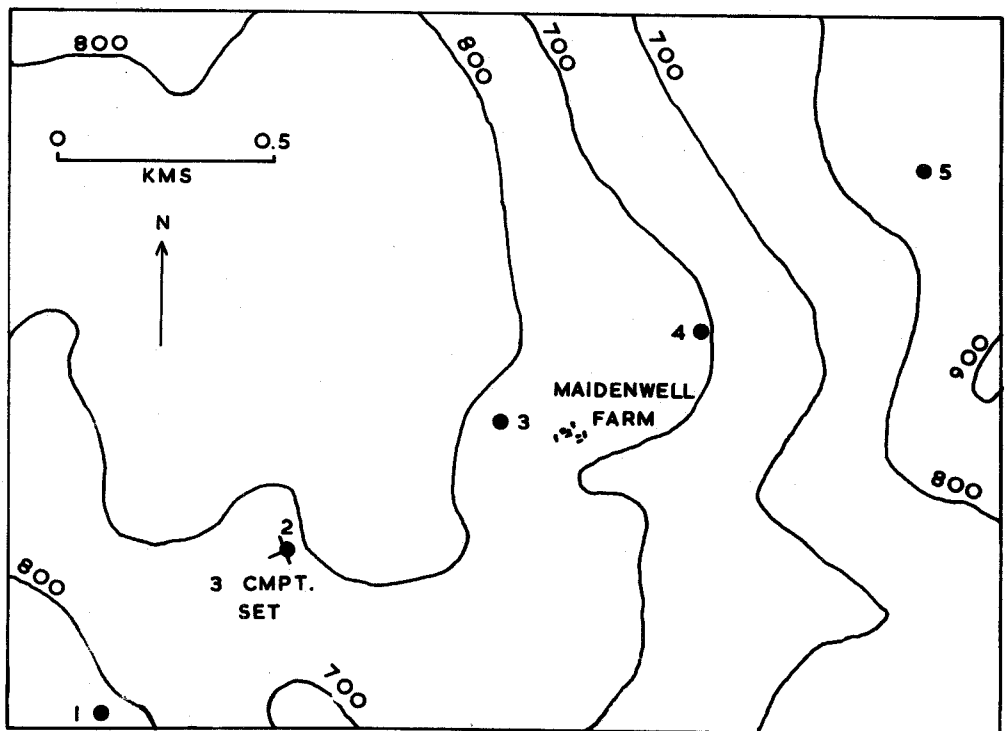
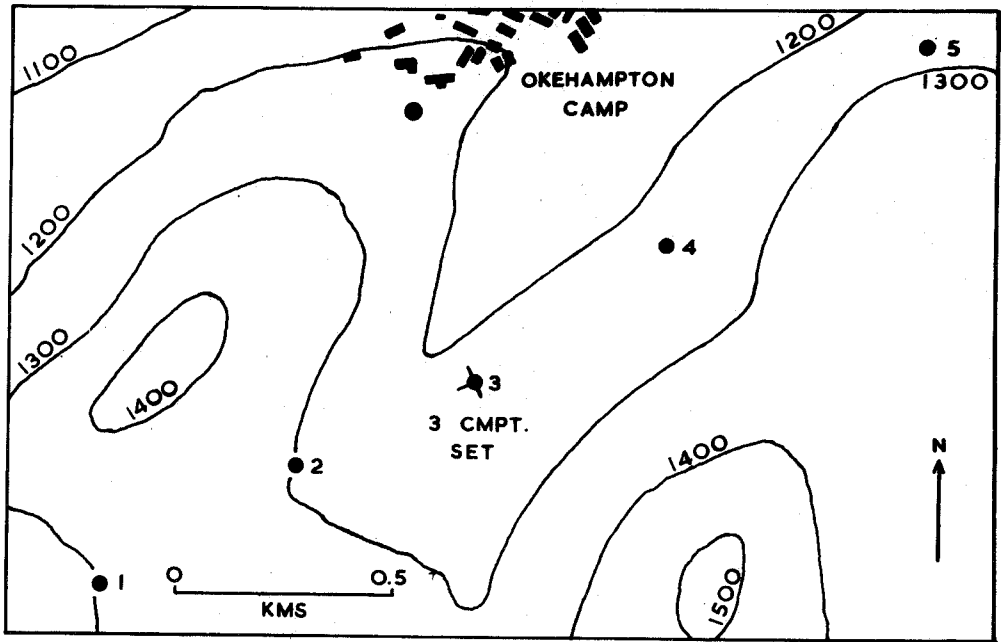


Fig.8. Sketch maps of the Dartmoor (above) and Bodmin Moor (below) array stations.

the whole project. A dipole aerial was erected to receive broadcasts from H.M.S. Hecla and reception was good throughout the whole period. The site is shown in fig.9. The apparatus used at this station was built in Durham and operated by Dr. A. L. Lucas now at the B.P. Research Centre, Sunbury-on-Thames. It is described in detail by Lucas (1966) but a summary is given below.

The apparatus may be divided into three main units.

#### I. FIELD RECORDING SYSTEM

This involves a transportable array with digital magnetic tape recording of ten seismic channels and timing and control information. At the time of recording, the digital information on any one channel may be replayed to a simple one channel digital-to-analogue converter, designed to drive a pen recorder. This section of the equipment is shown in schematic form in fig.10. The main units indicated are here described briefly.

##### 1. Geophone

10 B.P. Swamp Geophones (3c/s) are used.

##### 2. Pre-amplifier

The pre-amplifier has a fixed gain of 200 and is powered by mercury cells. It is cased in a PVC tube permanently sealed at one end with both input and output lines passing through the other which is sealed by compressing a rubber disc between two brass plates.

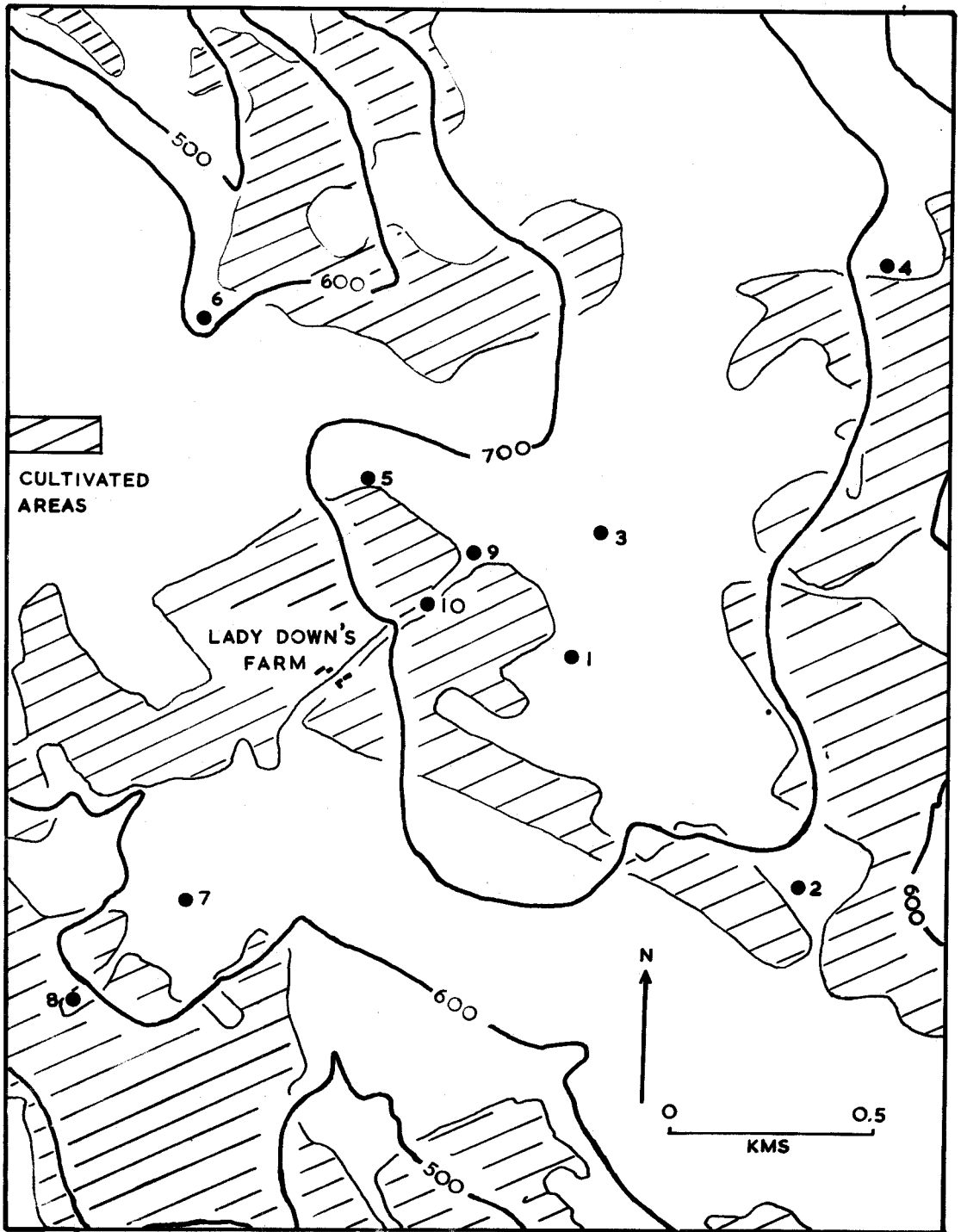


Fig.9. Sketch map of the Land's End array station.

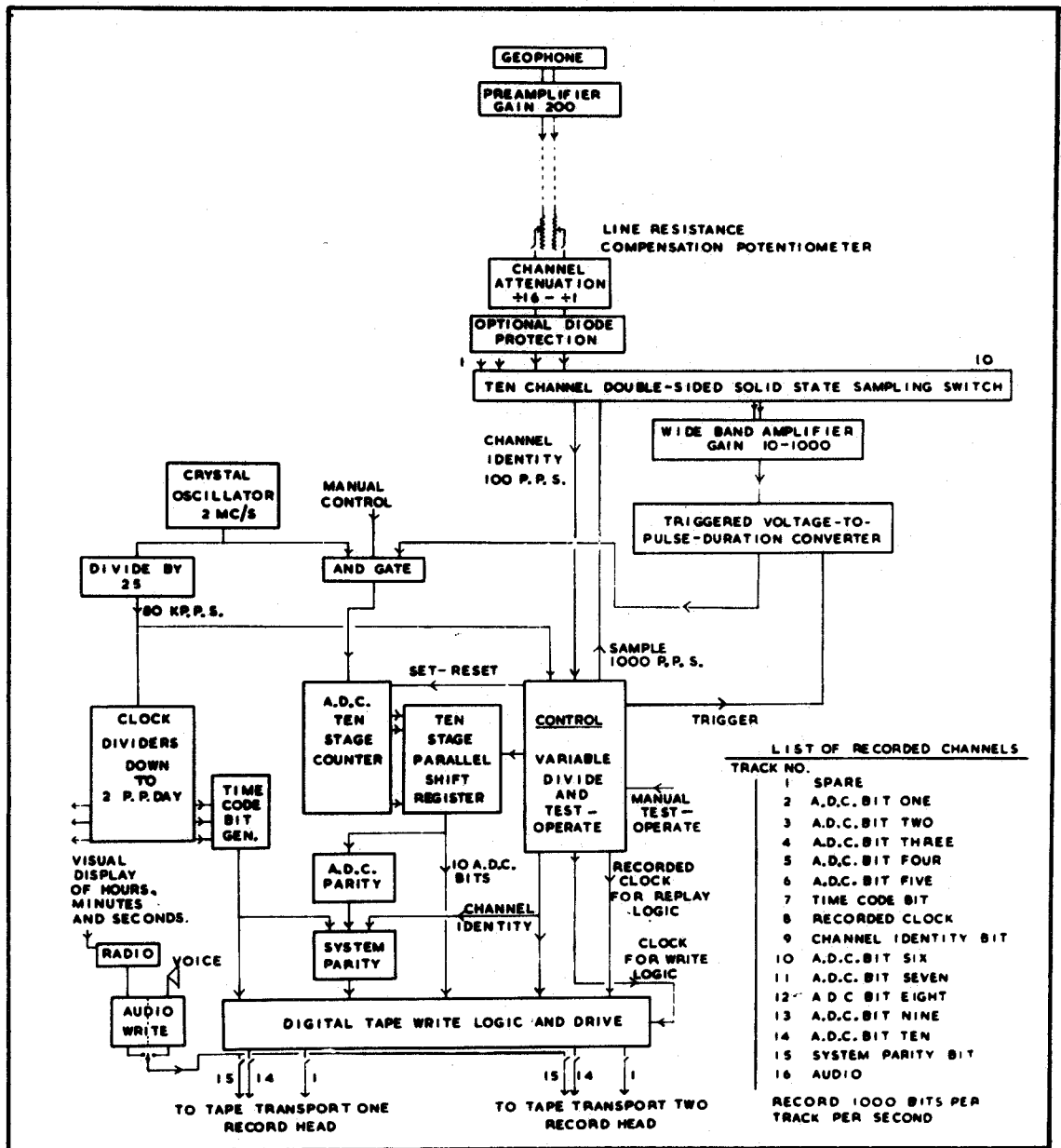


Fig.10. Schematic diagrams of seismic data processing system (after Lucas 1966).

1 - Array field recording system.

### 3. Channel attenuation

This function enables an attenuation of from  $\frac{1}{16}$  to  $\frac{1}{1}$  to be applied individually to the signals on the different channels.

### 4. Ten channel double-sided sampling switch

This unit was purchased as a complete unit. The drive pulse to the channel one switch is brought out and used for channel identity eventually being written on to the tape.

### 5. Wide band amplifier (Redcor 371-022)

This is a wide band, low level, differential d.c. amplifier. This has a maximum gain of 1,000 which makes the overall maximum gain of the system to be 200,000.

### 6. Triggered voltage to pulse duration converter

This transforms a voltage into a time interval. The AND gate output consists of the intervals of 2mc/s signal commencing whenever the ramp comparator is triggered and ending when the ramp voltage equals the input voltage to the A.D.C.

The rest of fig.10 indicates the functions required to write the information in logical form on to the tape.

Important points to note are

- (a) the standard system rate is 1kc/s, i.e. each seismic channel is sampled by the switch 100 times a second;
- (b) the crystal oscillator output is divided down to 2 pulses per day to produce the system clock which is shown visually and written on to the tape every second (time code bit);

(c) the oscillator output is also divided down to  $1\text{kc/s}$  which is used to control various logical functions and is also recorded on a channel of the tape for the replay logic;

(d) the output of the AND gate is counted by the A.D.C. 10 stage counter, the information from which is passed into a ten stage parallel shift register whose outputs are then written across the tape in the form indicated at the side of fig.10.

The system parity bit is generated from the A.D.C. parity, the channel identity and the time code bit as shown.

The amplified output of a microphone or the output of the radio receiver may be written on the audio track.

Two tape decks are used. They are the TDR4 model of Thermionic Products (Electronics) Ltd., with speeds from  $15/8$  i.p.s. to 15 i.p.s. and fitted with 16 track record and replay heads to S.B.A.C. spacing for 1 inch tape.

As has already been indicated, any one channel of information may be replayed on a pen recorder while recording is in progress. This is the only safe way of making sure that the information is being recorded correctly. Fig.11 shows schematically how this is done.

Each track of the replay head drives a 2 stage, capacitance coupled head amplifier through a capacitance and a  $1\text{k}\Omega$  resistance.

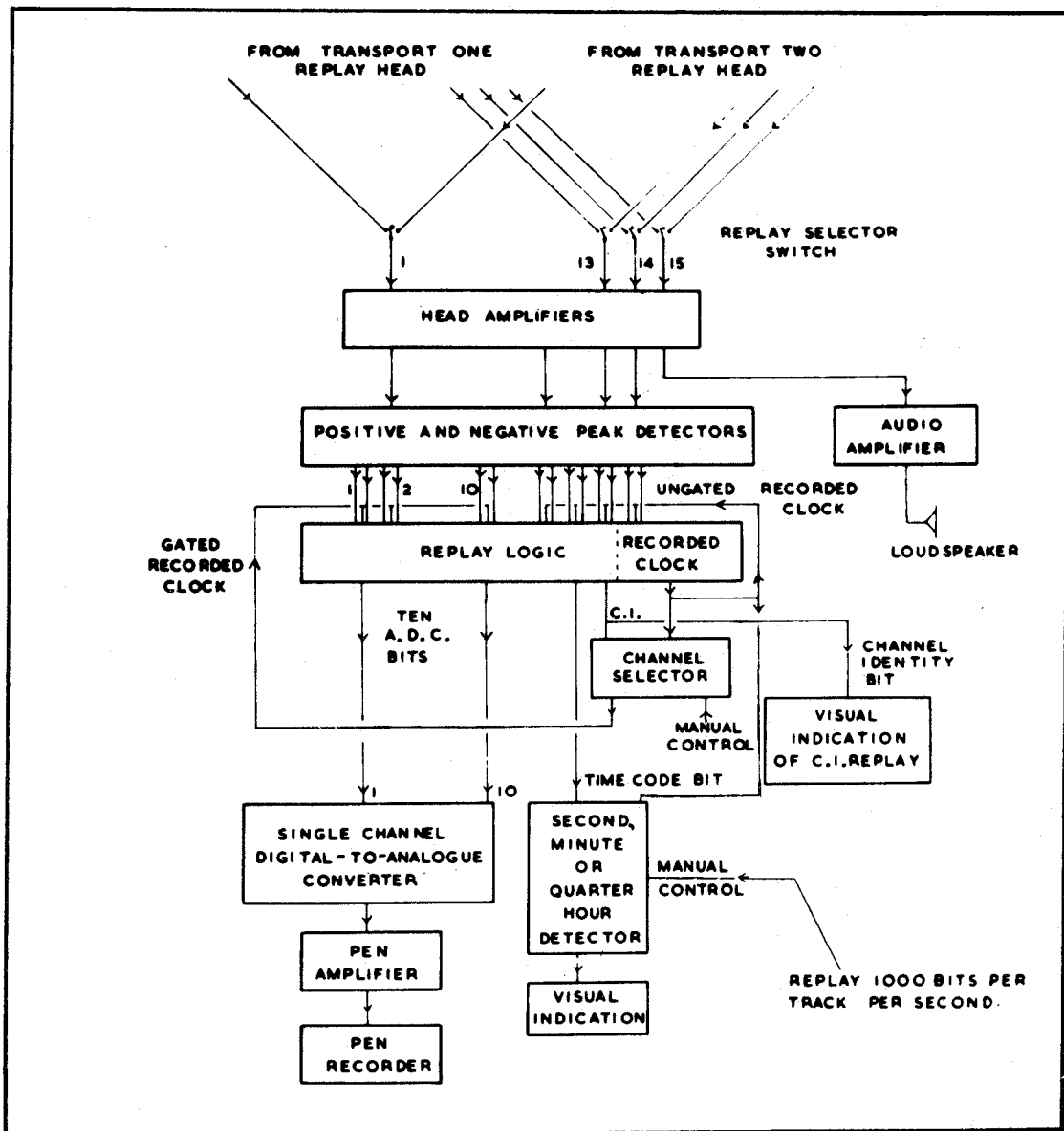


Fig.11. Schematic diagrams of seismic data processing system (after Lucas 1966).

2 - Array field replay system.



The positive and negative peak detectors (discriminators) give logic outputs by diode clipping at controlled threshold voltages which drive the replay logic boards. The channel selector for the single channel digital-to-analogue converter (D.A.C.) suppresses 9 out of 10 of the A.D.C. samples allowing samples of the one selected channel through to the single channel D.A.C. the output of which drives the pen recorder via an amplifier.

At the same time visual indication of correct channel identity replay is given by a red lamp which is driven by a monostable triggered by the channel identity replay logic. This logic should be a logical '1' for 1 millisecond in 10 which produces a steady visible flicker in the lamp.

A time code bit detector operated manually can be used to drive a green lamp every time a second, minute or quarter hour marker is detected. These monitoring facilities are used to ensure that information is being correctly written on to the tape.

## II. LABORATORY REPLAY SYSTEM

In the laboratory the recorded seismic information is replayed at real time speed to a 10 channel digital-to-analogue converter driving a multi-channel galvanometer recorder. Fig.12 shows the schematics of this process.

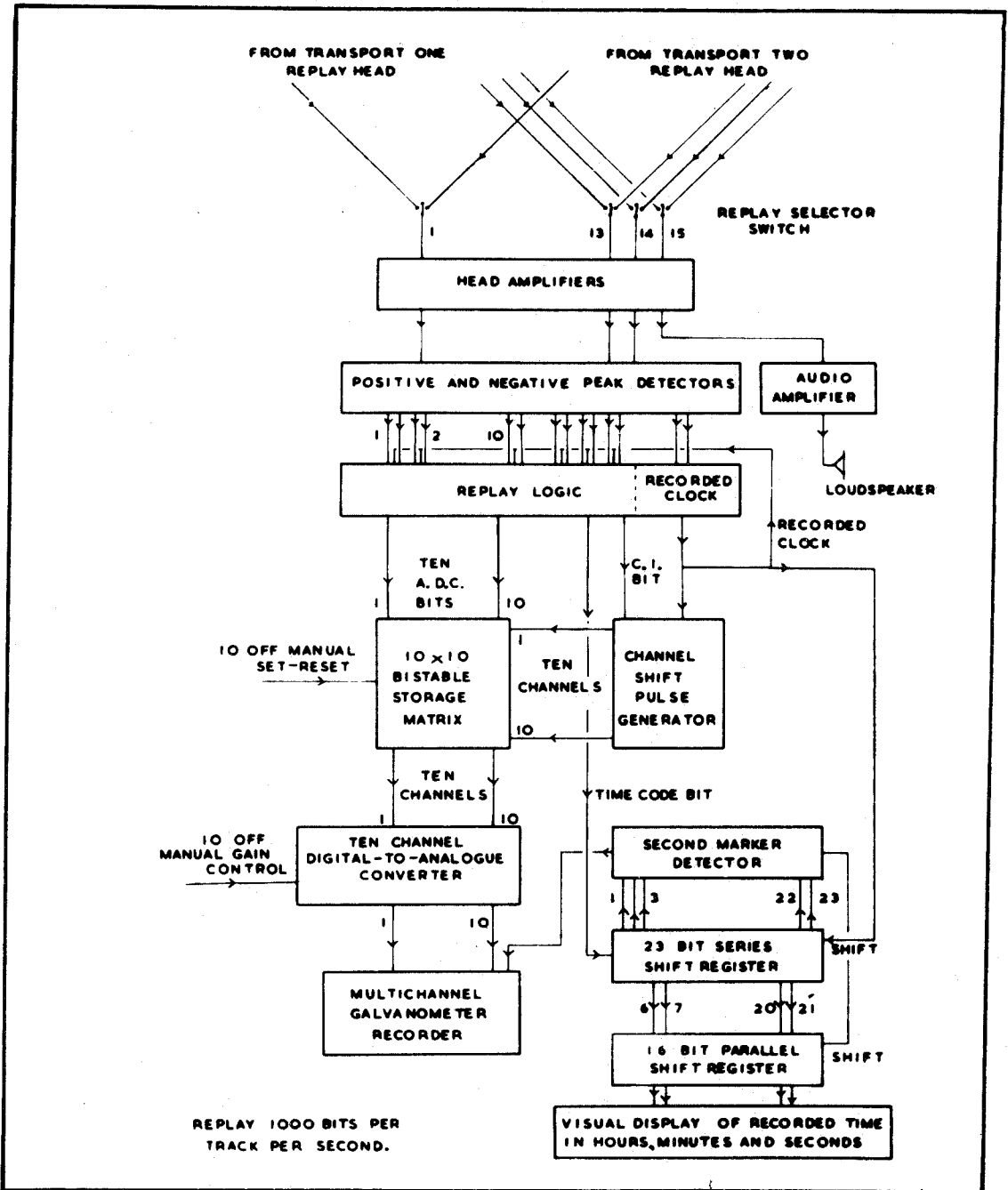


Fig.12. Schematic diagrams of seismic data processing system (after Lucas 1966).

3 - Laboratory replay system.

The head amplifiers, peak detectors, replay logic and audio channel of fig.12 use the same hardware as the field replay system although the channel selector switch must be in its non-operative position to allow all information through to the replay logic. The remaining elements of the diagram are concerned either with the 10 channel D.A.C. or the visual display of the recorded system time and as before will be discussed briefly in turn.

1. 23 bit series shift register

The contents of the time code bit replay logic are continually fed into a 23 bit series shift register.

2. Second marker detector

Any second marker is detected by an AND gate which examines the three oldest bits in the series shift register for the 101 opening phrase and the two newest bits for the 01 closing phrase.

3. 16 bit parallel shift register

When a second marker is detected the contents of the sixteen stages of the series shift register are shifted out into a 16 bit parallel shift register (N.B. the remaining 2 bits constitute the second, minute or quarter hour phrase).

4. Visual display of recorded time in hours, minutes and seconds

The contents of the above 16 bit parallel shift registers are displayed using 16 D.M. 160 tubes.

The channel shift pulse generator and the 10 x 10 bistable storage matrix are used to ensure that each channel of the 10 channel D.A.C. receives the 10 bits of information which constitute one sample of a particular seismic channel.

The 10 channel D.A.C. generates a drive current having a zero order hold form (i.e. a 'staircase') which drives galvanometers of an ultra violet recording oscillograph by using them directly in passive adder circuits. An example of a trace is shown in fig.13.

### III. PUNCH REPLAY SYSTEM

This transfers the recorded seismic information, timing, channel identification and parity information to punched paper tape using flux sensitive replay heads and a slow replay speed. The schematics of this facility are seen in fig.14.

The peak detectors and the replay logic use the same hardware as the field replay system while the 23 bit series shift register, the 16 bit parallel shift register and visual display of system time use the same hardware as the galvanometer replay system.

#### 1. Slow speed transport

This deck, having speeds of from 15/128 i.p.s., to 15 i.p.s., is fitted with a special head for flux sensitive replay.

This is necessary because the speed of operation of the synchronous punch is 100 characters per second so that for the recording system

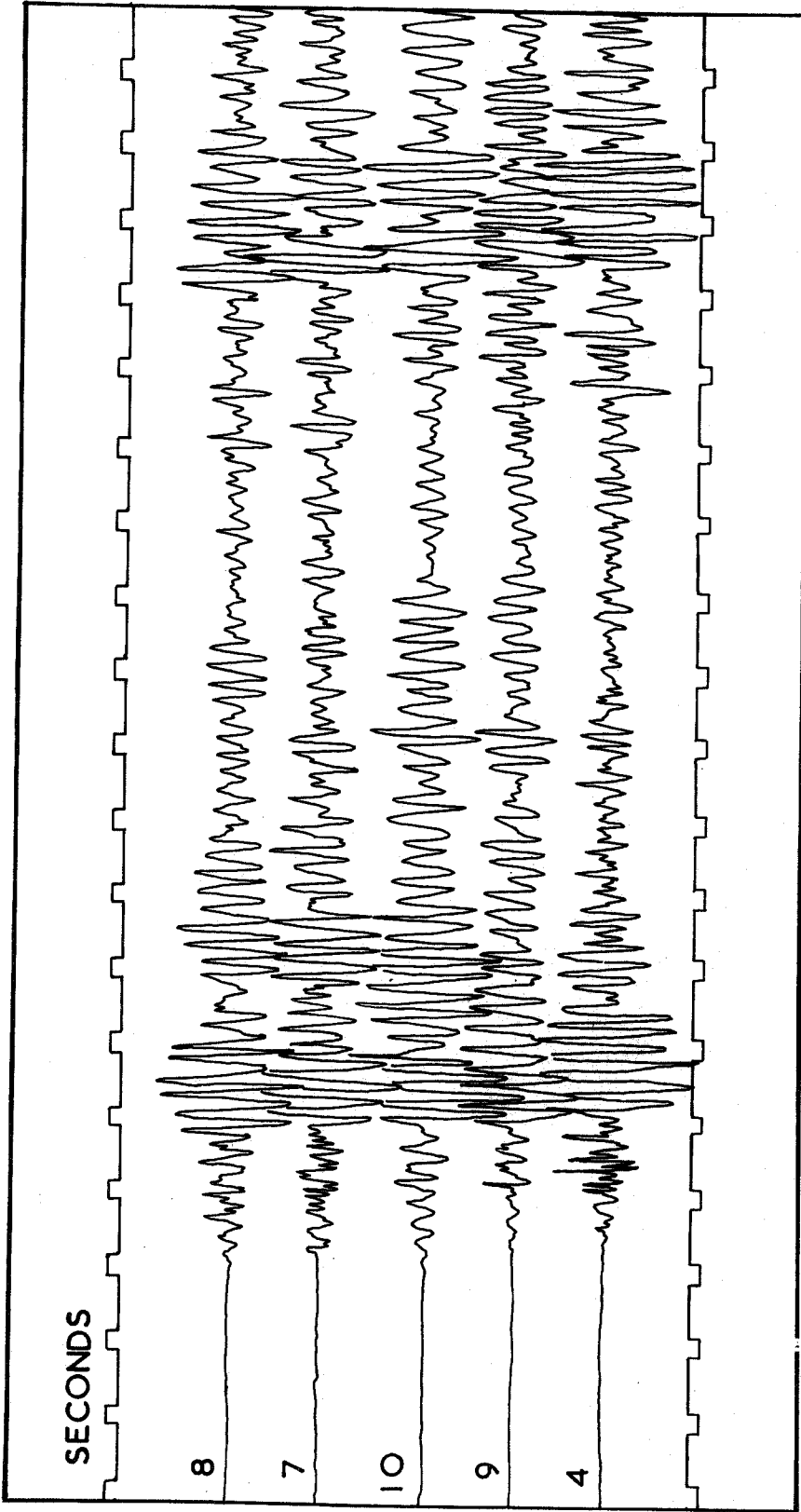


Fig. 13. U/V recorder trace of shot 11 of the south west England experiment as received by 5 of the geophones at the Land's End station.

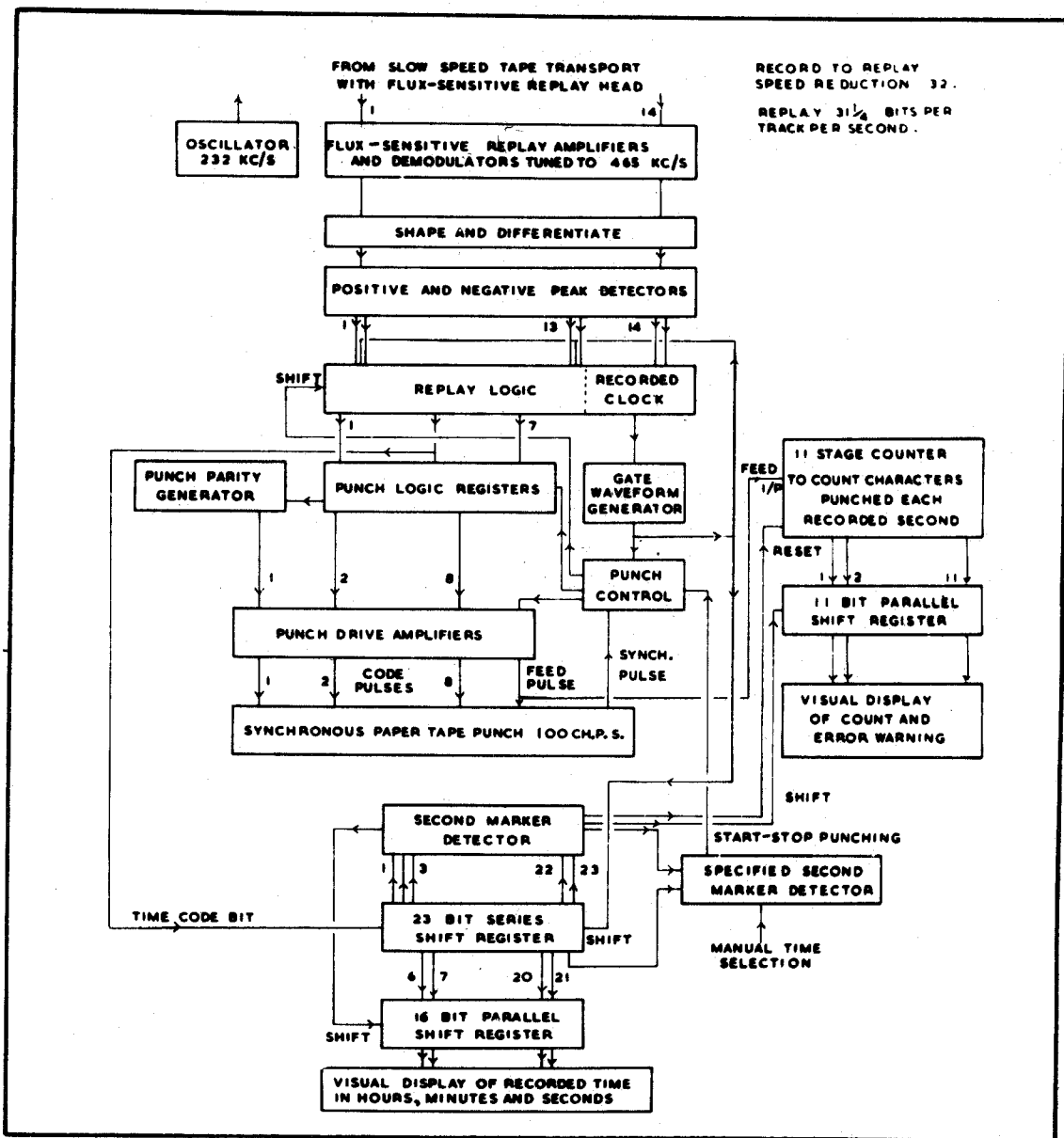


Fig.14. Schematic diagrams of seismic data processing system (after Lucas 1966).

4 - Punch replay system

rate of 1kc/s, a time scale expansion of 32 is used in order not to overload the punch.

## 2. 232kc/s.

The flux sensitive head uses a gapped ring modified so as to permit the reluctance of the ring to be switched between a high and a low value at a high frequency. The flux being driven round a ring by the magnetomotive force of the recorded signal is therefore 'chopped' at the switching rate, and the signal flux is converted to a fixed frequency alternating flux whose amplitude is proportional to that of the recorded signal. The two windings on each track are an oscillator winding and a read winding giving an amplitude modulated output at twice the oscillator frequency. The output of the read winding is amplified and demodulated to give the flux sensitive signal output which is then shaped and differentiated simulating the conventional replay process.

The gate waveform generator and punch control are instrumental in ensuring that the thirteen bits of information together with a punch parity bit from the parity generator are recorded on the tape in two 7 bit words.

## 3. Specified second marker detector

The system time at which it is required to start or stop punching may be set up on 18, 2-way, centre-off switches. This is vital bearing in mind that a 930ft reel of tape takes approximately 30 minutes to store 55 seconds of recorded data.

The contents of the 11 stage counter used to count the number of characters punched each recorded second are moved into an 11 bit parallel shift register the outputs from which are displayed on DM 160 tubes for about 32 seconds for each recorded second of data. If an error occurs in the system and the number of characters punched per recorded second is incorrect then a red error warning lamp is lit up.

All the hardware involved in these three units uses transistors as opposed to valves throughout and the only H.T. line is an unstabilised +50 volt line required for the DM 160 tubes. The analogue and digital circuits have all been constructed on veroboard circuit board except for the pre-amplifiers, the construction of which was contracted out using specially designed printed circuit boards. The system is built as a number of separate 19 inch chassis and these are placed into 19 inch cabinets. The equipment is run from an A.C. mains supply or from a mains generator fitted to a Land Rover.

The station recorded at a speed of 15/4 i.p.s. over the period of the shot times only and recorded all 45 shots. Some trouble with one or two channels was encountered, channel 3 refusing to work throughout the whole period. The main problem was with livestock damaging the land lines although considerable care was taken in routing the cable along the tops of walls and hedges. This problem was considerably reduced at the other



stations along the peninsula because of the design of the F.M. recording system at these stations.

Computer programmes had been developed by Dr. Lucas for handling the paper tapes on an Elliott 803 computer installed in Durham. However, early in 1967 Durham and Newcastle Universities acquired an IBM 360/67 computer which, in spite of its obvious advantages, posed the problem of having to change the data handling system completely. A special programme written in PL/1 was developed to read the paper tapes into the 360 and to store the data on computer magnetic tape. Appendix C describes this programme and some of the problems involved.

These last 5 stations were all situated on the granite outcrops along the south western peninsula. An effort to place the seismometers and geophones on the solid rock was made but often frustrated by the deep overburden of weathered granite and/or soil. Open shallow pits were dug at the Dartmoor, Bodmin Moor, Hensbarrow and Carnmenellis sites while the streamlined geophones at the Land's End station were augured into 3 or 4ft deep holes. No calibrations of instruments were made at any of these five stations.

G. Scilly Isles stations ( $49^{\circ}55.4'N.$ ,  $6^{\circ}18.4'W$ )

F.M. recordings were made of two vertical Willmore Mark II seismometers set approximately 400 metres apart and

recorded at high and low gain levels. The station recorded most of the 45 shots. It was operated by a team from the UKAEA seismology unit at Blacknest under the direction of Dr. H.I.S. Thirlaway.

H.	French Station	1	(48°33.1'N., 4°14.5'W)
I.	French Station	2	(48°27.9'N., 4°10.6'W)
J.	French station	3	(48°23.2'N., 4°07.6'W)
K.	French station	4	(48°17.8'N., 4°04.2'W)
L.	French station	5	(48°13.0'N., 4°01.6'W)
M.	French station	6	(48°08.2'N., 3°58.0'W)
N.	French station	7	(48°02.5'N., 3°52.7'W)
O.	French station	8	(47°56.7'N., 3°52.0'W)
P.	French station	9	(47°53.1'N., 3°46.9'W)
Q.	French station	10	(47°35.6'N., 2°42.8'W)

These ten stations were portable seismic stations consisting of single seismometers, the outputs of which were recorded on paper. The stations were set up in north western France extending line 3 from Landerneau to Rosporden. Stations 1 and 8 proved to be useless but all the other stations recorded most of the line 3 shots.

R. Eskdalemuir array station (55°20.0'N., 3°09.6'W)

This is the UKAEA seismic array station consisting of F.M. recordings of an 'L' shaped array of 20 Willmore Mark II seismometers (1c/s). The station is described by Truscott (1965).

Signal to noise levels were low because of the large distances of the station from the shots but most of the line 3 shots were recorded by the station and the data is incorporated in this study.

In addition to the above 18 land stations it was hoped that a sonobuoy station would have been occupied halfway along line 2 while lines 2 and 3 were being shot and that this station would then be removed to the end of line 1 for the final line of shots. Unfortunately, inclement weather conditions were expected and the stations were not set up. The other casualty was a land station installed near St. David's Pembrokeshire by the Birmingham University Geophysical group. Several problems were encountered rendering the data unusable.

From the foregoing it is obvious that although the shot firing routine was meticulously handled by the Hydrographics Department, the recording side of the experiment suffered various difficulties. The effect of these shortcomings will become apparent later. In spite of this, large amounts of data were collected and the next section deals with the preparation of the data for processing.

## 2.2 Data preparation

All the data collected from the British and Irish

stations was used in this study. Revoy (1969) has been working with the data collected from the French stations but the P-wave data from these stations has been communicated to Durham by M. Revoy and is also incorporated in this study.

As a first operation all the magnetic tape recordings of all the shots were played out on to paper. Doubtful arrivals on the F.M. records were enhanced by frequency filtering for identification purposes only. No filtering was applied to the digital records. First arrival onsets of unfiltered records were read off to the nearest 0.01 second and corrected to absolute time by adding in the time encoder corrections. Travel times of first arrivals were then calculated and corrected to a sea level datum by adding the approximate height corrections ( $t_h$ ) given by :-

$$t_h = \frac{\text{shot depth} - \text{station height}}{5\text{km/sec}}$$

In most cases this term is of the order of -0.05sec.

Another slight adjustment was made because of the uncertainty in the position of the shots. The station positions are accurate to within 200 metres but it will be noted that the shot positions with the least uncertainty are known only to within 500 metres. Some of the more distant shot positions are known only to within 2 or 3km. At close ranges, assuming a velocity of 5km/sec, a distance error of 0.5km is equivalent to a timing error of 0.1 second and at large ranges, assuming a velocity of

8km/sec, a distance error of 1km is equivalent to a timing error in excess of 0.1sec. It is thought that only in a few cases is the uncertainty less than 0.1sec. Thus the travel times have been corrected to the nearest 0.05 second. This correction is hardly necessary but it serves to emphasise the uncertainty in the travel times and it is in this form that they have been used throughout this study.

Shot - station ranges were calculated on a digital computer using two different methods, the one acting as an independent check on the other. The first method, originally programmed by A. L. Lucas (1966) uses formula 5 given by Bullen (1963, page 155). The second method, claimed to be much more accurate at short ranges, is known as the Thomas method which has been used in many American refraction experiments (Steinhart, personal communication). In fact both methods gave ranges which are within 0.2km of each other and in most cases within 0.1km but the results given by the Thomas method are used in this study.

Appendix B lists the onset times, ranges, sea level datum corrections and first arrival travel times for all the shots received at all the stations. Doubtful arrivals have not been included.

A further preparation of the data takes the form of stacked records of individual shots at each recording station. Individual traces of shots are mounted at their respective

distances on a reduced travel time, distance framework.

The reduced travel time is given by the relation :

$$T_{\text{calc}} = T_{\text{observed}} - \Delta/6.0$$

where  $T_{\text{calc}}$  is the reduced travel time in secs.

$T_{\text{observed}}$  is the observed travel time in secs.

$\Delta$  is the range between shot and station.

6.0 is a value selected as an estimate of  
crustal P-wave velocity.

The scale chosen is such that 5sec along the time axis equals 40km along the distance axis which is a scale that others using this technique, notably Landisman (personal communication), are advocating as a standard. It was found that traced drawings of the seismic records provided the easiest form of display. The use of these stacked records will become apparent in a later chapter.

## CHAPTER 3

The classical method of interpretation of the south west England seismic refraction data in terms of homogeneous layers separated by plane surfaces is described in this chapter. It is also assessed in terms of its usefulness for the interpretation of seismic refraction data in general. The problems inherent in the method are discussed and, in particular, the problem of inhomogeneity is emphasised. The upper crustal variations in the vicinity of the shots of the south west England experiment are described and the adjustments to the travel times which were made to correct for these variations are presented. The travel time graphs of first arrival data only at each receiving station are described and interpreted in terms of velocity-depth structure. The results of a time term analysis applied to two different sets of data are also given and the efficacy of such an approach to the analysis of data from the south west England experiment is discussed.

### 3.1 The classical method

In addition to the assumption of homogeneous plane layering, the classical method also assumes that the layers exhibit a step-like increase of velocity with depth. Travel time-distance graphs are constructed and straight lines are

fitted to the data, in this case, by the method of least squares which has been programmed for use on the IBM 360/67 computer (see Appendix D). For the simple case of a horizontal layer overlying a half space, the travel time graph takes the form of two segments, the inverse slopes of which represent the velocities above and below the discontinuity. The depth to the discontinuity is given by the formula

$$Z = \frac{T_i V_1 V_0}{2\sqrt{V_1^2 - V_0^2}},$$

where  $Z$  = depth to discontinuity,

$T_i$  = time intercept for  $V_1$  segment,

$V_0$  = velocity above the discontinuity,

$V_1$  = velocity below the discontinuity.

The above formula can be modified for the multi-layer case.

In crustal structure studies this method has been found to be the most effective in the evaluation of basement and sub-Moho velocities and in the determination of crustal thicknesses. It has been used as the basis for refraction experiments in most parts of the world. Many references may be given here but the reader is referred to James and Steinhart (1966) who give a critical review and comprehensive bibliography of explosion studies in the period 1960 - 1965.



The statistical uncertainties inherent in the seismic refraction method are discussed in detail by Steinhart and Meyer (1961). The basic assumption of planar homogeneous layers exhibiting step-like increases of velocity with depth are often violated in the field. Thus there are several sources of error inherent in the acquisition of least squares velocities and depths to refractors from travel time data. They are listed below :-

- (i) Errors in shot/station position.
- (ii) Errors in picking onsets.
- (iii) Deviations of the interface from a plane.
- (iv) Lateral velocity variations
- (v) Surface irregularities (topographic differences).
- (vi) Hidden changes of velocity with depth.
- (vii) Non-reversal of refraction lines.

Items (i), (ii), (iii) and (iv) will appear as residuals from the least squares lines and thus will be included in the estimate of uncertainty. Corrections can be applied to minimise the uncertainty due to item (v) but items (vi) and (vii) will provide sources of error which are more difficult to assess.

Any hidden changes of velocity with depth will result in incorrect estimates of depth to a particular boundary. An unreversed refraction line results in unreversed estimates of velocities. An unreversed velocity is, in itself, unreliable

and can greatly increase the estimates of uncertainties on other values dependent upon it for their evaluation. A properly planned refraction experiment should eliminate the possibility of an unreversed velocity. However, even the best planned experiment is not able to cater for all eventualities and some refraction lines, or parts thereof, may be unreversed by the failure of a certain shot or station required to give full reversal.

For the south west England experiment the estimates of uncertainties were calculated in the form of standard errors on the velocity and time intercept values given by least squares. The following sections presenting all the velocities obtained in the experiment by the least squares method will include discussions on the reliability of these values. Unreversed portions of the lines have been recognised and steps have been taken where possible to minimise the uncertainties resulting from this potential source of error. A histogram of travel time residuals from least squares lines reveals that their distribution is symmetrical and almost normal (see fig.15). Therefore the author is confident that, except where stated, the velocity values given are reliable within the 95% confidence level indicated by twice the standard errors. On the assumption of there being no changes of velocity with depth, the depth estimates given are also reliable within the 95% confidence

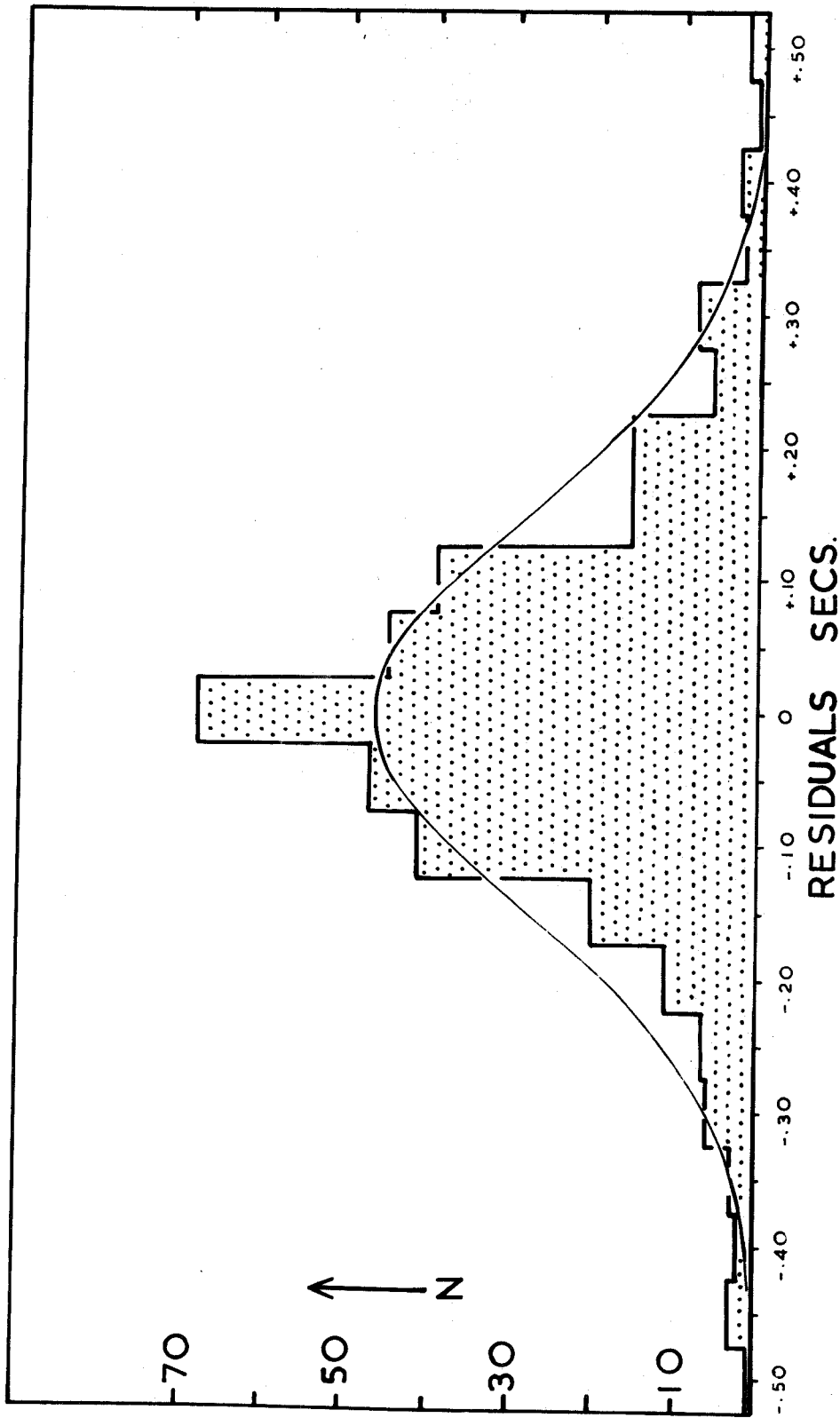


Fig.15. Histogram of the least squares residuals from the first arrival travel time data of the south west England experiment. The calculated normal curve is also included.

level indicated by twice their standard errors.

### 3.2 Adjustments for upper crustal variation

The classical method has been applied to the first arrival travel time data of the south west England refraction experiment. Attempts have been made to make allowances for the varying thicknesses of sedimentary material which are known to be present throughout the region. For line 1, this was a relatively simple matter. It was noted from previous work in the area (see Chapter 1 of this thesis) that the seismic stations set up earlier in the vicinity of this line indicated a thickening wedge of sediments at its western end. Most of the short refraction profiles were unreversed and there is no gravity control of the area so that true sediment thickness can only be estimated. Table 1 gives the sedimentary delay time for each shot position of line 1 used in this preliminary interpretation. These values were calculated using the sedimentary thicknesses indicated by the earlier stations, and were added to the first arrival travel times of the line 1 shots.

For lines 2 and 3 there is very little seismic control of the shallow structures. However, a gravity profile along the two lines was undertaken in 1966 and 1967 by the University of Durham and the Bouguer anomaly profile is shown in fig.16. The profile is being interpreted by Mr. B. Ward as part of the

Table 1. Sedimentary delay times for the line 1 shots

Shot no.	Delay time (sec)
1	.52
2	.33
3	.22
4	.15
5	.12
6	.11
7	.08
8	.07
9	.07
10	.06
11	.05
12	.05
13	.05
14	.05
15	.05
16	.05
17	.05
18	.05
20	.05

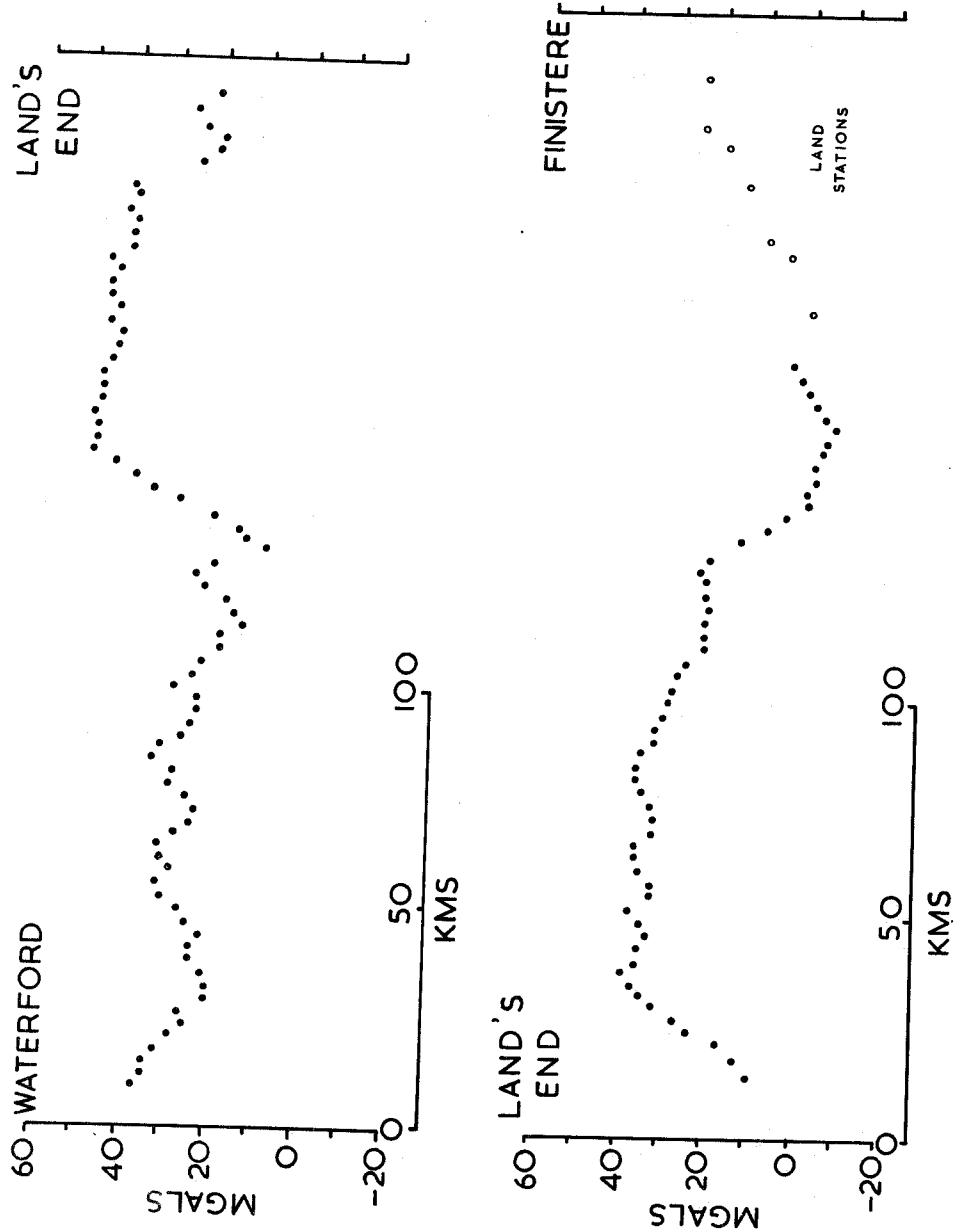


Fig.16. Bouguer anomaly profile along lines 2 and 3.

M.Sc. course at Durham but the author has attempted a simple interpretation of part of it aided by personal communication with Mr. Ward. The main features are the three gravity lows. The central low has been interpreted by Bott, Day and Masson-Smith (1958) and Ward (personal communication) to be caused by the south west England granite batholith. The southern low is interpreted by Ward (personal communication) to be a mass of granitic material extending to approximately 6 km depth. The northern low is assumed to be the westward extension of the sedimentary basin reported by Blundell et al (1968). An interpretation of the northern anomaly in terms of sedimentary depths is shown in the lowest section of fig.22. A density contrast of  $-0.15$  gm/cc and the smoothed Bouguer anomaly curve shown in fig.22 were assumed and depths were calculated using a computer programme (NTRAP) developed by Allerton (1968) at Durham University. A sedimentary velocity of  $3.0$  km/sec was used to calculate the sedimentary delay times at each shot point. However, it was found that these delays increased the scatter of the travel time data at both the Irish and Land's End stations and, in the absence of any other information, no corrections have been applied to the data from line 2.

The problem of limited data also occurs along line 3. The short seismic refraction profiles about 50 km to the east of the line give indications of a wedge of sediments thickening southwards to about 3 to 4 km depth in the middle of the Channel

(see Chapter 1). These profiles were mostly unreversed and it is uncertain how the sediments vary laterally especially in the region of line 3. The gravity profile gives no indication of a gravity low immediately to the south of Land's End and, indeed, maintains a relatively uniform high level for some distance between the two southern lows. Thus estimates of sedimentary delay times cannot be calculated with certainty and no corrections have been applied to the data from this line.

### 3.3 First arrival travel time graphs

First arrival travel time graphs for every station are presented in this section. The travel times have been plotted in their reduced form ( $T - \Delta/6$ ) against distance ( $\Delta$ ). The striking feature of all these graphs (except those of Dartmoor and Eskdalemuir, which only give one segment) is that the data is best fitted by two major straight line segments with a crossover distance of about 120 km. The arrivals representing seismic waves which have travelled distances greater than 120 km fit lines giving velocity estimates of approximately 8.0 km/sec. These arrivals are interpreted as the head wave from the Mohorovicic discontinuity at the base of the crust and will subsequently be referred to as  $P_n$  arrivals. The other arrivals, representing seismic waves which have travelled less than 120 km, fit lines which give velocity estimates of a little lower than 6.0 km/sec.



These arrivals are interpreted as the head wave refracted from the crystalline basement and will subsequently be referred to as  $P_g$  arrivals. The results given by the least squares process, which has been applied to the travel time data of all the stations, are given in table 2.

No secondary  $P_g$  arrivals have been picked from the data at any of the stations. The amplitude of the first arrival out to about 120 km falls off rapidly and becomes almost lost in noise near that distance. A second arrival which follows the  $P_n$  arrivals at distances greater than 120 km and arrives approximately at the calculated  $P_g$  time is not thought to be a true  $P_g$  arrival because of its large amplitude. This matter will be discussed further in a later chapter. Secondary  $P_n$  arrivals, at distances less than 120 km, have not been recognised at any station although they will be present. They are masked by other, more energetic arrivals coming in at a similar time.

At close ranges one or two of the stations give evidence of lower velocity segments and most stations show small positive  $P_g$  intercepts. There is also considerable scatter of the data about the straight line segments. These observations reflect the variability of the near-surface geological structure with an irregular basement surface and lateral irregularities in the topmost layers of the Earth's crust. These layers consist generally of variable thicknesses

Table 2. Results of the least squares process of fitting straight lines to the travel time data of the south west England experiment

Station	Line	Phase	Velocity	Standard error on Velocity	Time intercept	Standard error on time intercept	No. of Obs.
Dartmoor	1	$P_n$	8.00	$\pm .07$	5.55	$\pm .23$	13
Bodmin Moor	1	$P_n$	7.93	$\pm .04$	5.46	$\pm .13$	11
Bodmin Moor	1	$P_g$	5.77	$\pm .10$	-0.12	$\pm .31$	5
Carmenellis	1	$P_n$	7.98	$\pm .06$	5.85	$\pm .20$	8
Carmenellis	1	$P_g$	5.92	$\pm .03$	0.36	$\pm .06$	8
Land's End	1	$P_n$	7.99	$\pm .08$	5.57	$\pm .25$	8
Land's End	1	$P_g$	5.88	$\pm .03$	0.18	$\pm .06$	10
Scilly Isles	1	$P_n$	7.72	$\pm .16$	4.97	$\pm .43$	4
Scilly Isles	1	$P_g$ east	5.94	$\pm .03$	0.19	$\pm .02$	6
Scilly Isles	1	$P_g$ west	5.79	$\pm .03$	-0.10	$\pm .07$	8
Waterford	2	$P_n$	8.62	$\pm .09$	8.06	$\pm .24$	7
Waterford	2	$P_g$	5.88	$\pm .07$	1.04	$\pm .17$	6
Land's End	2	$P_n$	8.15	$\pm .29$	6.68	$\pm .71$	5
Land's End	2	$P_g$	5.62	$\pm .06$	0.03	$\pm .15$	7
Eskdalemuir	2	$P_n$	8.18	$\pm .12$	7.59	$\pm .93$	12
Land's End	3	$P_n$	7.63	$\pm .38$	6.09	$\pm .93$	3
Land's End	3	$P_g$	5.61	$\pm .07$	0.15	$\pm .17$	8
French sts.	3	$P_n$	8.07	$\pm .05$	6.14	$\pm .12$	12
French sts.	3	$P_g$	5.80	$\pm .07$	0.24	$\pm .19$	22

of low velocity sediments and locally, in the granite batholith area, of weathered granite.

The travel time graphs and interpretation of the results from each line of shots will now be considered separately.

### 3.3.1 Line 1 travel time graphs

Only stations situated along the line of the shots have been used in this study of the line. The French and Irish stations received one or two of these shots but not enough to plot on a travel time graph. The arrivals could not be seen, even after processing, on the Eskdalemuir array records. The travel times are corrected for the inferred wedge of sediments at the western end of the line and the travel time graphs of individual stations are described below.

#### (a) Dartmoor (fig.17)

All the shot points for this station fall in the  $P_n$  range (i.e.  $> 120$  km). Several of the more distant shots provided onsets which were difficult to pick with certainty and they are not included.

#### (b) Bodmin Moor (fig.17)

The two well-defined segments,  $P_g$  and  $P_n$ , are observed.

## (c) Carnmenellis (fig.18)

The two well-defined segments,  $P_g$  and  $P_n$ , are observed here also. The arrival from shot 13 at a distance of about 80 km is approximately half a second later than would be expected and it has not been included in the least squares fit.

## (d) Land's End (fig.18)

The  $P_n$  segment is well-defined but the  $P_g$  segment is slightly curved in the range 0 - 50 km in the form of a travel time graph of arrivals representing seismic waves which have travelled through a medium having a steady increase of seismic velocity with depth. However, this form of graph can also result from a thickening wedge of sediment. The maximum delay is only about 0.25 sec representing a maximum thickness of 1.0 km assuming a sedimentary velocity of 2.5 km/sec. At distances of approximately 55 and 72 km the two arrivals are slightly early. These points represent shots 12 and 13 which were exploded close to the shores of the Scilly Isles and, presumably, upon the outcropping granite with no consequent sedimentary delay time.

## (e) Scilly Isles (fig.19)

The arrivals at this station form two groups, one comprising arrivals travelling from west to east and the other comprising arrivals travelling in the opposite direction. The  $P_n$  velocity is low which reflects the problem of the thickening wedge of sediments at the western end of the line. The standard error of the slope of the line is large and this reflects the

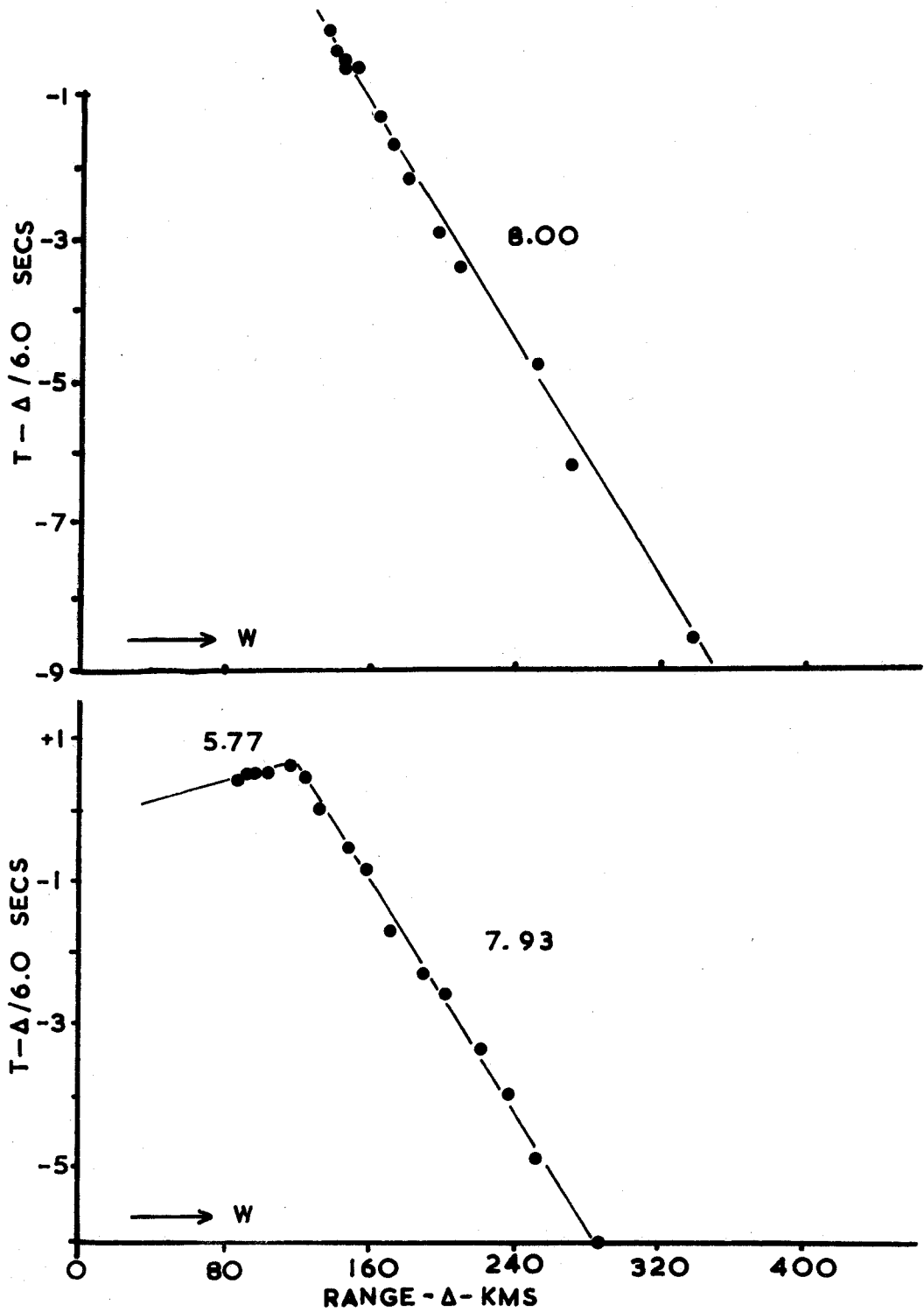


Fig.17. First arrival travel time graphs for the Dartmoor station (above) and the Bodmin Moor station (below).

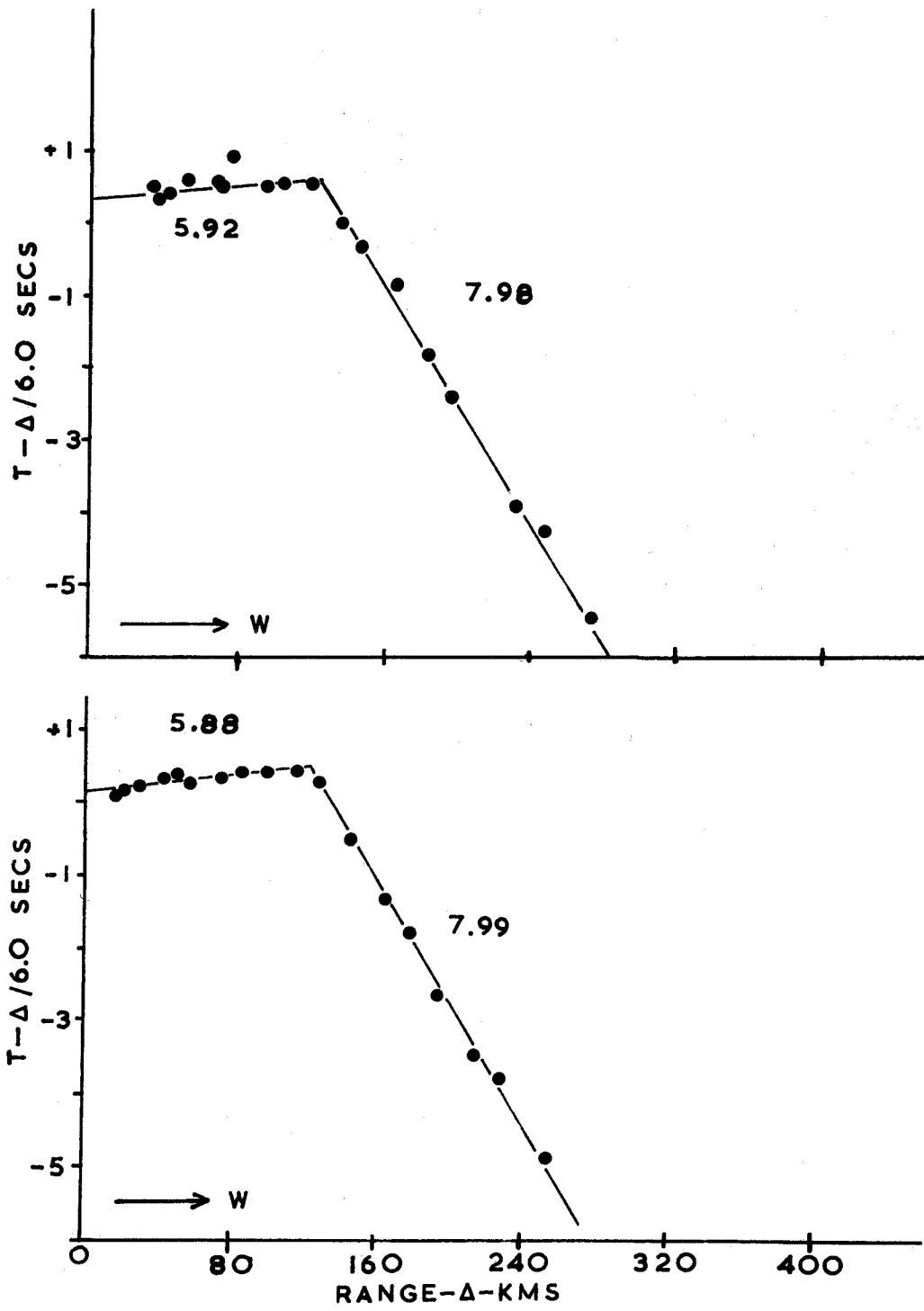


Fig.18. First arrival travel time graphs for the Carnmenellis station (above) and the Land's End station for the line 1 shots (below).

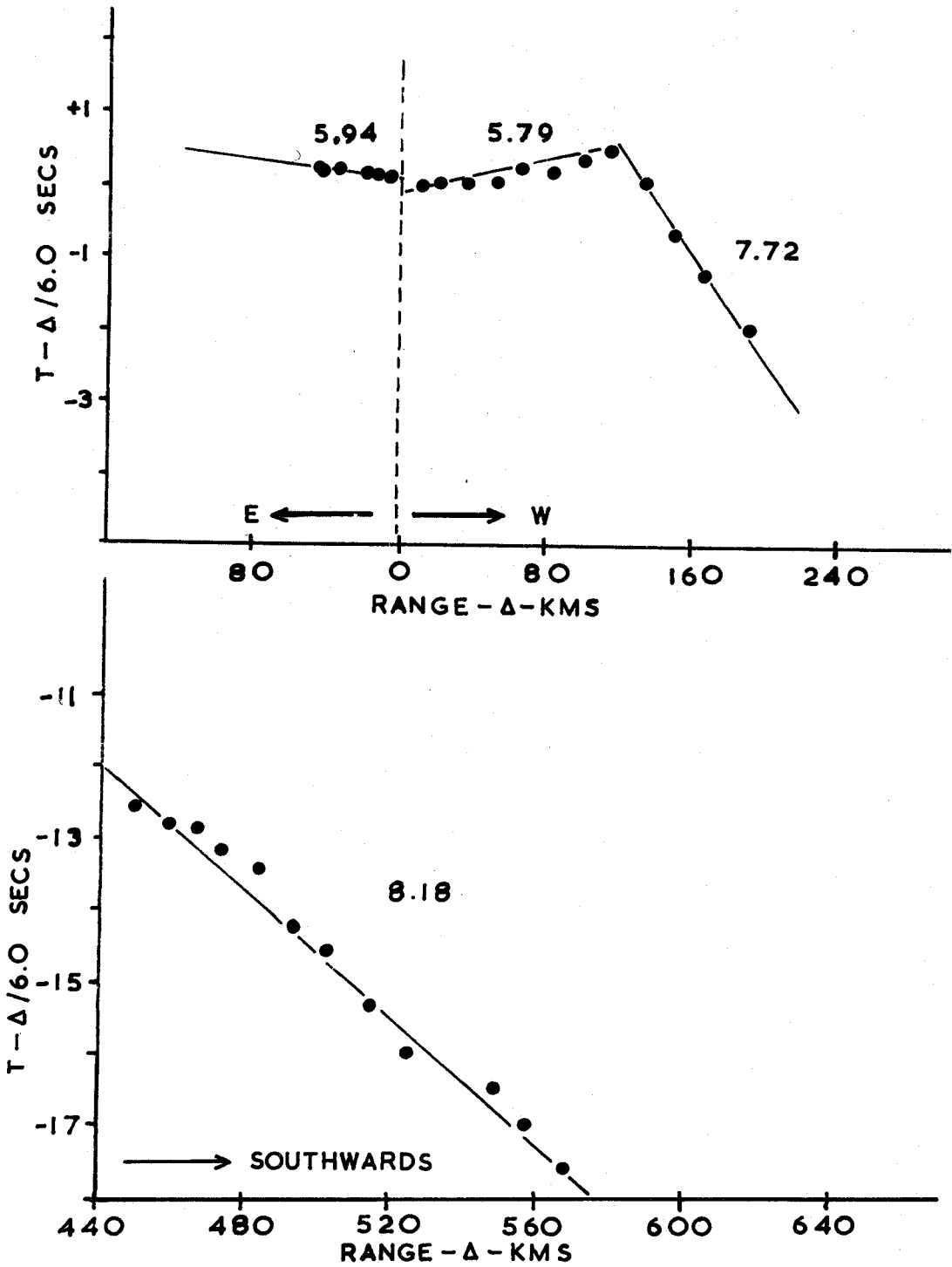


Fig.19. First arrival travel time graphs for the Scilly Isles station (above) and the Eskdalemuir station (below).

paucity of points and inaccuracies of the delay times used in the analysis in order to make allowances for the wedge of sediments. The scatter on the western  $P_g$  line can be explained by an uncorrected variation in thickness of sediments beneath shots 5 to 8. The eastern  $P_g$  line gives a slightly higher velocity than the western one but the difference is not significant. Slightly varying sediment thicknesses on either side of the Scilly Isles could account for this variation.

### 3.3.2 Interpretation of line 1 travel time data

The  $P_g$  velocity measured at all the stations is remarkably constant within the error limits given. The estimates of velocity at each station can be combined to give an overall estimate of  $P_g$  velocity of  $5.85 \pm .05$  km/sec. This velocity represents the seismic P-wave velocity within the granite and it is pertinent here to look at the work which has been carried out on the behaviour of P-wave velocities in granites under varying pressure and temperature conditions.

Birch (1958, 1960), studying the effects of pressure only, found that the P-wave velocity in granites increased rapidly to pressures equivalent to about 3 km depth and thereafter increased only slowly as the pressure increased to the equivalent of a crustal thickness of 30 km. Hughes and Maurette (1956), studying the combined effects of temperature and pressure, found



similar results to those of Birch except that the velocity tended to remain constant or decrease a little after the initial increase of velocity with depth. Thus there is evidence that the P-wave velocity within a granite is almost constant below a depth of about 3 km but that there is a considerable increase of velocity down to this depth.

Assuming the rate of increase of velocity with depth indicated by Birch (1960), the energy of shots more than 20 km away from a station will have travelled down to about 3 km and thus should indicate the maximum velocity present in the granite. For the south west England experiment few shots are situated less than 20 km away from each station with the result that the velocity obtained from the travel time data should represent this maximum velocity. Nevertheless, a study of the travel time graphs indicates that the near shots do tend to weight the estimates of the velocity to lower values and thus it is expected that the maximum velocity may be a little higher, perhaps about 5.9 - 5.95 km/sec. However, because of the evidence that the P-wave velocity tends to decrease a little with increased pressure and temperature, it may be assumed that 5.85 km/sec is a reasonable estimate of the mean velocity within the granite. The significance of this observation will be discussed in a later chapter.

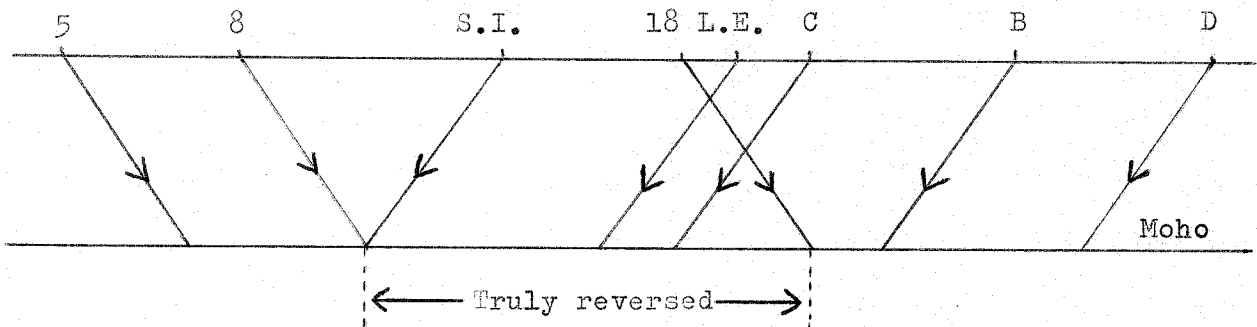
The  $P_n$  velocity seen at all the stations except that of the Scilly Isles is also remarkably constant. The combined estimate is  $7.95 \pm .05$  km/sec. However, this velocity has been obtained looking in the direction of shot to station, i.e. it is the apparent velocity in one direction only. In order to obtain an estimate of the true  $P_n$  velocity and to calculate the dip (if any) of the Moho, the line may be reversed by plotting the travel times of the first arrival of a particular shot at each of the recording stations. In this way the apparent velocity in the direction stations to shots can be ascertained. There is still the problem that the apparent velocities have been measured in different portions of the line, i.e. in the region of the shots and in the region of the stations. If the dip of the refractor changes along the line, the true  $P_n$  velocity is impossible to calculate. If the refractor can be assumed to be a plane dipping uniformly across the whole region then the two apparent velocities can be used to give an estimate of the real  $P_n$  velocity and the dip of the refractor.

This has been done for line 1 of this experiment. The first arrival travel time data for shots 3, 5, 7 and 8 arriving at the Land's End, Carnmenellis, Bodmin Moor and Dartmoor stations were fitted by a least squares straight line in the usual manner. If the angle of dip is small ( $< 3^\circ$ ) then the real  $P_n$  velocity is the average of the apparent

velocities in both directions. By fitting a straight line to the travel time data of a number of shots at an equal number of stations one obtains this average velocity.

Thus the real  $P_n$  velocity is found to be  $8.07 \pm .07$  km/sec.

This would indicate that the Moho is dipping at an angle of 34 minutes towards the west but because of the errors involved, this dip can be regarded as negligible.



Vertical scale  
exaggerated

D = Dartmoor.

B = Bodmin Moor.

C = Carnmenellis.

L. E. = Land's End.

S. I. = Scilly Isles.

5, 8, 18 = shot numbers.

Fig. 20. The extent of line 1 giving a truly reversed

$P_n$  velocity.

The above result has assumed that the Moho is a plane dipping uniformly across the whole region. If the apparent velocities in both directions could be measured in the same region then a truly reversed  $P_n$  velocity and an estimate of dip would be obtained. Fig.20 shows the extent to which this can be done for line 1. The apparent velocity given by the travel time data from shots 8 to 18 as seen at the Dartmoor station is the apparent velocity in one direction beneath the Scilly Isles and Land's End stations. Similarly, the apparent velocity given by the arrival times of any shot at the Scilly Isles, Land's End, Carnmenellis and Bodmin Moor stations is the apparent velocity in the opposite direction in the same region. The position and length of the reversed section depends on the critical distance which is the distance between the source and point of emergence of a ray which has been critically reflected at the Moho. It will be shown in a later chapter that this distance is about 65 km. Therefore the reversed portion extends from about 32 km WSW of the Scilly Isles to approximately 16 km ENE of the Land's End station, a distance of about 108 km.

Shot 3 was the only shot in the  $P_n$  range at all four stations. It gives an apparent  $P_n$  velocity in one direction of  $7.91 \pm .14$  km/sec. The Dartmoor data gives an apparent  $P_n$  velocity in the opposite direction of  $8.00 \pm .12$  km/sec. Therefore, within the error limits given there is no significant dip of the Moho beneath the region of the Scilly Isles and Land's End stations and the  $P_n$  velocity is not significantly different from the apparent velocity in the direction shots to stations. However, because only one shot was used to give the reversed velocity this estimate of real  $P_n$  velocity is not as accurate as that gained by using the four shots and stations. Thus the preferred estimate of real  $P_n$  velocity along line 1 is  $8.07 \pm .07$  km/sec.

The individual values of intercept time,  $P_g$  and  $P_n$  velocity for each station were substituted in the depth formula given at the beginning of this chapter and the results are given in table 3. The crustal thickness thus estimated assumes that the crust is homogeneous with the  $P_g$  velocity remaining constant throughout. It will be shown later that the velocity increases with depth within the crust resulting in a higher average crustal velocity and a corresponding increase in the crustal thickness. The results do not significantly differ from station to station. Thus the combined estimate of crustal thickness along line 1 is  $22.8 \pm 1.1$  km which will be a minimum estimate of the true crustal thickness in the vicinity of the stations.

Station	Depth
Dartmoor	21.55 $\pm$ 1.67km (P <sub>g</sub> vel. = 5.85km/sec assumed)
Bodmin Moor	22.96 $\pm$ 2.03km
Carnmenellis	24.16 $\pm$ 1.08km
Land's End	23.37 $\pm$ 2.32km
Scilly Isles	21.75 $\pm$ 3.97km

Table 3. Minimum depths to the Moho for stations along line 1

The small positive  $P_g$  intercepts indicate that the main crustal layer is covered by a layer of low velocity material, either weathered granite or sediments. Except at the end of the line where the sediments are assumed to reach about 2 km thickness, the low velocity material is calculated to be about 0.5 km thick, assuming a sedimentary velocity of 2.5 km/sec. This figure is an average one but it does show that only a thin veneer of a low velocity material exists along line 1 and, in subsequent interpretations of this line, it has been ignored.

### 3.3.3 Line 2 travel time graphs

The Land's End, Irish and Eskdalemuir stations only have been used in the analysis of line 2. Other stations received insufficient arrivals from the shots of this line to plot travel time graphs. The travel times have not been corrected for upper crustal delays.

#### (a) Waterford (fig.21)

The  $P_n$  segment is well-defined with an apparent velocity of  $8.6 \pm .09$  km/sec. The  $P_g$  segment shows that shots 42, 43 and 44 have progressively larger positive residuals but that residuals from shots 45 southwards are similar. All the shots giving  $P_g$  as a first arrival are situated in the region of the low Bouguer anomaly, interpreted as the westerly extension of a sedimentary basin in the Irish Sea (see section 3.2). Shots 42, 43 and 44

are situated over deepening parts of the basin so that the least squares  $P_g$  velocity of 5.88 km/sec may not be a good estimate of the  $P_g$  velocity in this region.

(b) Land's End (fig.21)

The scatter on the data from this station is large. It is all the more difficult to explain for the  $P_g$  segment when one notes that the travel times of the same shots fit a good  $P_n$  segment at the Irish station. The travel time of shot 31 has been ignored in the least squares analysis. At first sight both the  $P_g$  and  $P_n$  velocities would seem to be significantly different from those at the other end of the line. The possibility that this is not a correct assumption will be discussed in a later section.

(c) Eskdalemuir (fig.19)

All the shots from line 2 are in the  $P_n$  range. A least squares fit of all the data except shot 27 gives a  $P_n$  velocity of  $8.18 \pm .12$  km/sec. However, the scatter of the data makes it difficult to obtain a reliable estimate of the  $P_n$  velocity. The arrival from shot 27 is difficult to pick with certainty and its approximate position marks a discontinuity in the travel time graph which will be discussed later.

### 3.3.4 Interpretation of line 2 travel time data

The reason for the greater uncertainties in the velocities



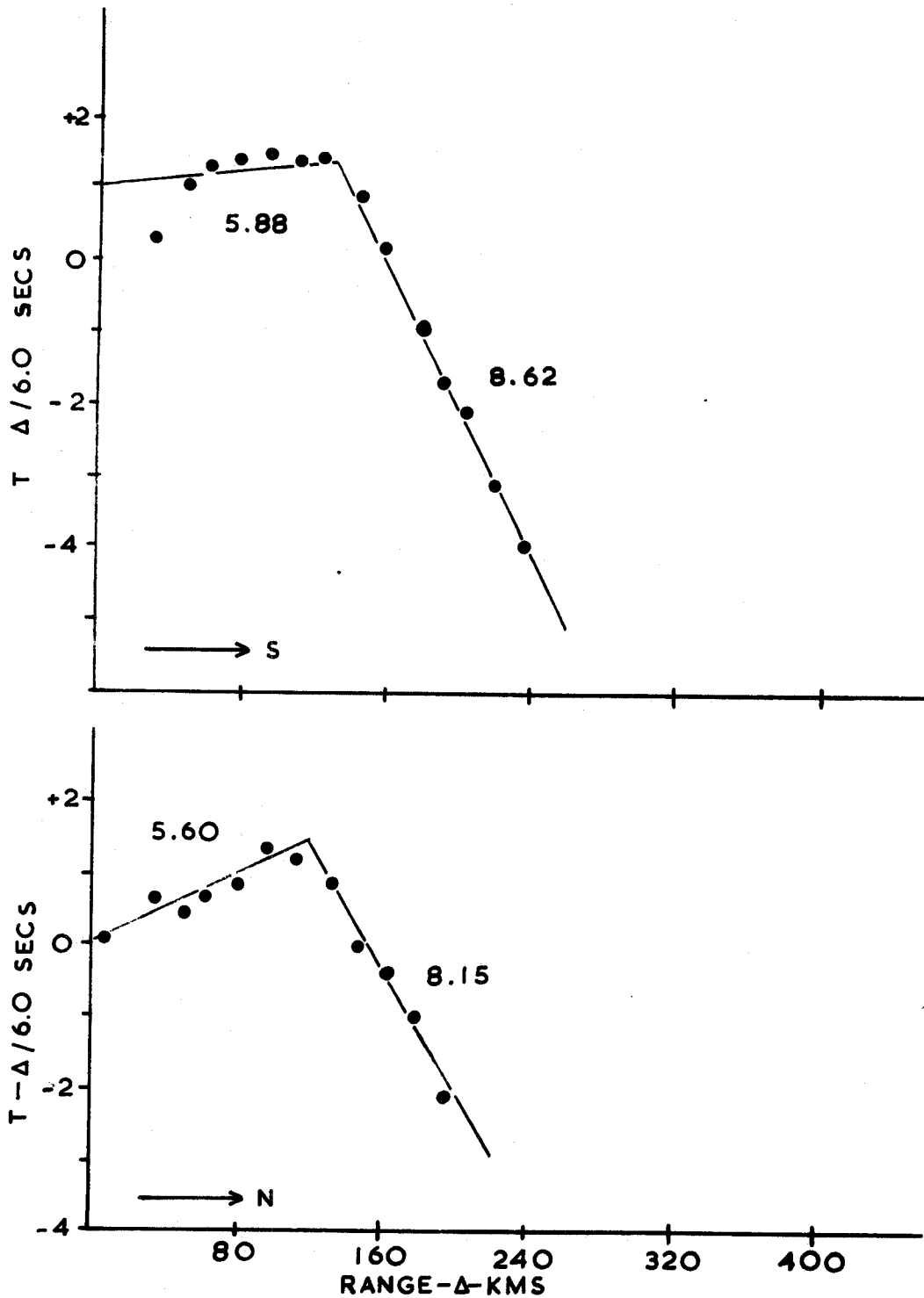


Fig.21. First arrival travel time graphs for the Waterford station (above) and the Land's End station for the line 2 shots (below).

given by the travel time data from this line can be found in the fact that the travel times have been uncorrected for upper crustal variation. The presence of the sedimentary basin in the northern half of the line creates a major problem in this respect.

There is not enough information available for more reliable estimates of these velocities to be obtained but at least some reasonable values can be assumed from the data of the northern half of the line in order to extract a little more information concerning the shape and depth of this basin. A  $P_g$  velocity of 5.9 km/sec and a  $P_n$  velocity of 8.1 km/sec have been assumed to calculate  $P_g$  and  $P_n$  residuals (observed - calculated) at the Irish, Land's End and Eskdalemuir stations for shots 42 to 24. The residual graphs, presented in fig.22, are similarly shaped confirming the fact that part, if not most, of the observed scatter is caused by variations in the upper crustal layers. If these variations are assumed to be due to varying thicknesses of low velocity material within a sedimentary basin, then estimates of the thicknesses of this material at each shot point can be obtained using the  $P_g$  residuals. The basin has been assumed to be basically wedge-shaped thickening in a southerly direction away from the Irish coast. The thicknesses thus obtained are shown in fig.22. These estimates can be increased or decreased by changing the sedimentary velocity or

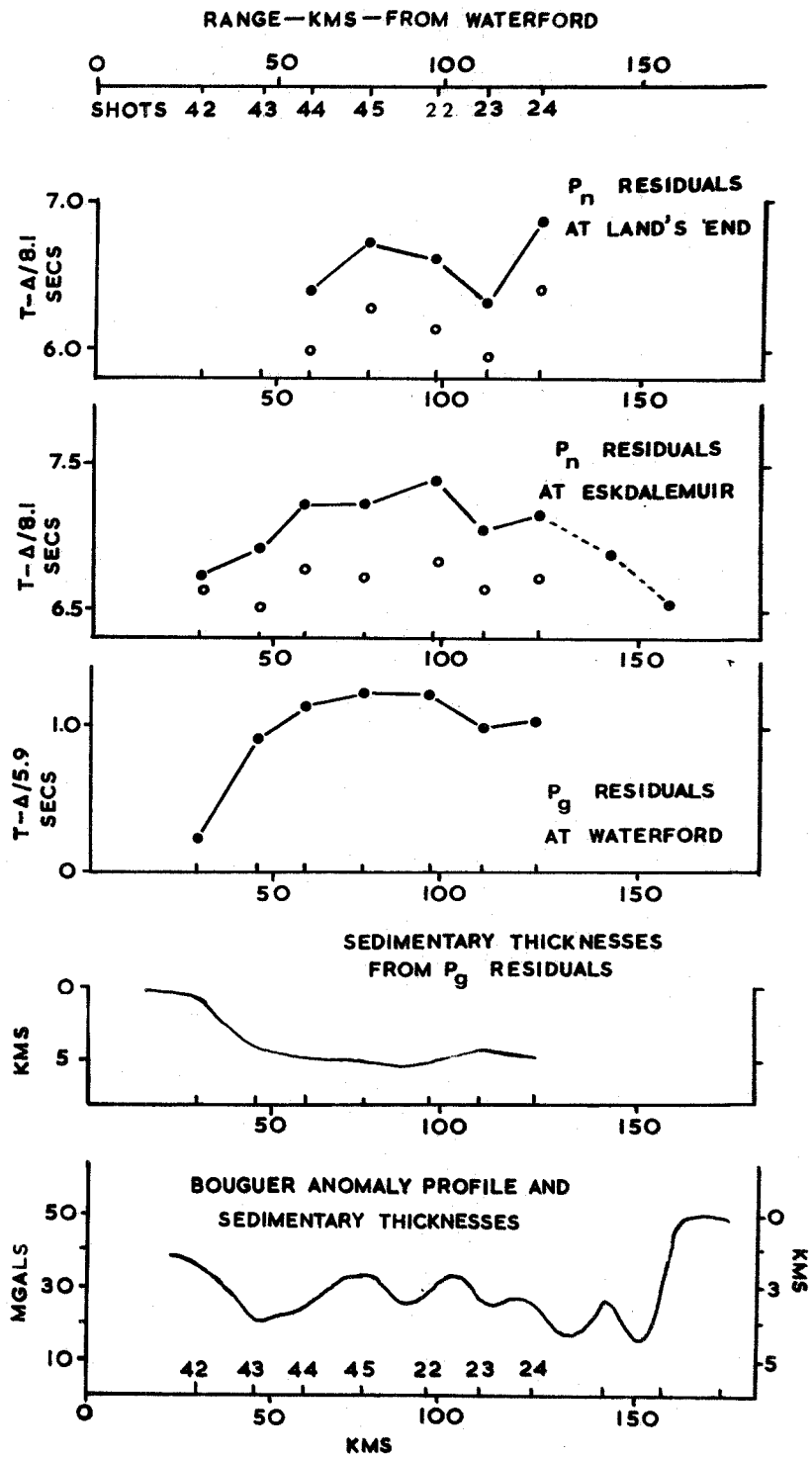


Fig.22. Residual data and an interpretation of the Bouguer anomaly profile along the northern part of line 2.

by assuming a different basic shape. However, the velocity of 3.0 km/sec is that indicated by Blundell et al (1968) and the assumption of a wedge-like shape would appear to be reasonable in this case. The apparent difference in shape and depth of the basin as revealed by the seismic data when compared with that given by the gravity data can be explained most probably by the fact that the gravity data has not been corrected for cross-coupling errors. However, the high frequency components seen superimposed upon the broad gravity low may be real and possibly due to shallow phenomena within the basin itself.

Assuming the sedimentary depths given by the  $P_g$  residuals then  $P_n$  delay times due to the presence of these sediments can be calculated for the Eskdalemuir and Land's End stations. If the observed arch-like shape of the residual graphs is due solely to the presence of the sedimentary basin then the subtraction of these delays from the  $P_n$  residuals should result in its total disappearance (see open circles on fig.22). For the Eskdalemuir data this would appear to be the case but for the Land's End data the shape is modified only slightly. This may be due to observational errors but it is equally possible that it could be real. The significance of this possibility will be discussed in a later chapter.

The unreliabilities of the  $P_n$  and  $P_g$  velocities obtained from the data of shots 25 to 21 are too large for

useful information to be extracted from residuals. The  $P_g$  velocity of 5.60 km/sec is suspiciously low when compared with the 5.8 km/sec velocity found by Merriweather (see Chapter 1 of this thesis). Shots 25 and 26 are situated over the southern margin of the sedimentary basin and thus arrivals from these shots will be delayed, weighting the  $P_g$  velocity estimate to a lower value. Therefore it is probable that the real  $P_g$  velocity is in excess of 5.6 km/sec. The geological similarities north and south of Land's End tend to suggest that the  $P_g$  velocities should be similar also. It will be shown in a later section that the  $P_g$  velocity south of Land's End is 5.8 km/sec and it is thought likely that this is a better estimate of the real  $P_g$  velocity along the southern part of line 2. The apparent difference of  $P_g$  velocity in the northern and southern regions of line 2 is therefore not thought to be as great as the travel time data would suggest.

The  $P_n$  velocity, as given by the travel time data at the Irish station, is unusually high. The travel times of arrivals from the shots of the southern half of line 2 at the Eskdalemuir station also form a higher velocity segment than the  $P_n$  value given by all the data from this station. On the other hand the  $P_n$  velocity seen at the Land's End station is more normal although the scatter of the data is large. This difference in  $P_n$  velocity as seen from the two ends of the

line may be explained by the presence of a dip of the Moho towards the north. However, the amount of dip and true  $P_n$  velocity are difficult to obtain with certainty because of two major problems. Firstly, the distance between the Irish and Land's End stations is not large enough to permit overlap of the two segments thus apparent velocities are seen for different regions of the line. (This problem is overcome to some extent when the Eskdalemuir and Land's End stations are used. In this case the  $P_n$  segments overlap in the region of shots 42 to 26 and thus the northern part of the line can be properly reversed.) Secondly, the standard errors on the apparent  $P_n$  velocities are large and the  $P_g$  velocity is not accurately known. However, assuming this velocity to be 5.8 km/sec, and that the Moho dips uniformly along the line of shots, the apparent velocities seen at the Irish and Land's End stations give a Moho dip of 1.5 degrees towards the north with a real  $P_n$  velocity of 8.35 km/sec. The Eskdalemuir and Land's End  $P_n$  velocities give a real  $P_n$  velocity of 8.22 km/sec and a Moho dip of 0.5 degrees in a northerly direction. In spite of the large uncertainties involved there is thus some evidence of a northward dipping Moho somewhere along line 2 with a slightly higher  $P_n$  velocity than that found along line 1. The fact that the gravity regional tends to decrease northwards along the northern half of the line is in agreement with a northward thickening crust in this region.

The above estimates of dip and sub-Moho velocity have been obtained assuming a homogeneous layer above the Moho with a velocity of 5.8 km/sec. The discontinuity in the region of shots 26 and 27 on the Eskdalemuir travel time graph has already been noted (see section 3.3.3). This discontinuity coincides approximately with the steep gravity gradient along the gravity profile described in section 3.2 which can be interpreted as being caused by the simple inwardly dipping, possibly fault bounded margin of the sedimentary basin. An alternative interpretation of this gradient may be that it is caused by a thrust from the south carrying denser material over less dense sedimentary material beneath (see fig.23). This

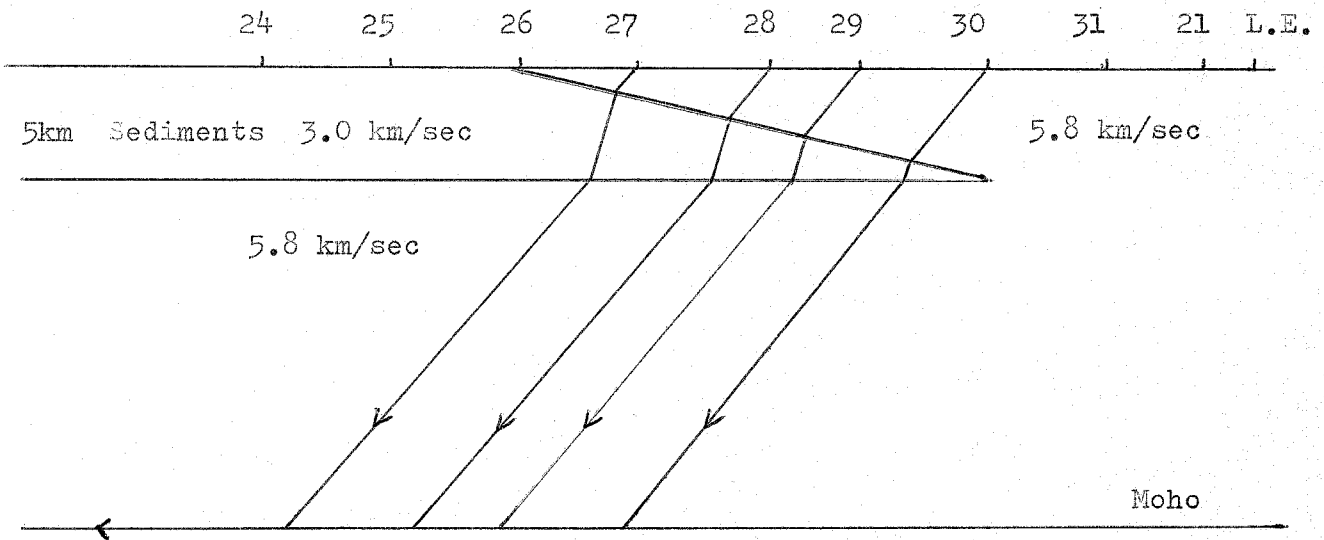


Fig.23. Suggested structure in the upper crust along the southern half of line 2.

gradient coincides with the approximate westward extension of the line of the gravity gradient over Exmoor described by Bott, Day and Masson-Smith (1958) and Al Sadi (1967). This has been interpreted by them to be a thrust which has carried the outcropping Devonian rocks northward across a large basin of Carboniferous and Devonian rocks.

A southward thickening wedge of higher velocity material resting on lower velocity material would have the effect of progressively decreasing the reduced travel times of seismic waves transmitted from shots situated on the wedge to the Irish and Eskdalemuir stations (see fig.23). This would result in an anomalously high value for the apparent  $P_n$  velocity as seen at these two stations. It is calculated that a real  $P_n$  velocity of 8.0 km/sec would become an apparent velocity of 8.6 km/sec at the Irish station if a wedge of high velocity material was present thickening from 0 to 5 km in the region between shots 26 and 30 at the expense of less dense sedimentary material beneath. Depending on the exact nature of the wedge, the Moho could then be flat-lying or slightly dipping in either direction at least along the southern half of line 2. The evidence for this suggestion of a thrust is tenuous but it is in the author's opinion that the seismic data from the region south of shot 26 may be better explained by such a complex structure than by the assumption of a Moho dipping uniformly along the length of line 2.



### 3.3.5 Line 3 travel time graphs

Arrivals recorded at the Land's End station and at the French stations 2, 3, 4, 5, 6, 7, 9 and 10 are presented here. No corrections for varying thicknesses of sediments have been incorporated in the travel time data.

#### (a) Land's End (fig.24)

The  $P_g$  and  $P_n$  segments are not at all obvious. Shots 39, 40 and 41 only are in the  $P_n$  range thus the least squares velocity of  $7.6 \pm .38$  km/sec is unreliable as the large standard error suggests. The  $P_g$  segment exhibits an offset between shots 35 and 36. The least squares  $P_g$  velocity using shots 32 to 39 is  $5.61 \pm .07$  km/sec and the reliability of this estimate will be discussed in a later section.

#### (b) French stations (fig.24)

The data available from these stations is severely limited by the poor quality of the seismograms. Paper records only were obtained and the outputs of the seismometers were not filtered before recording. Consequently, long period micro-seismic noise tends to obscure arrivals particularly of distant events.

Insufficient data is available from any one station to give a good estimate of the apparent  $P_n$  velocity. Therefore

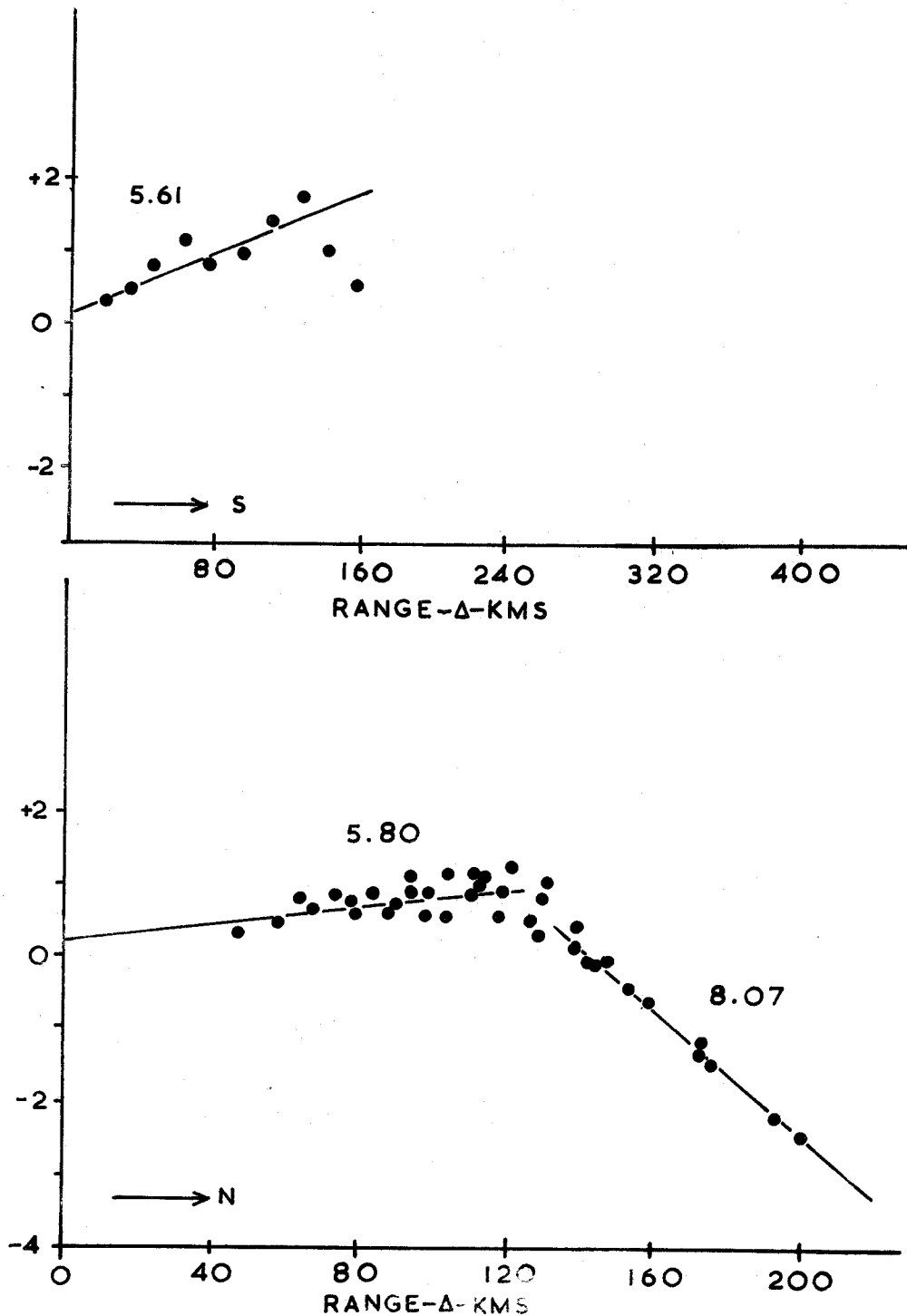


Fig.24. First arrival travel time graphs for the Land's End station for the line 3 shots (above) and the French stations (below).

all the  $P_n$  arrivals have been plotted on a single graph to which a straight line segment has been fitted by least squares. This gives an estimate of the real  $P_n$  velocity assuming that the Moho is a uniformly dipping plane surface. The  $P_n$  velocity is thus estimated to be  $8.07 \pm .05$  km/sec although the reliability of this value is probably not as good as its standard error would suggest.

Apparent  $P_g$  velocities were obtained by fitting least squares lines to the data of the French stations 2, 3, 4, 5 and 6. These gave velocities of about 5.7 km/sec. It is known from the geology of the area that the thickness of low velocity material increases generally northwards from the Brittany coast. This velocity estimate will, therefore, be anomalously low. The velocity obtained from least squares fits of the travel times of arrivals from individual shots to several stations is approximately 5.85 km/sec. This is an estimate of the apparent  $P_g$  velocity in the direction stations to shots. A least squares fit of all the  $P_g$  data gives a velocity of  $5.80 \pm .07$  km/sec. This is assumed to be the best estimate of the real  $P_g$  velocity available from the data.

### 3.3.6 Interpretation of line 3 travel time data

A study of the  $P_n$  residuals from the least squares straight line shows that they are all less than  $\pm 0.1$  sec

which would suggest that the Moho is not dipping significantly. Revoý (1969) concluded from a more sophisticated study of the data that there is no significant dip of the Moho in the region between shot 38 and the French station 7. The author would extend the regions beneath which there is a flat-lying Moho to include most of the shots from line 3 and adds that there is no significant difference between the sub-Moho velocity along this line and along line 1.

Assuming a  $P_g$  velocity of 5.8 km/sec and a  $P_n$  velocity of 8.07 km/sec, the estimate of minimum thickness of the main crustal layer is calculated to be  $22.5 \pm 1.8$  km. This is an estimate of the average thickness of the main crustal layer from the position of shot 33 to the French station 10. It has been shown that the thickness of the low velocity sedimentary material is expected to be of the order of 3 km in the central part of the line of shots thinning to zero thickness near the French coast. The travel time data have not been corrected for this variation and, although attempts have been made to obtain reversed  $P_n$  and  $P_g$  velocities, the values thus obtained may be slightly in error. The overall effect will be that the minimum estimate of thickness of the main crustal layer given above will tend to be an overestimate in the region of the shots and an underestimate in the region of the stations, i.e. the depth to the bottom of the main crustal layer is

probably constant but the thickness of the layer is decreased at the expense of the low velocity sedimentary material in the region of the shots.

In order to elucidate the structure of the uppermost crustal layers along line 3,  $P_g$  and  $P_n$  residuals have been calculated in a similar manner to those for line 2. A few observations of the shots from the northern end of the line recorded at the Scilly Isles and Bodmin Moor stations are also used here. It is found that if the  $P_g$  velocity is assumed to be 5.6 km/sec for the northern end of the line then some of the residuals at the Scilly Isles, Land's End and Bodmin Moor stations are negative. A velocity of 5.8 km/sec is required to make all these residuals positive and it is concluded that this is a better estimate of the real  $P_g$  velocity in the northern part of line 3. It is thus not significantly different from that found in the south. Therefore a  $P_g$  velocity of 5.8 km/sec and a  $P_n$  velocity of 8.0 km/sec have been assumed for the calculation of the residuals which are presented in fig.25.

The  $P_g$  residual graphs of all stations for shots 32 to 37 exhibit a similar shape. Arrivals from shots 34 and 35 are delayed relative to the other shots. This delay is real because of the similarity at all stations. The variability may be explained by the azimuthal variation of the direction between shots and stations and by the presence of observational errors.

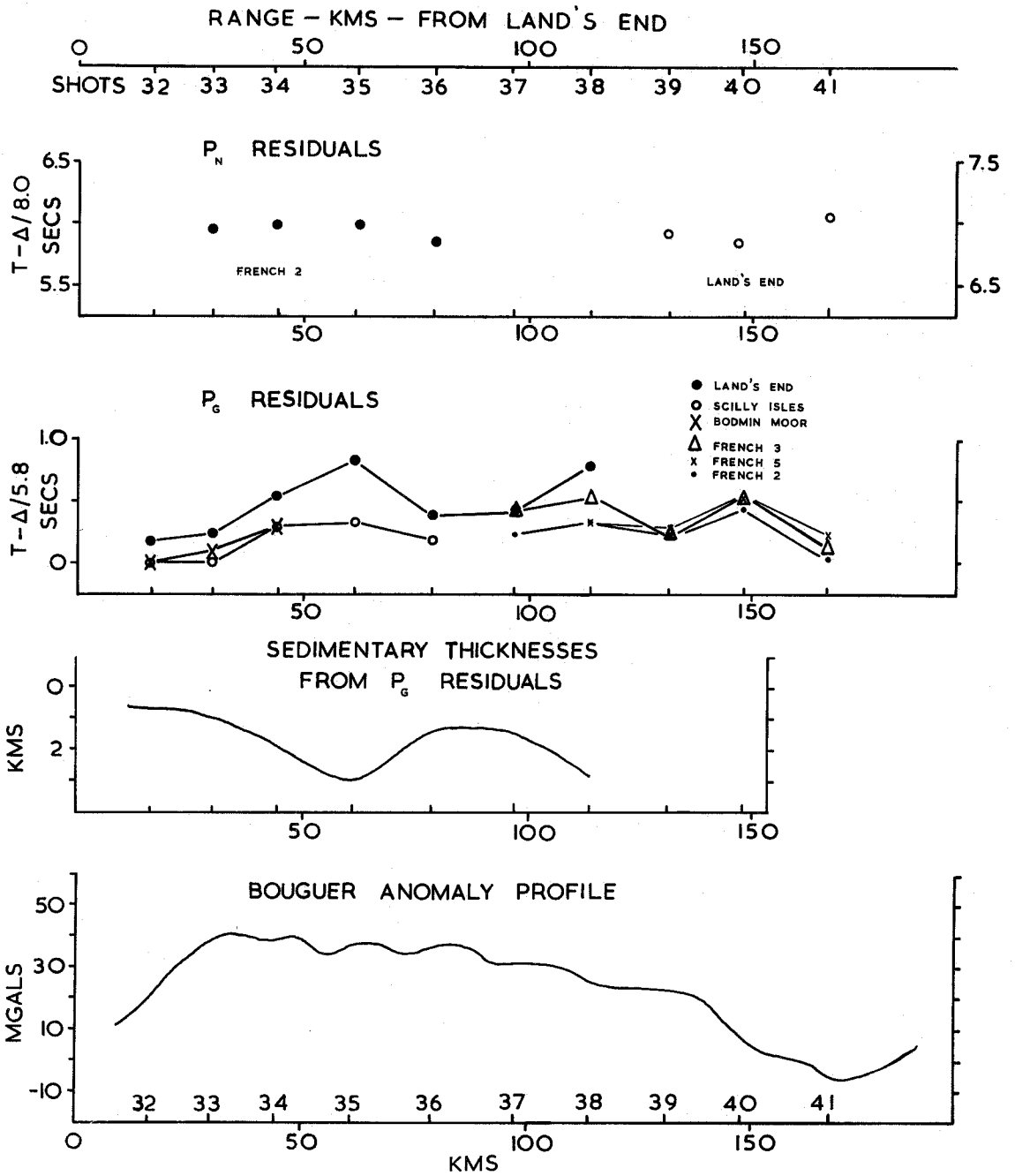


Fig.25. Residual data from line 3.

The interpretation of this shape in terms of variation in velocity - depth structure is not a simple one. It is possible that it could reflect the topography of the basement beneath changing thicknesses of low velocity but homogeneous sediment. Fig.25 presents such an interpretation. A sedimentary layer with a velocity of 3.0 km/sec is assumed to be resting on an undulating basement surface. The thickness of the sediments increases southwards to reach a maximum near shot 35. The sedimentary basin then thins considerably beneath shots 36 and 37. A study of the literature dealing with sedimentary depths in this region reveals that the cone of critically refracted waves from shot 36 is situated over what is postulated to be the deepest part of a sedimentary basin extending along the English Channel (see Day et al 1956, Hill and Vine 1965). Even allowing for inconsistencies in the data of Day et al, due mainly to non-reversal of the refraction lines at many of the seismic stations, it would be difficult to postulate that there is a basement rise in the region of this shot. Thus an alternative explanation must be found.

The work of Day et al (1956) on the depths of boundaries within the sedimentary sequence shows that a saddle-like structure occurs above the basement in the region under study. It is postulated that the residual graph shape

described above is due to the increased thickness of relatively high velocity Palaeozoic rocks at the expense of low velocity Mesozoic rocks and possibly of basement material in the region south of shot 35. There are so many variables in this picture that any attempt to estimate relative thicknesses from the south west England experiment data is unwarranted.

The  $P_g$  residual graphs for the French 2, 3 and 5 stations also exhibit a similarity of shape. The other French station graphs, although similar, have not been included for the sake of clarity. Very little can be inferred from the pattern of the residuals because there is no azimuthal variation in the stations giving these graphs. The relative delays are small enough to be completely explained by shot position errors. In fact, the completely opposite trend exhibited by the Land's End  $P_n$  residuals would tend to confirm that this is the case.

#### 3.4 Time terms

The time term approach to the interpretation of seismic refraction data, originally described by Schiedegger and Willmore (1957) and Willmore and Bancroft (1960), has been used in the analysis of data from several seismic refraction experiments, notably by Berry and West (1966a) with a later re-interpretation by O'Brien (1968), by Smith,



Steinhart and Aldrich (1966) and by Blundell and Parkes (1968). The method was applied to the first arrival travel time data collected from the south west England experiment using the computational technique described by Berry and West (1966a) and programmed for the IBM 360/67 computer. A description of the programme and listing appears in Appendix E.

As has already been indicated, an examination of the travel time curves shows that the travel time data can be divided into two groups, each of which is associated with a particular refracting horizon. Each travel time observation can be divided into three parts; firstly, the time taken for a seismic wave to travel from a shot to a detector at the sub-refractor velocity, neglecting the presence of the upper layer; secondly and thirdly, the delays introduced in the vicinity of the shot and station by the seismic waves travelling at a lower velocity down to and up from the refracting horizon. Within each group, therefore, the travel time data between a system of shots and stations can be fitted by a series of equations of the type

$$T_{ij} = \Delta_{ij}/v + a_i + b_j ,$$

where  $T_{ij}$  = the theoretical travel time between the  $i$  th shot and the  $j$  th station,

$v$  = velocity below the refractor,

$a_i$  =  $i$  th shot time term,

$b_j$  =  $j$  th station time term.

In an experiment involving  $n$  shots and  $m$  stations it can be seen that a maximum of  $n \times m$  travel time observations is possible. In practice some of these observations will not be made. However, there will be substantially more observations than the  $n + m$  number of time terms and one velocity which are the unknowns. Thus it is possible to apply the method of least squares to find a set of  $n + m$  time terms and, optionally, the velocity  $v$  which best fit the above system of equations. There is a problem in that the solution thus gained will not be unique with the time terms being determined only to within an additive constant. One important requirement, therefore, in the time term approach involves the physical interchange of at least one shot and station position or the arbitrary assignment of a numerical value to one of the time terms.

For the south west England experiment shot 21 was exploded on granite within 6 km of the Land's End station. Shot 13 was exploded similarly with respect to the Scilly Isles station. These two pairs were thus used to satisfy the interchange requirement.

Before the results are presented it must be emphasised that the use of the time term approach for the interpretation of the south west England data is questionable for several reasons. Firstly, implicit in the method is the assumption that the velocity beneath the refractor is constant. We have

seen that there is some evidence from the data that this is not the case as far as the south west England experiment is concerned. A possible higher  $P_n$  velocity is indicated along line 2 when compared with line 1. Secondly, the distribution of shots and stations is not ideal for such an approach. The method requires a distribution such that fully reversed coverage in the vicinity of each shot and station is acquired. In this way true subrefractor velocities are obtained. Unbiased time term values, except those representing points near the periphery of the configuration of shots and stations, can then be calculated and any trends exhibited by the time terms will be real. For the south west England experiment it has been shown that some portions of the refraction lines are not properly reversed. This is especially the case for the  $P_g$  travel time data where short sections of line 1 only are reversed in the required manner. Thirdly, the potential number of observations has been considerably reduced for the various reasons which have already been mentioned in Chapter 2. Thus in several cases there is only one observation of a particular shot. The effect of these problems will be seen in the results of the analysis.

The data were divided into two groups, one representing  $P_g$  arrivals and the other,  $P_n$  arrivals. Doubtful data such as the observation of shot 13 at the Carnmenellis station were removed and travel time data uncorrected for the thickening

wedge of sediment at the end of line 1 were used. The formulae given by Berry and West are used to give estimates of the statistical uncertainties inherent in the time terms. The standard deviations quoted represent the inconsistency of the data contributing to the individual time term while the standard errors represent the unreliabilities of the time terms themselves. Because of the problems enumerated above these are minimum uncertainties. If the assumptions inherent in the method are applicable to a particular set of data then they can be regarded as reliable but if there is any violation of the assumptions then anomalous trends will occur in the time terms which will not be apparent in the uncertainty estimates. Solutions leaving the velocity as an unknown to be determined by the least squares process were obtained for each data set as well as solutions obtained by constraining the velocity to a number of fixed values. The fit of the time term model to the observational data was measured by using the standard deviation of the solution as given by Berry and West.

#### P<sub>g</sub> solution

A list of the P<sub>g</sub> time terms and the sub-refractor velocity is given in table 4. The velocity obtained was derived from the least squares process as one of the unknowns. A set of constrained velocities was used to indicate the change in the goodness of fit of the model to the observational data

Table 4.

P<sub>g</sub> time terms

Refractor velocity = 5.82km/sec      Standard deviation of the  
 solution = 0.2sec

Shot/station name	Time term sec	Standard deviation	Standard error	No. of obs.
Shot 5	Line 1	0.07		1
6	"	-0.07		1
7	"	-0.16		1
8	"	0.07		1
9	"	-0.17	0.02	2
10	"	-0.08	0.04	3
11	"	0.0	0.02	3
12	"	-0.08	0.01	3
Scilly Isles	"	0.01	0.19	27
Shot 14	"	0.13	0.05	3
15	"	-0.12	0.55	4
16	"	0.06	0.06	4
17	"	0.06	0.07	4
18	"	0.03	0.04	4
19	"	0.22	0.23	2
20	"	0.15	0.13	4
Land's End	"	0.08	0.14	28
Carnmenellis	"	0.09	0.34	10
Bodmin Moor	"	-0.03	0.14	15
Waterford	Line 2	0.12	0.0	8
Shot 42	"	0.03		1
43	"	0.69		1
44	"	0.87		1
45	"	0.89		1
22	"	0.87		1
23	"	0.61		1
24	"	0.66		1
25	"	0.55	0.0	2
26	"	0.74		1
27	"	0.21	0.15	3
28	"	0.39	0.24	3
29	"	0.12	0.20	3
30	"	0.24	0.18	3
31	"	-0.34	0.07	3
Land's End	"	0.08	0.14	28
			0.03	

Table 4 (Contd.)

P<sub>g</sub> time terms

Refractor velocity = 5.82km/sec

Standard deviation of the  
solution = 0.2sec

Shot/station name	Time term sec	Standard deviation	Standard error	No. of obs.
Land's End Line 3	0.08	0.14	0.03	28
Shot 32 "	0.07	0.06	0.03	3
33 "	0.13	0.10	0.06	3
34 "	0.41	0.10	0.06	3
35 "	0.56	0.27	0.19	2
36 "	0.30	0.08	0.06	2
37 "	0.45	0.08	0.06	2
38 "	0.71	0.06	0.03	4
39 "	0.46	0.05	0.02	4
40 "	0.63	0.08	0.03	6
41 "	0.38	0.07	0.03	6
French 2 "	-0.23	0.06	0.03	5
3 "	-0.15	0.06	0.03	4
4 "	-0.16	0.05	0.02	4
5 "	-0.07	0.05	0.03	3
6 "	-0.43	0.20	0.14	2
7 "	-0.24	0.01	0.01	2

as a function of the velocity (see fig.26). However, the shot - station configuration is not of the type necessary to obtain good velocity control (see Parks 1967). For this reason this  $P_g$  solution must be assumed to be unreliable, although the subrefractor velocity and time term values seem to be of the right order in most cases.

#### $P_n$ solution

Two  $P_n$  solutions were attempted. Firstly, one including the data from the line 3 shots and French stations and, secondly, excluding them. The results from each solution are presented in tables 5 and 6. Once again the velocities obtained were derived from the least squares process as one of the unknowns. It was noticed in the first solution that all the French station time terms were considerably less than the line 3 shot time terms. The difference is large enough to be assumed unreal and to be due to the poor control of velocity that is obtained along this line. Several stations are situated at one end of a line of shots and only four observations of those shots are seen from the other end of the line. A weighting system could be devised to off-set this problem but as there are only four observations from the one direction it was not thought worthwhile. Therefore the line 3 and French stations data were abandoned for the second solution.

Table 5.

P<sub>n</sub> time terms, first solution

Refractor velocity = 8.04km/sec

Standard deviation of the solution = 0.23sec

Shot/station name	Time term sec	Standard deviation	Standard error	No. of obs.	
Shot 1	Line 1	3.74	.11	.07	3
2	"	3.41	.09	.05	3
3	"	3.07	.13	.06	5
4	"	3.17	.02	.01	2
5	"	3.20	.08	.05	3
6	"	3.02	.11	.06	3
7	"	3.26	.16	.08	4
8	"	3.10	.05	.02	5
9	"	2.86	.01	0	2
10	"	2.77			1
11	"	2.80	.22	.15	2
12	"	2.75	.04	.03	2
Scilly Isles	"	2.75	.07	.03	7
Shot 14	"	2.86	.07	.04	3
15	"	2.96	.01	.01	2
16	"	3.01	.19	.13	2
17	"	2.78	.03	.02	2
18	"	2.84			1
19	"	2.79			1
20	"	2.85			1
Land's End	"	2.63	.14	.03	16
Carmenellis	"	3.00	.06	.02	8
Bodmin Moor	"	2.94	.23	.06	14
Dartmoor	"	2.79	.10	.03	13
Eskdalemuir Line 2	"	3.06	.17	.05	13
Waterford	"	3.17	.16	.05	12
Shot 42	"	3.26			1
43	"	3.42			1
44	"	3.65	.09	.06	2
45	"	3.83	.16	.11	2
22	"	3.66	.35	.20	3
23	"	3.48	.07	.05	2
24	"	3.73	.29	.21	2
25	"	3.49	.19	.11	3
26	"	3.33	.46	.32	2
27	"	3.52	.35	.24	2
28	"	3.37	.20	.14	2



Table 5. (Cont.)

P<sub>n</sub> time terms, first solution

Refractor velocity = 8.04km/sec

Standard deviation of the solution = 0.23sec

Shot/station name	Time term sec	Standard deviation	Standard error	No. of obs.
Shot 29 Line 2	3.37	.05	.04	2
30 "	3.12	.19	.13	2
Land's End "	2.63	.14	.03	16
Land's End Line 3	2.63	.14	.03	16
Shot 33 "	4.38			1
34 "	4.43			1
35 "	4.48	.12	.06	4
36 "	4.25	.16	.08	3
37 "	4.23	.34	.24	2
38 "	4.70	.10	.06	3
39 "	4.54	.26	.18	2
40 "	4.49	.30	.17	3
41 "	4.83	.56	.33	3
French 2 "	1.65	.02	.01	3
3 "	1.65	.11	.08	2
4 "	2.15	.34	.24	2
5 "	1.58	.21	.12	3
7 "	1.57	.16	.09	3
9 "	1.74	.19	.13	2
10 "	1.27	.37	.21	3

Table 6.

 $P_n$  time terms, second solution

Refractor velocity = 8.05km/sec

Standard deviation of the solution = 0.17sec

Shot/station name	Time term sec	Standard deviation	Standard error	No. of Obs.	
Shot 1	Line 1	3.72	.09	.05	3
2	"	3.39	.10	.06	3
3	"	3.09	.16	.07	5
4	"	3.13	.01	.01	2
5	"	3.21	.02	.01	3
6	"	3.04	.05	.03	3
7	"	3.28	.18	.09	4
8	"	3.11	.05	.02	5
9	"	2.90	.05	.04	2
10	"	2.85			1
11	"	2.85	.25	.18	2
12	"	2.80	.07	.05	2
Scilly Isles	"	2.79	.06	.02	7
Shot 14	"	2.90	.05	.03	3
15	"	2.98	.01	.01	2
16	"	3.04	.18	.13	2
17	"	2.80	.03	.02	2
18	"	2.86			1
19	"	2.81			1
20	"	2.86			1
Land's End	"	2.72	.10	.03	13
Carmenellis	"	3.03	.06	.02	8
Bodmin Moor	"	2.89	.13	.04	13
Dartmoor	"	2.79	.11	.03	13
Eskdalemuir	Line 2	3.16	.16	.05	13
Ireland	"	3.20	.15	.05	12
Shot 42	"	3.23			1
43	"	3.40			1
44	"	3.61	.12	.08	2
45	"	3.79	.13	.09	2
22	"	3.66	.29	.17	2
23	"	3.44	.04	.03	2
24	"	3.69	.25	.18	2
25	"	3.51	.19	.11	3
26	"	3.32	.47	.33	2
27	"	3.51	.34	.24	2
28	"	3.38	.19	.13	2
29	"	3.38	.04	.03	2
30	"	3.12	.18	.13	2
Land's End	"	2.72	.10	.03	13

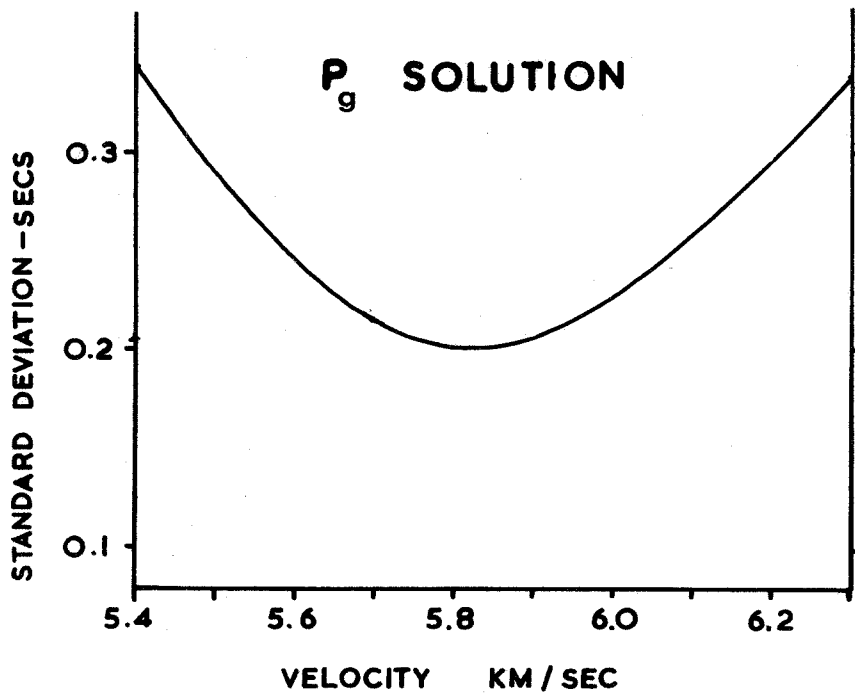
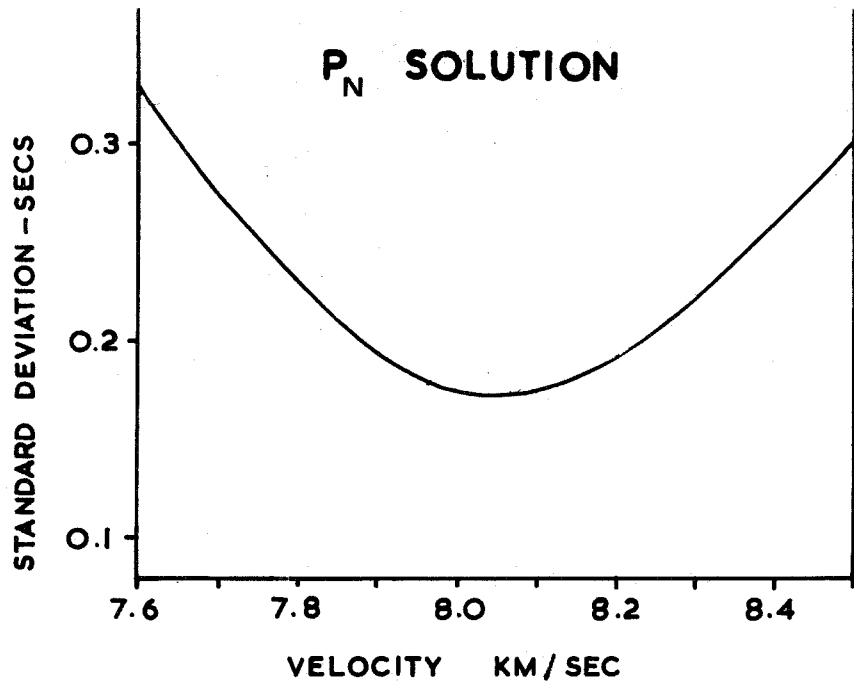


Fig.26. The standard deviation of the solution versus the refractor velocity for the P<sub>n</sub> (2nd solution) and P<sub>g</sub> time term solutions.

This has little effect on the remaining time terms which reflects the poor interrelatedness of the data from line 3 with that from the other lines. The subrefractor velocity is changed very little but the standard deviation of the solution is greatly improved. A set of constrained velocities was applied to the data in a similar manner to that of the  $P_g$  data. The resulting changes of standard deviation with velocity are given in fig.26. The shot-station configuration is better as far as this solution is concerned but there is still a possible problem of subrefractor velocity variation. However, the results from this solution are assumed to be reliable enough for the observed trends to be real.

The time terms are seen to increase generally towards the west along line 1. This is almost certainly due to the effect of the wedge of sediments at the western end of the line. The time terms are also relatively large in the northern half of line 2 reflecting the delay times introduced by the presence of the sedimentary basin in this region.

Unfortunately the structure of the upper crustal layers is not well enough known for these time terms to be converted to depths. A more reliable evaluation of the  $P_g$  time terms would have been useful in this respect. However, a feature of the time term approach is that data from different experiments distributed through time can be combined together as long as

some of the station or shot positions are re-occupied. When the velocity-depth distribution throughout the region is known in more detail than the data from the south west England experiment may be used in conjunction with the new data to give even better estimates of the time terms and of the depths they represent.

## CHAPTER 4

The results described so far have been those derived from the analysis of first arrival travel time data only. They are important in that they form the foundation upon which the final interpretation of all the data will be based. First arrival onsets are the least ambiguous of those along a seismic record and thus the reliability of these results should be well known. However, a study of later arrivals is necessary if a complete and fully meaningful interpretation is to be accomplished.

The problem of recognising discrete phases and of picking their onset times is increased by the presence of a high background of noise which is usually present along a seismic record after the first arrival. This is mainly due to the presence of signal generated noise produced by the local structure immediately in the vicinity of the shot and station. When teleseismic waves are involved, the noise may form recognisable phases which can be traced from one detector to the next (Key 1967, 1968). In explosion seismology such coherence is unusual. The noise typically consists of isolated bursts of energy with no lasting character from detector to detector.

This chapter describes methods which have been used to process later, as well as first, arrivals on the records. The results are presented and used with those obtained from

the first arrival travel time data to give an overall interpretation in terms of velocity - depth structure.

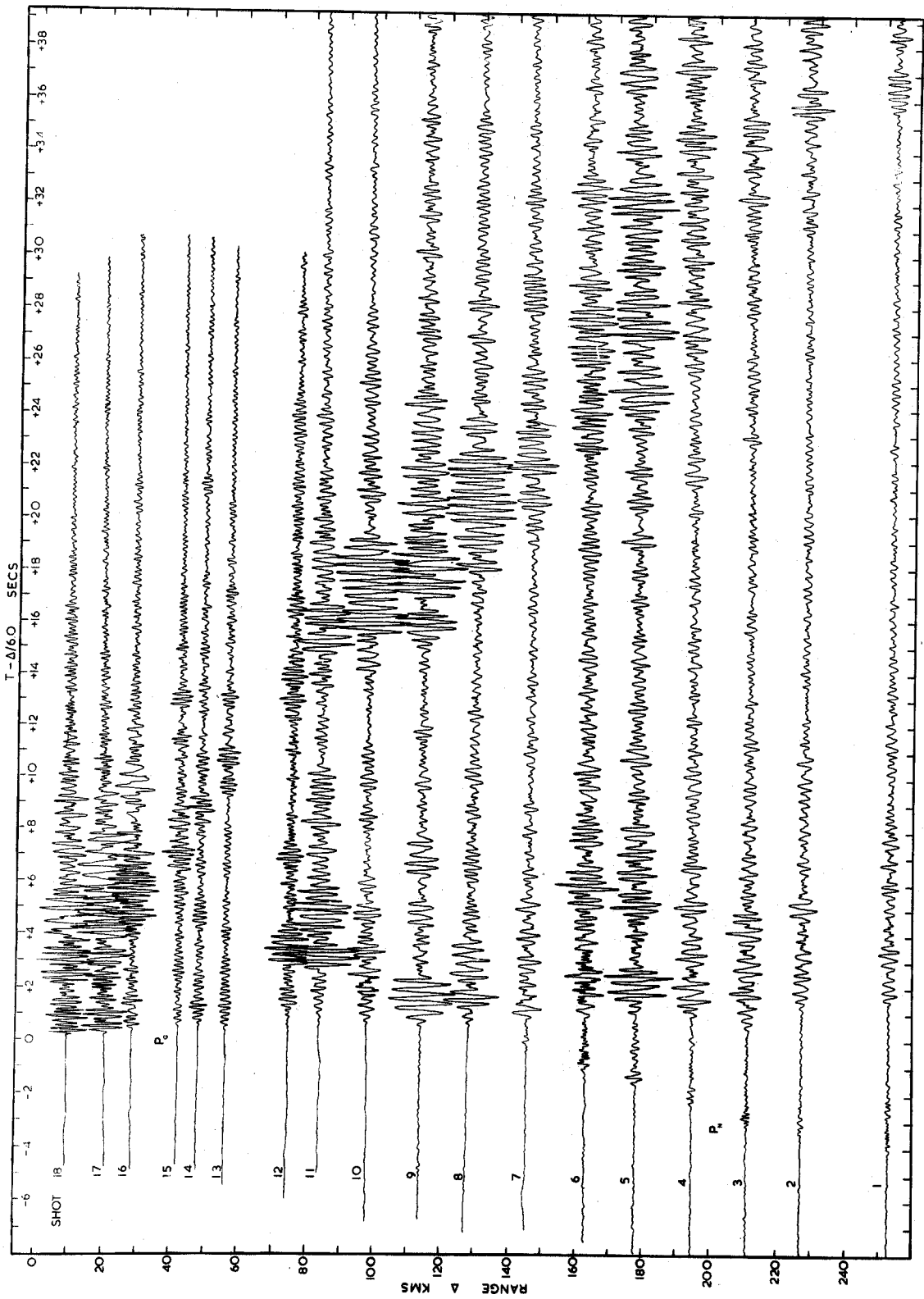
#### 4.1 Stacked records

The stacked records, prepared in the manner described in Chapter 2, can give a complete picture of all the arrivals seen at each particular station. If certain phases can be correlated over large distances from trace to trace then it is fairly certain that they are important and worthy of further inspection. Any isolated bursts of energy can be recognised and eliminated as far as the broad interpretation is concerned. The stacked records are therefore used to indicate persistent secondary phases, a study of which can improve the overall interpretation of the data.

A study of these records reveals a basic pattern of arrivals which is common to all of them. There are minor variations but the overall picture presented by each record is remarkably consistent especially for the line 1 shots. As an example, the record of the shots of line 1 as received at the Land's End station is shown in fig.27. Stacked records of the line 1 shots at the Scilly Isles, Bodmin Moor and Carnmenellis stations, the line 2 shots at the Waterford and Land's End stations, and the line 3 shots at the Land's End and French stations will be presented in the following sections.

Fig.27. The stacked record of the line 1 shots at the Land's End station.





The major feature of all these records, as exemplified by that shown in fig.27, is the presence of a large amplitude secondary arrival which appears abruptly at a distance of about 60-80 km and at a reduced time ( $T - \Delta/6.0$ ) of about +2 to +3 seconds (see trace of shot 12 on fig.27). In nearly all cases this arrival can be correlated from shot to shot and at greater distances becomes the first large amplitude arrival after the  $P_n$  arrivals. On most records many other phases arrive within a few seconds after the  $P_g$  and  $P_n$  phases at distances greater than about 80 km but there is no other phase which is as persistent as this large amplitude secondary phase. Shear waves are present on most records running diagonally across them and they exhibit several features which will be described in later sections. Surface waves are present on the traces of near shots at most stations but their periods are less than one second and are of little use for interpretation purposes.

The author is aware that other important phases are probably present on these records but their interpretation is always ambiguous. It will be shown that there is no ambiguity in the interpretation of the large amplitude secondary arrival and thus the rest of this chapter is mainly concerned with this arrival and its use in the interpretation of the data from the south west England experiment.

## 4.2 Amplitude measurements

In many refraction experiments described in the literature little attention is paid to the amplitude characteristics of the various phases, except for a few notable exceptions (Berry and West 1966b, Roller 1965, Richards 1960, Werth, Herbst and Springer 1962). A study of the problems involved helps to explain this omission but the author believes that some attempt should be made to reconcile the amplitude-distance relationships of the various phases to the crustal models proposed.

The problems of amplitude measurement and interpretation are described in detail by Steinhart and Meyer (1961). The main problems are those due to instrumental characteristics, changing source conditions and local variations in the vicinity of the detectors. For the south west England experiment the problem of changing source conditions is minimised by the fact that all the shots were of the same size, they all exploded on the sea bed and none of them 'blew out'. There are still problems of variation of lithology with consequent different coupling characteristics at each shot point but this is not thought to be of major importance. The effects of local variations in the vicinity of the detectors are minimised if the amplitude measurements are always taken from one seismometer and as far as this

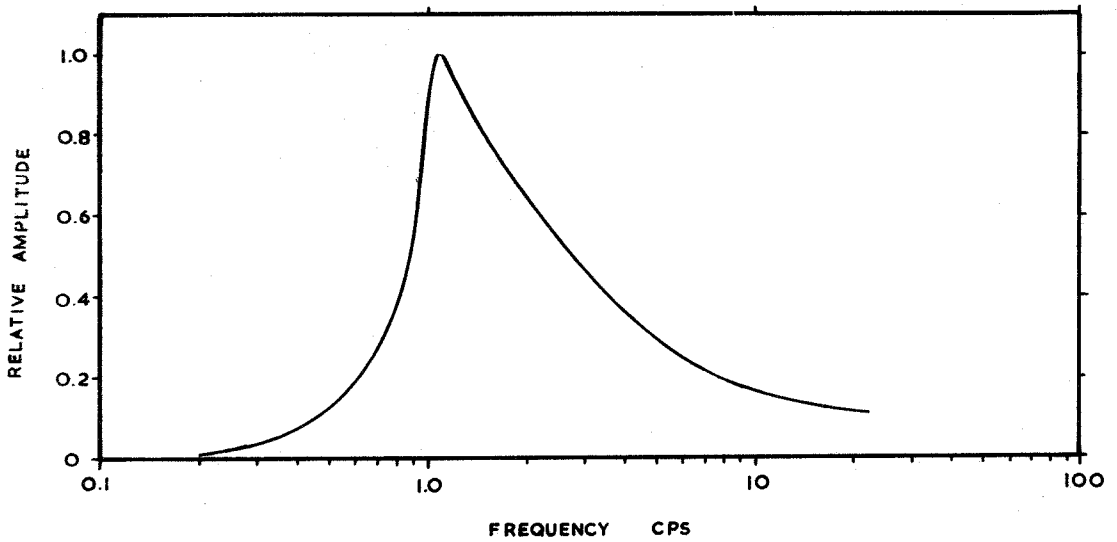
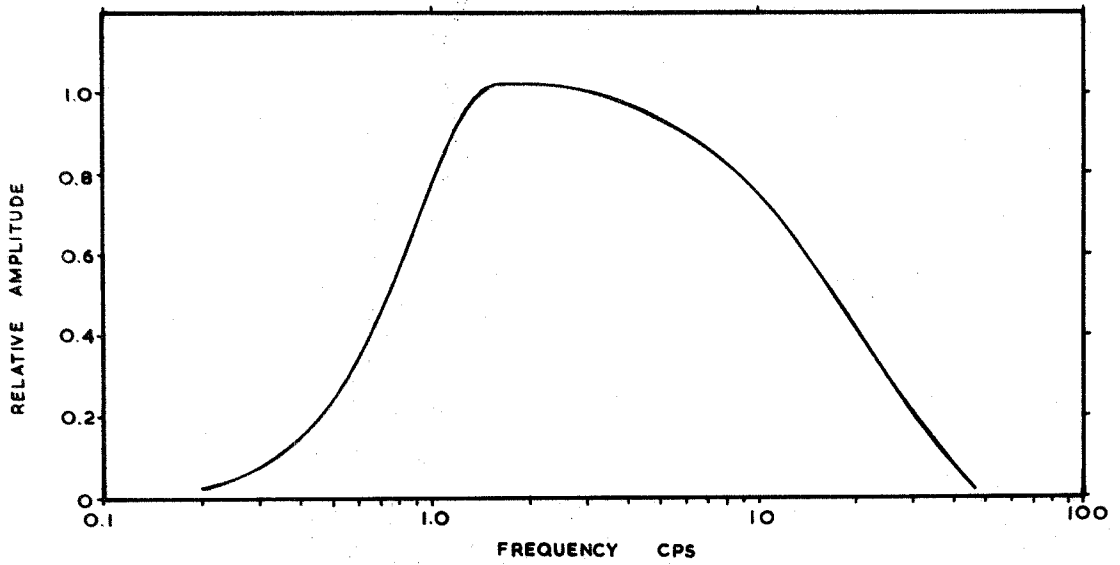


Fig.28. Frequency responses of the recording systems at the Scilly Isles station (above) and at the Carnmenellis and Bodmin Moor stations (below).

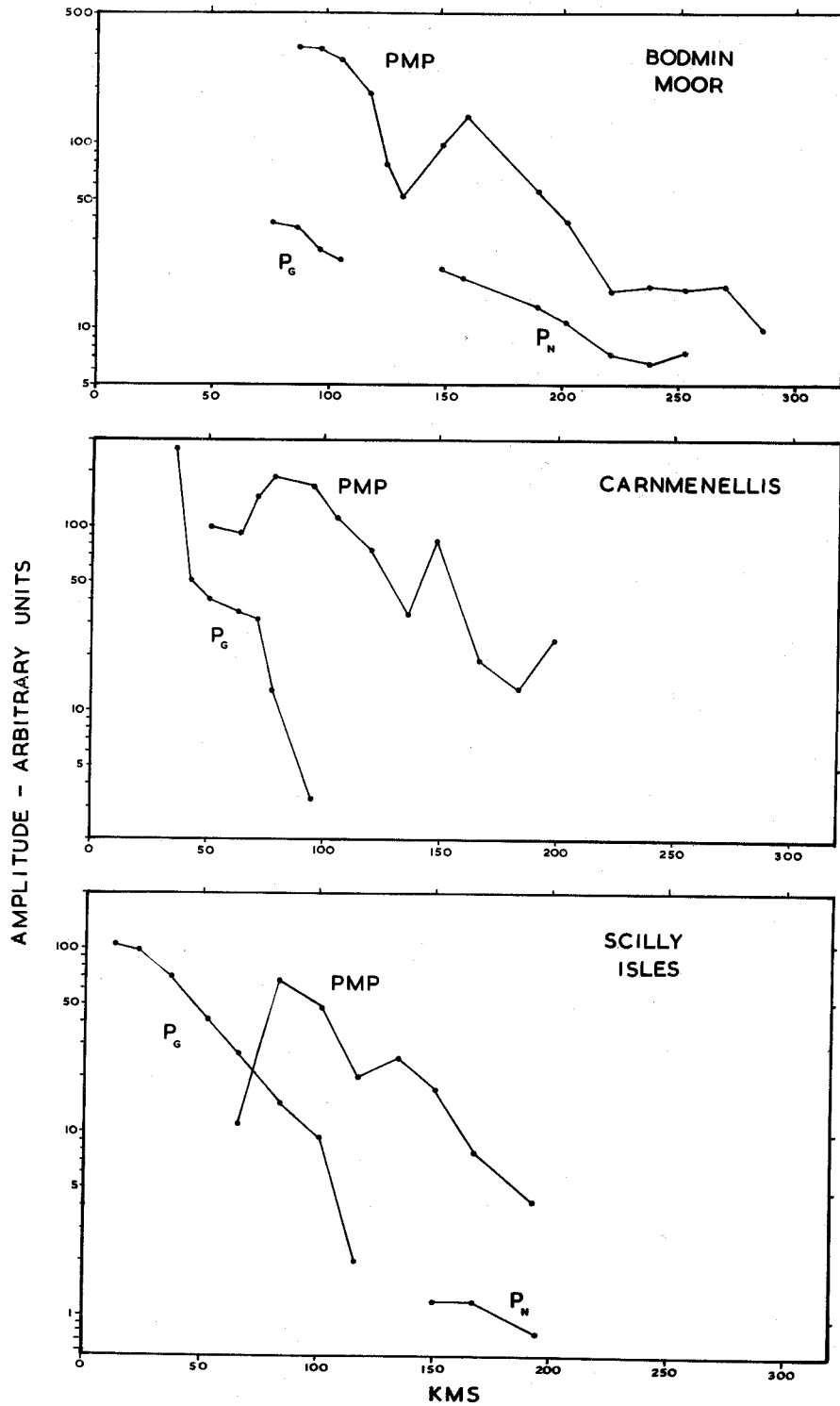


Fig.29. Amplitude-distance graphs for various phases at the Bodmin Moor, Carnmenellis and Scilly Isles stations.

experiment is concerned, it is thought that the major problem is the instrumental one. The frequency response of the system at the Scilly Isles is well known (see fig.28), but the frequency response curve for the system at the Bodmin Moor and Carnmenellis stations has had to be calculated using an assumed seismometer damping coefficient of 0.27 (see fig.28). The exact value of this coefficient is unknown although it is not thought to differ much from that assumed. Frequency response curves for the B.P. swamp geophones at the Land's End station are not available and those of the systems at the Waterford and French stations are unknown. However, in spite of these difficulties, amplitude measurements at three of the stations may be assumed to be reliable enough for interpretative purposes.

Maximum peak to peak amplitudes of the first few cycles of the  $P_g$ ,  $P_n$  and large amplitude secondary arrivals at the Carnmenellis, Bodmin Moor and Scilly Isles stations were measured and the dominant frequency of the arrival was noted. After adjustment for frequency response and changes in gain, the measurements were plotted on the amplitude-distance graphs shown in fig.29. Amplitudes of the same phases at other stations have been measured but the uncertainties are much larger and the curves are not presented here.

#### 4.3 Velocity filtering

Velocity filtering is another processing technique

which has been applied to the data to aid recognition of phases. Several of the recording stations consist of arrays of seismometers. In recent years the use of such arrays has become well established in seismology. In refraction seismology, arrays are used to improve signal to noise ratios, to indicate apparent velocities of coherent arrivals across the arrays and to give information about azimuthal and frequency content of arrivals.

There is considerable literature dealing with the theory of seismic arrays. One of the most comprehensive treatments is that of Birtill and Whiteway (1965). They deal thoroughly with the theory and indicate the optimum sizes and shapes of arrays which should be used. A special report by the UKAEA (1965) has a section on array design and processing methods while Iyer (1968) describes a method of wave-number filtering applicable to array data.

The main processing method used in this study is that of velocity filtering with the purpose of obtaining the apparent velocities of certain arrivals along a seismic record. These apparent velocities can then be used to identify the phases which give information about the structure of the media in the vicinity of the array. In this particular study a similar method has been applied to both analogue and digital data. Ryall (1964) describes it as the U.K. method and compares it with other methods aimed at achieving similar results.

Seismometer outputs are delayed by amounts equivalent to a specified velocity across the array. The outputs are then split into two groups and summed. The sums are then multiplied together (cross correlated) and smoothed by integrating over a time window. The operation is repeated for a number of different velocities and the maximum value of the smoothed function is then taken to indicate the correct phasing conditions for an arrival having a particular velocity across the array. An azimuthal search can also be made by assuming a constant velocity and changing the phasing conditions for different azimuths.

For the Bodmin Moor and Dartmoor arrays the analogue apparatus developed by the UKAEA seismology unit was used to process the F.M. recorded data in its analogue form. Delay increments are inserted by running a tape loop over a bank of replay heads, the amount of delay being controlled by the speed of the loop. The data is then frequency filtered before it is processed on an analogue computer. A 2.0 second exponential window is used in the smoothing operation. The pen recorder output consists of traces representing successive stages of the processing sequence. However, various problems were encountered, not least of which was that of the unequal spacing of seismometers. This resulted in the insertion of inaccurate delays and it was decided finally that no reliable



phase velocities could be measured using the analogue apparatus. Measurements of phase velocities on the seismograms themselves were also assumed to be unreliable because of the inaccuracies involved in measuring the onset times across so short an array.

For the Land's End array a digital processing method was used. A computer programme was written in Fortran IV for use on the IBM 360/67. A description and listing of this programme appears in Appendix F. After the insertion of delays, four outputs from each arm of the array are summed and multiplied together. Although the digitising interval is .01 second, an interpolation routine is used to enable small increments of delay to be introduced. A square time window of 0.2 seconds is used in the smoothing routine. No frequency filtering is attempted during the processing.

It was found that the phase velocity of a discrete arrival travelling across the array could be measured to within  $\pm 0.1$  km/sec (see Appendix F). However, the reliability of the phase velocities obtained from the programme may be impaired by several factors. Firstly, the programme assumes plane wave fronts and thus, because of the size of the Land's End array, the phase velocities of arrivals which have travelled less than about 15 km will be measured inaccurately. Secondly, the arrival of two phases together will result in the phase velocity given by the programme having a value probably somewhere

between the real phase velocities of both arrivals. Thirdly, if the coherence of a particular arrival is poor for any reason then there may be some ambiguity in the result given by the programme. Nevertheless, a study of the seismic records themselves will supply most of the information which will indicate whether a particular phase velocity is reliable or not. The results obtained from this programme are presented in Appendix F.

As no on-line graph plotter is available on the 360/67, the output of this programme consists of punched cards bearing the smoothed output for several different velocities. This data is fed into an IBM 1130 computer and plotted on the graph plotter with the aid of a computer programme written by Mr. C.W.A. Browitt of the Geology Department, University of Durham (see Appendix G). The velocity filtered record of shot 2 is shown as an example in the pull-out supplement at the back of this thesis.

#### 4.4 The analysis and interpretation of all the data

This section describes the results obtained from the amplitude and velocity filtering measurements of all three lines of shots. It also discusses the nature of the large amplitude secondary arrival and describes its use in the determination of the eventual crustal models which are proposed for the three lines of the south west England experiment.

#### 4.4.1 Analysis of $P_g$ and $P_n$ arrivals

The amplitude measurements of the  $P_g$  arrivals at the Carnmenellis and Scilly Isles stations and  $P_n$  arrivals at the Bodmin Moor station are shown in fig.29. The rapid decrease in amplitude of the  $P_g$  arrival and the more gentle decrease of that of the  $P_n$  arrival is typical of the behaviour of these two phases (see Berry and West 1966b, Roller and Healy 1963). A similar pattern is seen at the Land's End station. The relatively large amplitude of the  $P_n$  arrival is evidence of a strong first order (i.e. step-like) velocity discontinuity and the persistence of these arrivals from shot to shot is indicative of the extensive uniformity of this refractor.

Phase velocity measurements of the  $P_g$  and  $P_n$  arrivals have been made for several of the line 1 shots. In most cases the phase velocities of the  $P_g$  arrivals are in the range 5.4 to 5.6 km/sec but those from shots 15 and 18 are considerably less at 5.1 and 5.2 km/sec respectively. The apparent  $P_g$  velocity measured from shot 18 is probably unreliable because of the proximity of the shot to the station but there is no obvious explanation of the low value obtained from shot 15. The generally low apparent velocities of the  $P_g$  arrivals when compared to the  $P_g$  velocity obtained from the first arrival travel time data may be explained by the presence of a 'dip' of the 5.85 km/sec refractor in the

immediate vicinity of the array. The station is situated about 700 ft above sea level with the land surface and, presumably, the refractor dipping towards the sea. The direction of dip as far as line 1 is concerned is, therefore, towards the west and a dip in this direction of no more than two degrees would be adequate to explain the low  $P_g$  phase velocities.

Only four of the shots in the  $P_n$  range have been velocity filtered. Two of them, shots 1 and 2, give unambiguous  $P_n$  phase velocities of 7.9 km/sec tending to confirm that there is an almost flat-lying Moho beneath the vicinity of the station. Of the other two, the  $P_n$  arrival from shot 4 has an ambiguous phase velocity of 8.0 or 8.5 km/sec reflecting its poor coherence across the array while that from shot 8 has a phase velocity of 7.7 km/sec. A study of the seismograms of this shot indicate the near-presence of a secondary arrival which is most likely to be the cause of the apparently low  $P_n$  phase velocity as measured by the programme.

#### 4.4.2 Analysis of later arrivals

Apart from the large amplitude secondary arrival which will be described in the next subsection and the S-wave arrivals, there are no other persistent phases which could be used for interpretation purposes. It is expected that some of the arrivals which are seen, especially in the few seconds

after the onset of the  $P_n$  and large amplitude secondary arrivals, are of the nature of reflections, refractions or diffractions, some of them probably from the steeply dipping granite margins. Their phase velocities are usually in the range 5.6 to 6.8 km/sec.

Although the author has studied the S-waves in less detail, several facts about them have emerged. Firstly, the S-waves from the nearer shots have phase velocities of about 3.3 km/sec which is the expected  $S_g$  velocity. Secondly, the amplitude of the S-waves increases suddenly at a distance of about 80 km. Thirdly, the phase velocities of these large S-wave arrivals are higher than the  $S_g$  velocity (about 4.2 km/sec) and tend to increase slightly as the source of energy approaches the detector. They are tentatively interpreted as S-wave reflections from the Moho but no further study of them has been made.

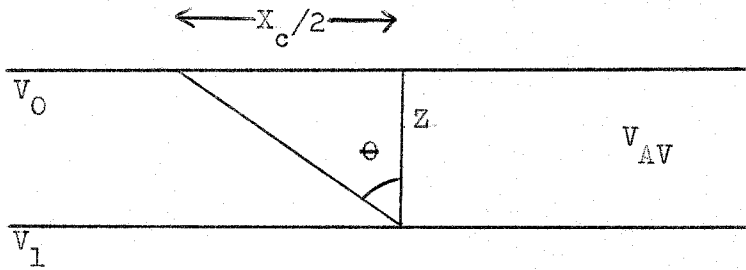
#### 4.4.3 The nature and use of the large amplitude secondary arrival

The large amplitude secondary arrival is interpreted to be predominantly a wide angle (supercritical) reflection from the Mohorovicic Discontinuity, henceforth designated PMP. Three lines of evidence support this interpretation. Firstly, the amplitude-distance characteristics of the phase in relation to  $P_g$  and  $P_n$  are similar to those of PMP in the theoretical

model used by Berry and West (1966b) to calculate amplitudes of various arrivals. Its amplitude at all three stations reaches a maximum at a distance of approximately 80 km with a secondary peak, not predicted by the model, occurring at varying distances within the range of 130 to 160 km (see fig.29). At distances beyond about 80 km the amplitude of this arrival is generally at least an order of magnitude larger than the amplitude of  $P_g$  and beyond 120 km it is significantly larger than that of  $P_n$ . Secondly, it is shown in figs. 31, 32 and 33 that the travel times of these arrivals are fitted by a curved line appropriate to a Moho reflection. Thirdly, it is found by velocity filtering that the apparent velocity of this arrival increases from about 5.6 km/sec for the more distant shots, through 6.1 km/sec for shot 9 (114.2 km), 7.1 km/sec for shot 11 (83.6 km) to 8.4 km/sec for shot 12 (73.7 km). This pattern of apparent velocity is to be expected for a wide angle reflection. For a uniform crust, the velocity at large distances should be asymptotic to  $P_g$  and at the critical distance it should be equal to that of  $P_n$ .

The PMP phase is most useful in that it can supplement the information already gained from the first arrivals. The distance at which it attains its maximum amplitude can be used to give an estimate of the critical distance, where a ray which has been critically reflected at the Moho emerges at the surface.

Knowledge of this parameter can be used in conjunction with first arrival data to obtain estimates of the maximum limiting depth to the Moho, the real depth to the Moho and an average velocity within the crust. The theory is as follows :-



$x_c$  = critical distance.

$\theta$  = critical angle.

Consider a model of the crust (shown above) of uniform thickness  $Z_1$ , average velocity  $V_{AV}$ , and velocity at the top  $V_0$ , overlying a substratum of velocity  $V_1 > V_0$ . First, let us suppose the crust to be of uniform velocity  $V_{AV} = V_0$ . Then

$$Z_1 = \frac{T_i V_1 V_0}{2 \sqrt{V_1^2 - V_0^2}}, \quad (1)$$

where  $T_i$  is the intercept time of the  $V_1$  segment.

If the velocity  $V_0$  increases with depth, then (1) will underestimate the true thickness, i.e.  $Z_1 \leq Z$ . Therefore (1) gives a minimum estimate of crustal thickness.

On the other hand, the crustal thickness  $Z_2$  for a uniform velocity  $V_0$  is related to the critical distance  $x_c$  by

$$Z_2 = \frac{x_c \sqrt{V_1^2 - V_0^2}}{2V_0} \quad (2)$$

If the velocity  $V_0$  increases with depth, then (2) will overestimate the true thickness, i.e.  $Z_2 \geq Z$ . Therefore formula (2) gives a maximum estimate of crustal thickness.

If we use  $V_{AV}$  in place of  $V_0$  in formulae (1) and (2), then both should give a good approximation of the true thickness  $Z$ . Estimates of  $Z$  and  $V_{AV}$  can then be obtained by solving the equations as follows :-

From (1)

$$Z = \frac{T_i V_1 V_{AV}}{2 \sqrt{V_1^2 - V_{AV}^2}} \quad (3)$$

and from (2)

$$Z = \frac{x_c \sqrt{V_1^2 - V_{AV}^2}}{2 V_{AV}} \quad (4)$$

Multiplying (3) by (4) we have

$$Z^2 = \frac{V_1 T_i x_c}{4}$$

and therefore

$$Z = \frac{\sqrt{V_1 T_i x_c}}{2} \quad (5)$$

By substituting  $Z$  in either (3) or (4) an estimate of  $V_{AV}$  is obtained thus :-

$$V_{AV} = \frac{x_c V_1}{\sqrt{4Z^2 + x_c^2}} \quad (6)$$

or

$$V_{AV} = \frac{2 Z V_1}{\sqrt{T_i^2 V_1^2 + 4Z^2}} \quad (7)$$



Critical reflections have previously been used for the selection of hypothetical models of the Earth's crust (Steinhart and Mayer 1961, Berry and West 1966b, Roller and Healy 1963). In nearly all of these studies, geometric ray theory has been used to compute the theoretical position of  $x_c$ . However, it has been shown by Cerveny (1966) that the use of geometric theory to predict amplitudes is seriously in error in the region of the critical distance. He has found that the amplitude of the reflected wave reaches its maximum not at the critical distance but at some point beyond it. Cerveny gives two reasons for this. Firstly, the head wave interferes with the reflected wave for some distance beyond the critical point. Secondly, geometric ray theory is a poor approximation in the region of the critical point.

The stations at Scilly Isles, Carnmenellis and Bodmin Moor all indicate a maximum amplitude distance of  $80 \pm 5$  km. The maximum amplitude distance of PMP at the Land's End station is also  $80 \pm 5$  km. The frequency content of the arrival varies little from shot to shot at Land's End and thus the observed maximum amplitude as seen on the trace from shot 11 is the real maximum amplitude. The closely similar estimate for all four stations is to be expected for a homogeneous crust with an almost horizontal lower boundary as indicated by the first arrival data. A similar value for this parameter for the Dartmoor station has thus been assumed. If this maximum

amplitude distance is taken to be coincident with the critical distance, then as shown above it can be used to obtain an absolute maximum estimate of crustal thickness. However, we have seen that the estimate of the real critical distance is improved by using Cerveny's results with a consequent better estimate of the maximum crustal thickness. For the five stations under discussion here, the critical distance has thus been re-estimated to be  $65 \pm 5$  km.

Table 7 gives the absolute maximum crustal thicknesses, the better estimates of maximum crustal thickness using Cerveny and the estimates of real crustal thickness and average crustal velocity for each station. The results from each station are not significantly different from one another. They give an absolute maximum crustal thickness of  $37.4 \pm 1.2$  km and a better estimate of maximum thickness using Cerveny of  $30.0 \pm 1.2$  km. The estimate of real crustal thickness is  $27.0 \pm 1.2$  km and the estimated average crustal velocity is  $6.15 \pm .13$  km/sec.

The main source of error in these estimates is that inherent in the estimate of critical distance. The spacing of the shots is such that an estimate of the maximum amplitude distance is only reliable within  $\pm 5$  km. The error on the estimate of the critical distance from the results given by Cerveny is difficult to assess because of the interdependence of the various factors that determine this distance in relation to the observed maximum amplitude distance. However, the author

Station	Scilly Isles	Land's End	Carmenellis	Bodmin Moor	Dartmoor
Maximum crustal thickness	km 35.3 ± 2.8	39.0 ± 2.5	36.5 ± 3.1	37.7 ± 2.7	38.6 ± 2.9
Better estimate of maximum crustal thickness	km 28.6 ± 2.7	29.8 ± 2.4	29.6 ± 3.0	30.7 ± 2.6	31.4 ± 2.8
Estimate of real crustal thickness	km 25.0 ± 3.0	26.9 ± 1.0	27.5 ± 1.1	26.5 ± 1.2	26.9 ± 1.2
Average crustal thickness	km/sec 6.15 ± .36	6.15 ± .16	6.10 ± .14	6.15 ± .07	6.20 ± .15

Table 7. Estimates of crustal thickness and average crustal velocity for the stations recording the line 1 shots. The Dartmoor results have been obtained assuming a similar critical distance to that found at the other stations.

is confident that it will be unlikely to exceed that quoted above.

We have, therefore, a seemingly simple model of the Earth's crust along line 1 consisting of a single layer, about 27.0 km thick, with an average P-wave velocity of 6.15 km/sec underlain by a flat-lying Moho with an upper mantle  $P_n$  velocity of 8.07 km/sec. The velocity of 6.15 km/sec, although relatively low as far as crustal velocities are concerned, is nevertheless higher than the 5.85 km/sec velocity which has been shown to be the average velocity within the granite (see section 3.3.2). This means that somewhere within the crust an increase of velocity with depth must occur.

Estimates of the depth to which the granite extends are of the order of 10 to 12 km (Bott et al 1958, Midford 1966). It is postulated that the velocity of 5.85 km/sec extends to this depth (see section 3.3.2). An increase of velocity must occur beneath this level to account for the average crustal velocity of 6.15 km/sec. The nature of this increase, whether abrupt or gradual, ought to be apparent from the data.

If the increase is due to an abrupt velocity discontinuity then head waves from such a discontinuity should be seen on the records although not necessarily as first arrivals. On the assumption of a step-like velocity discontinuity at a depth of 10 km, an average lower crustal

velocity of 6.33 km/sec would be necessary to give the average crustal velocity of 6.15 km/sec. If this depth is 12 km then the resulting average lower crustal velocity is 6.52 km/sec. It is calculated that head waves from a step-like discontinuity at about 10 to 12 km should be seen as first arrivals at ranges between about 100 and 120 km. No indications of any such first arrivals are seen on any of the travel time graphs although it may be argued that there are few shots in the appropriate distance range with the result that they may be mistaken as  $P_g$  arrivals. To test this, the apparent velocity of the first arrival from shot 9 as recorded at the Land's End station 114 km away obtained by velocity filtering was 5.3 km/sec. This is close to the typical  $P_g$  velocity. Thus there is no indication of a head wave from any intermediate refractor occurring as a first arrival. Nor does the velocity filtering indicate any persistent secondary phase with an apparent velocity of the right order. Furthermore, there are no recognisable super-critical reflections from such a boundary. Thus there is no evidence for any significant abrupt increases of velocity at any depth within the crust beneath the granite batholith.

This implies that there must be a gradual increase of velocity with depth in the lower crust possibly beginning at a depth of about 10 to 12 km. The presence of a lower crustal layer exhibiting a gradual increase of velocity with

depth automatically implies the presence of several features which should be recognisable to some extent on a seismic record. Let us assume a model of the crust consisting of an upper crustal layer 11 km thick with a velocity of 5.85 km/sec and a lower crustal layer extending to a depth of 27 km exhibiting a linear increase of velocity with depth such that the average crustal velocity is 6.15 km/sec. Travel times have been calculated for this model for all the P phases which travel through such a structure. The model and a reduced travel time graph of these phases are presented in fig. 30.

The effect of a lower crustal layer exhibiting an increase of velocity with depth can be clearly seen. Three cusp points are present, the most prominent of which is at 65 km where  $P_n$  arrivals and supercritical PMP arrivals are first seen. The  $P_n$  segment is tangential to the PMP segment at this point which is at the critical distance. At greater distances the two segments diverge with the PMP curve eventually reaching a second cusp point at a distance of 148 km. At this point the PMP phase ceases to exist where it has a ray in common with a body wave which has been continuously refracted through the lower crustal layer. This distance will be referred to as the grazing incidence distance. The short segment between the pair of cusps at 148 and 126 km represents a refracted phase which has travelled most of its path in the lower crust. The

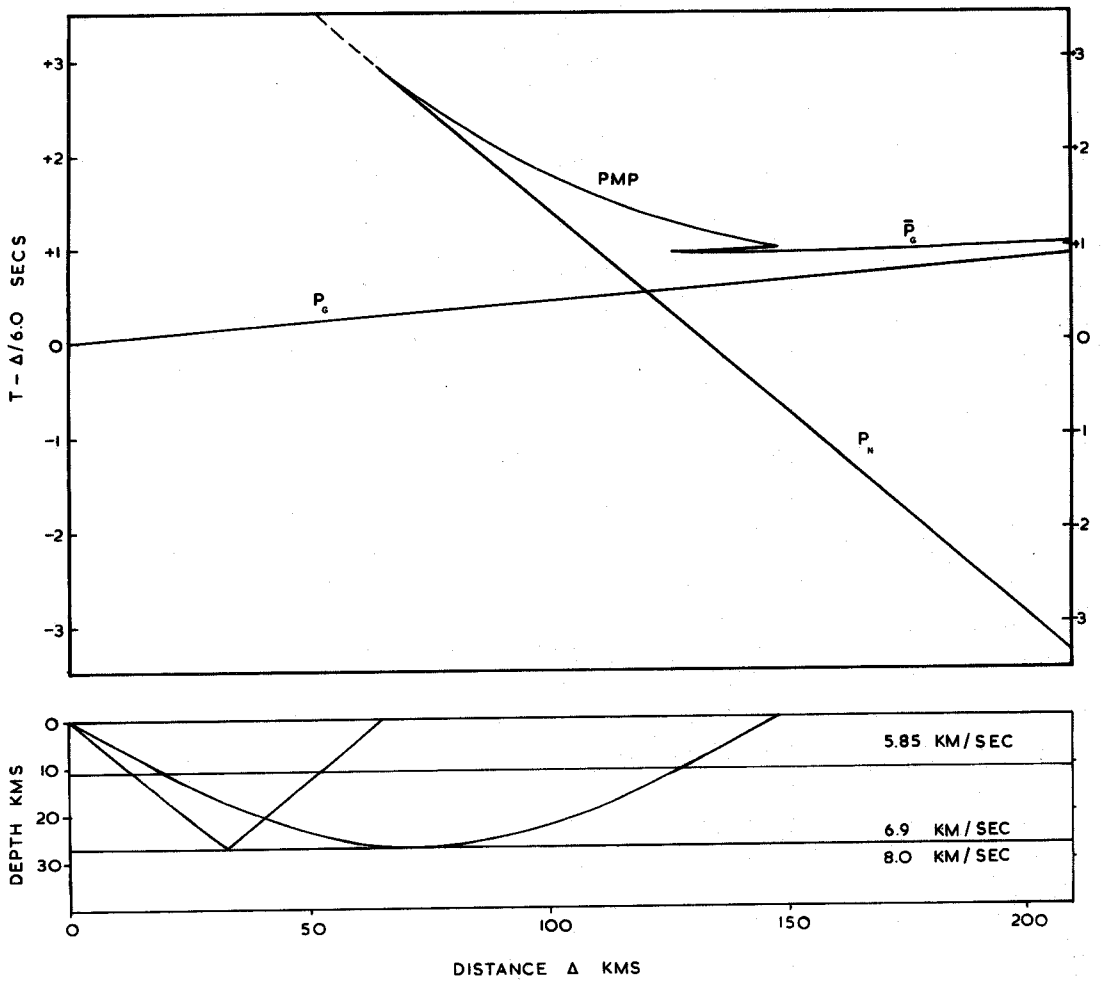


Fig.30. A crustal model and calculated reduced travel time graphs for the P-waves travelling through it.

other segment which is asymptotic to the  $P_g$  segment represents a phase which has travelled most of its path in the upper layers of the crust. This latter phase is a guided wave trapped between the upper layers of the lower crust and the ground surface. It is analogous to the crustal guided wave  $\bar{P}$ , described by Shurbet (1960) and Ryall and Stuart (1963) and thus will be designated  $\bar{P}_g$  for the purposes of this interpretation.

The problem of recognising these phases on a seismic record is complicated by the similarity of their travel times especially in the region of the short segment between the pair of cusps. In this region four phases all arrive within a short time of each other. On a record it is unlikely that several discrete arrivals will be seen. The most likely observation is that of a single phase but with a significantly increased amplitude in this particular region. This is explained by the interference of the several phases which are arriving in such a short space of time. The secondary amplitude maxima seen on the Scilly Isles, Carnmenellis and Bodmin Moor records may be explained in this way. At distances greater than the secondary amplitude maxima the phase which seemed to be a continuation of the PMP phase is shown to be the completely different  $\bar{P}_g$  phase.

The basic crustal model used to calculate travel times (see fig. 30) was proposed because of the observation that a gradual increase of velocity with depth must occur beneath the



granite. The model has been shown to provide an explanation of the important secondary amplitude maximum of PMP at each station. It has provided no evidence contradicting with any other observations which have been made and is therefore postulated to be a realistic type of model for the crust along line 1 of the south west England experiment.

Assuming the increase of velocity with depth to be linear, the knowledge of the critical distance ( $C_1$ ) and the grazing incidence distance ( $C_2$ ) can be used to obtain estimates of the depth at which the increase of velocity begins. The theory by which  $C_1$  and  $C_2$  are used is given in Appendix H. Two non-linear simultaneous equations in  $K$  (the constant of increase of velocity) and  $Z_1$  (the thickness of the upper crustal layer) are obtained which are solved by a substitution method on the computer.

This method has been applied to the data from the Scilly Isles, Carnmenellis and Bodmin Moor stations. A major problem with this method is that of the accurate measurement of  $C_2$ . A consequence of the interference of the several phases in the region of the short segment between the two cusps is that the observed maximum amplitude distance is probably not exactly at the real  $C_2$  distance but some way before it. The problem of determining the real  $C_2$  distance is similar to that of determining the critical distance  $C_1$  from the observed maximum amplitude

distance. In this case, however, no theoretical evidence is available which could help in the acquisition of a better estimate of the real  $C_2$ . Thus the observed secondary maximum amplitude distances have been used as the best available estimates of  $C_2$ . The values of  $V_0$  (the velocity in the upper crustal layer),  $V_2$  (the velocity immediately below the crust, i.e.  $P_n$  velocity),  $H$  (the total crustal thickness),  $C_1$  and  $C_2$  used in the computation for each station and the results thus obtained are presented in table 8. It was found that the solution is more sensitive to errors in  $C_1$  than to those in  $C_2$ . For instance if  $C_2$  is underestimated by 10 km the estimate of depth  $Z_1$  is decreased by 1 km only.

The results indicate that the velocity begins to increase at a depth of about 10 km at a point 80 km WSW of the Bodmin Moor station and at a depth of 12.5 km about 67 km WSW of the Scilly Isles. The apparent increase in the thickness of the uniform upper layer towards the west is thought to be significant although it may not be as great as estimated. The major significance of these results is that they confirm that a relatively uniform crustal layer interpreted as granite extends to a depth of about 10 or 11 km.

#### 4.4.4 Line 1, final interpretation

The velocity-depth model of the Earth's crust along

Station	$V_0$ km/sec	$V_2$ km/sec	$C_1$ km	H km	$C_2$ km	K km/sec/km	$Z_1$ km
Scilly Isles	5.85 ± .05	8.07 ± .07	65 ± 5	27 ± 1.2	134 ± 5	.08 ± .005	12.5 ± 1.0
Carmmenellis	5.85 ± .05	8.07 ± .07	65 ± 5	27 ± 1.2	148 ± 5	.065 ± .0025	11.0 ± 1.0
Bodmin Moor	5.85 ± .05	8.07 ± .07	65 ± 5	27 ± 1.2	160 ± 5	.055 ± .0025	10.0 ± 1.0

Table 8. Estimates of depths to the top of the lower crustal layer including the data used in their evaluation.

line 1 is presented in fig.34. In order to test the fit of the model, travel times of various phases have been calculated for each station and compared to those observed. Stacked records of the Scilly Isles, Carnmenellis and Bodmin Moor stations are presented in figs. 31, 32 and 33 respectively with lines indicating the calculated travel times for the particular  $P_g$  and  $P_n$  velocities as seen at each station in addition to the PMP and  $\bar{P}_g$  phases calculated assuming the model. Because of the problems of recognising the onsets of discrete arrivals in the region of the short segment between the pair of cusps (see fig.30), travel times of the  $\bar{P}_g$  phase have only been calculated for distances beyond where the PMP phase disappears.

For the Bodmin Moor and Scilly Isles stations the fit of the PMP phase is good, predicted onsets all being within 0.1 sec of those observed. For the Carnmenellis station the fit is not so good although the major discrepancy seen on the trace from shot 13 is explained by the fact that the whole trace is displaced by half a second (see first arrival travel time data, section 3.3.1). The goodness of fit of the  $\bar{P}_g$  phase is difficult to evaluate for the Carnmenellis and Scilly Isles stations and at the Bodmin Moor station for some shots it is rather poor. When the model is applied to the Land's End data it is found that the  $\bar{P}_g$  fit is good with all but one of the predicted onsets falling within 0.1 sec of the observed. However, there

Fig.31. The stacked record of the line 1 shots at the Scilly Isles station.

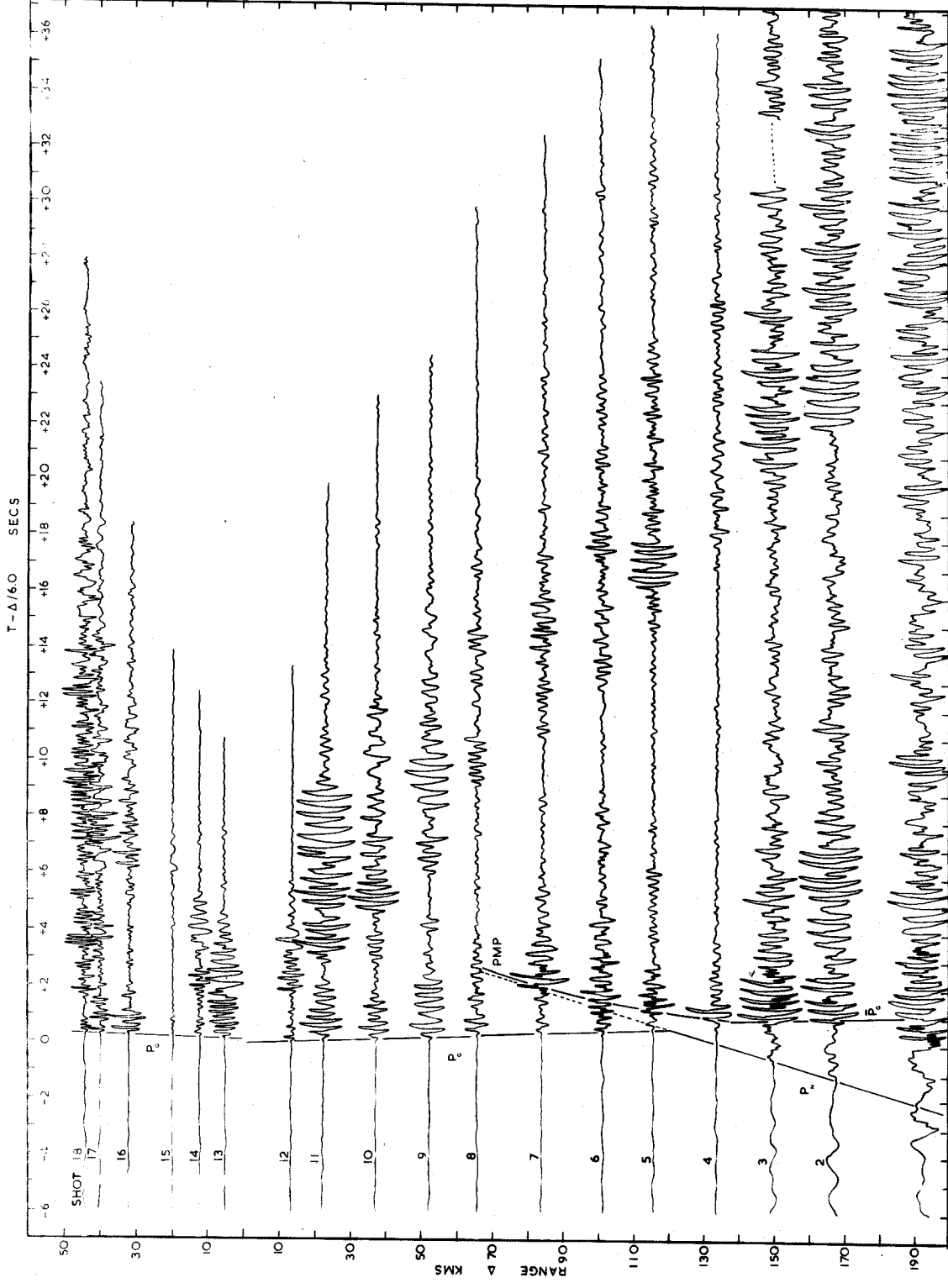


Fig.32. The stacked record of the line 1 shots at the  
Carmenellis station.

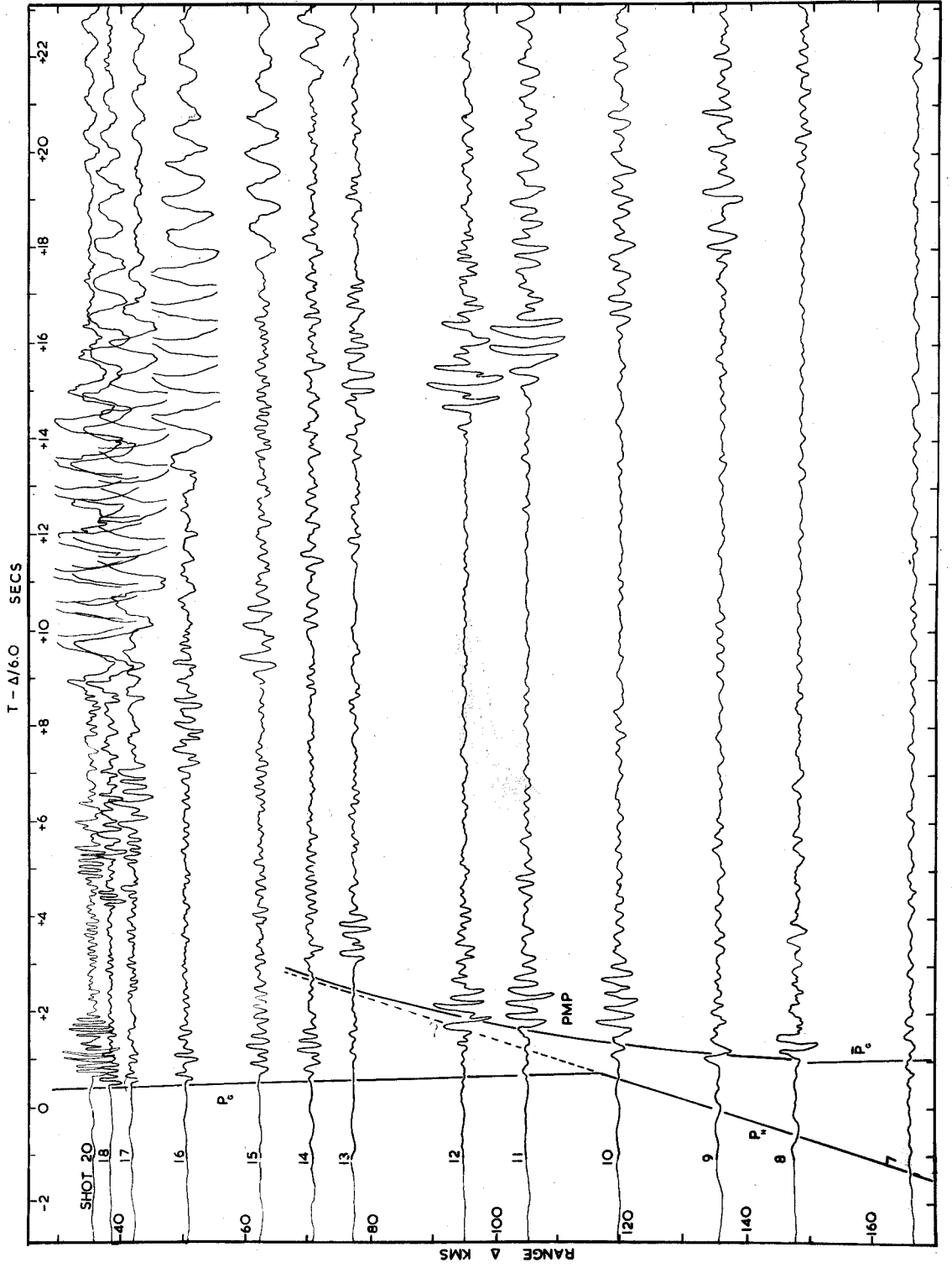
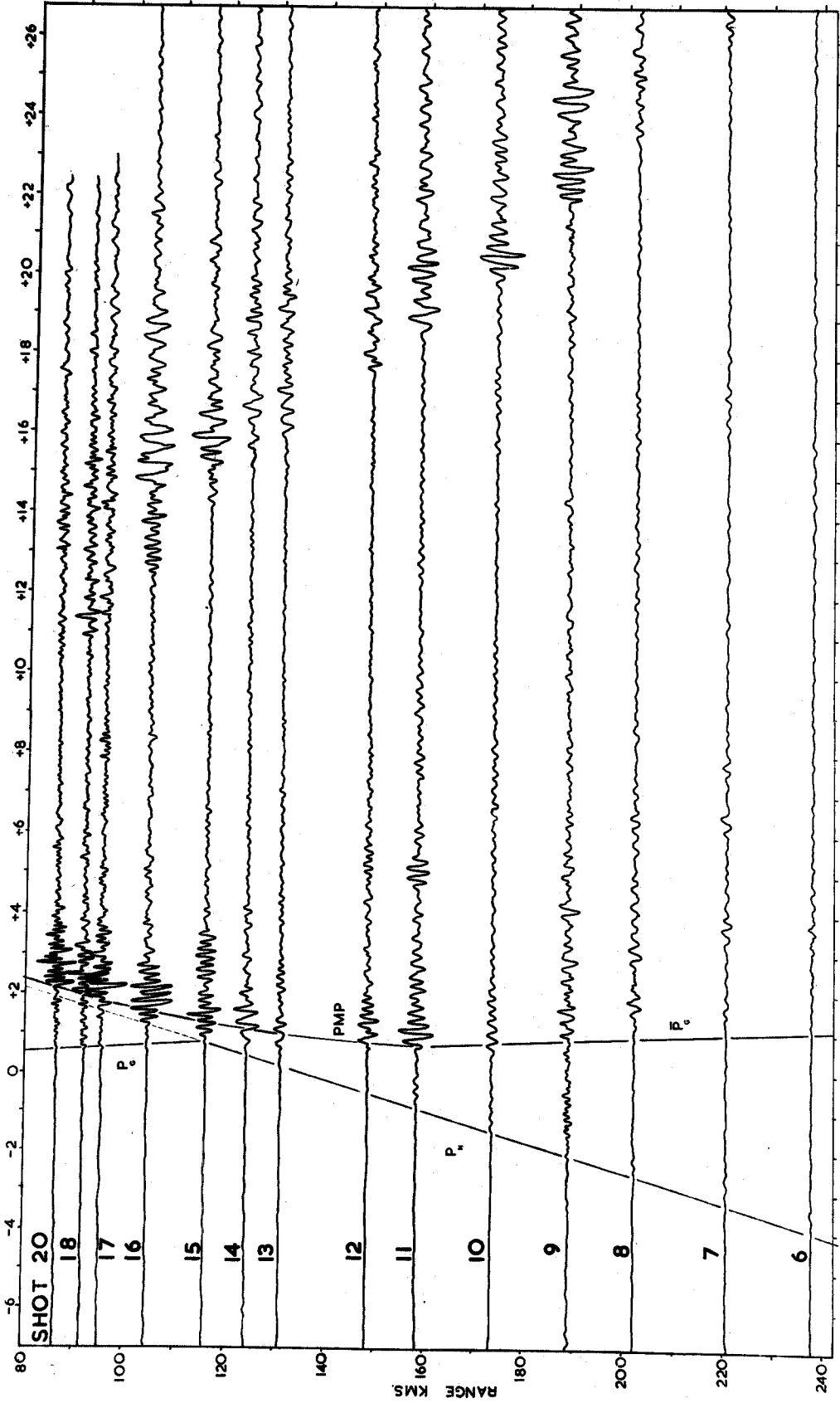




Fig.33. The stacked record of the line 1 shots at the Bodmin Moor station.

T-A/6.0 SECS



is a discrepancy in the fit of the PMP phases from the two nearer shots. In both cases the observed travel time of this phase is 0.2 sec later than that predicted although the observed onsets of this phase from the other shots are close to their predicted times.

The discrepancy in the travel time of the  $P_n$  arrival and that of the PMP arrival at the critical distance as seen in figs. 31, 32 and 33 is evidence that the  $P_n$  velocities observed at each station are underestimates of the real  $P_n$  velocity. This agrees with the results obtained from the reversal of the line using four shots and four stations. It is possible therefore that there may be a significant dip along line 1. However, it is thought more likely that the adjustments to the first arrival travel time data may not have fully compensated for the effects of the wedge of sediments at the end of the line with the resulting underestimates of real  $P_n$  velocity. There may be a dip of the Moho towards the west along line 1 but it will almost certainly be much less than the 34 minutes indicated by the first arrival travel time data.

The overall fit of the model to the travel time data is good although there are some inconsistencies most of which fall within the error limits which have been quoted. The major discrepancy is that of the fit of the calculated travel times of the PMP arrival to those observed at the Land's End station although this may easily be explained within the basic framework

of the model proposed here. A slight adjustment in the thickness of the upper crustal layer or a slightly different assumption of the type of increase of velocity with depth would be enough to explain the discrepancy. Reliable amplitude measurements at this station may have provided the real explanation.

The crustal model presented in fig. 34 has evolved from measurements of both seismic refraction and reflection data. Only unambiguous phases along the seismic record have been used in its evaluation and due respect has been paid to the errors involved. The model has been shown to fit the observed travel times of various phases and also to provide an explanation of the amplitude characteristics of the important secondary phases. It is difficult to obtain any other model which explains the major observations as well and as simply as this one.

However, this interpretation has been obtained assuming that there are no velocity reversals within the crust. Their presence is difficult to detect although a few workers, notably Gutenberg (1950, 1951, 1954, 1955), Mueller and Landisman (1966), Landisman and Mueller (1966) and Fuchs and Landisman (1966) have presented evidence of low velocity channels at different levels within the crust. The work of Fuchs and Landisman is especially interesting in that the stacked records they present are similar in many respects to those of the south west England experiment. The major difference is their interpretation of the presence of a low velocity layer at a depth of 8 to 11 km. A careful study

has been made of the data from the south west England experiment for evidence similar to that upon which Fuchs and Landisman base their interpretation. The little there is may be explained more easily in terms of the model proposed here. As has already been discussed (see section 3.3.2) there may be a slight decrease of velocity with depth within the granite but this will certainly not be of the order of that envisaged by Gutenberg and Fuchs and Landisman. The present author would not disagree with the possible presence of a low velocity channel along the profiles of Fuchs and Landisman in Germany but the data from the south west England experiment presents very little evidence for such a channel and its presence along any of the profiles of this experiment is unlikely.

The model in fig. 34 is therefore preferred and presented as a feasible model of the crustal structure along line 1. The geological implications of this model will be discussed in the next chapter.

#### 4.4.5 Line 2, results and interpretation

Several problems arise in the interpretation of the data from this line. Firstly, no reliable amplitude-distance measurements can be made because of the unknown nature of the frequency responses at both the Waterford and Land's End stations. Secondly, several of the channels at the Land's End array were not working properly for shots 42 to 24 so that there are no

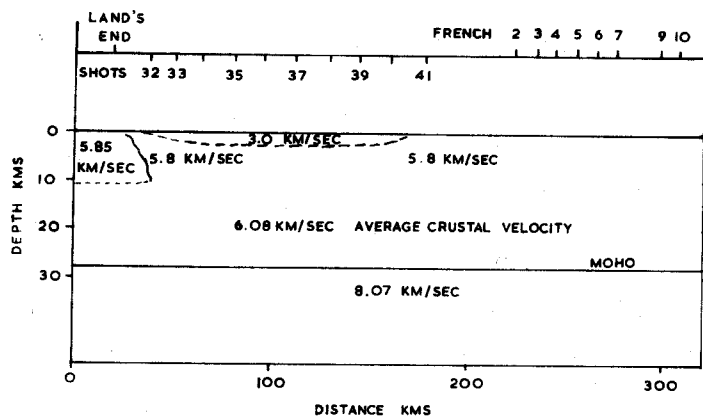
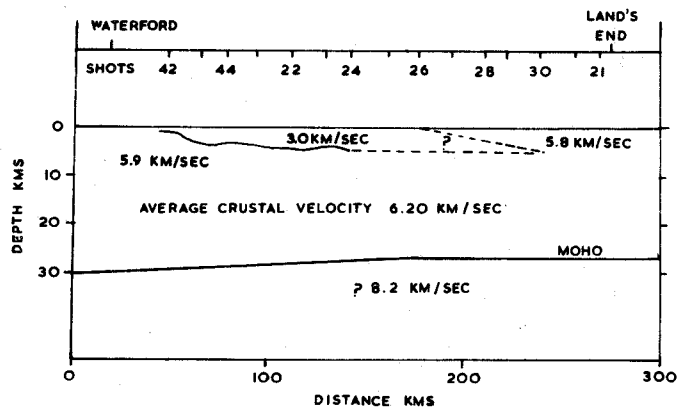
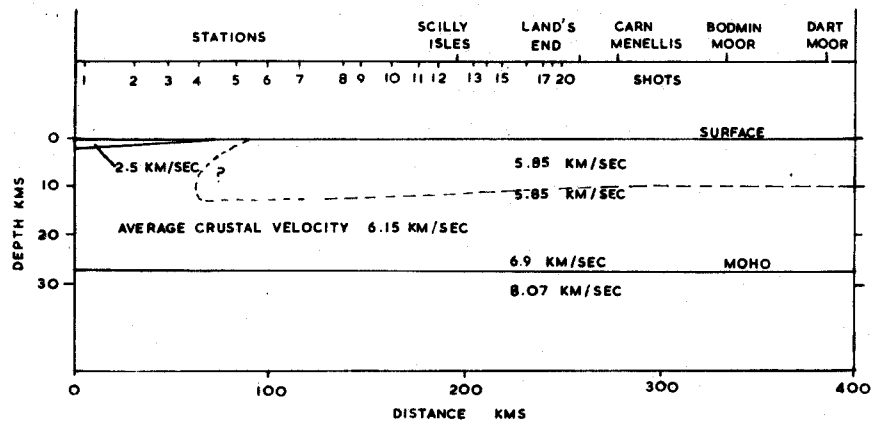


Fig.34. The crustal model for lines 1 (upper), 2 (middle) and 3 (lower) of the south west England experiment.

reliable velocity filtering results for these shots. Most of the remaining shots from this line have not been available for processing because of the computer input problem which is described in Appendix C. Thirdly, there is no unambiguous model for the first arrival data. Thus the interpretation of the results from this line is rather speculative in nature.

Stacked records of the Waterford and Land's End stations are presented in figs. 35 and 36. A stacked record of the Eskdalemuir station was not prepared because of poor signal to noise ratios and because, for most shots, only  $P_n$  arrivals with phase velocities of about 8.1 km/sec were discernible. The Land's End record especially is more complicated than those described for line 1 but the PMP arrival is clearly visible on both records reaching a maximum amplitude at a distance of about 65 km from the Land's End station and 80 km from the Waterford station.

It has been shown in section 3.3.4 that there is some evidence of a dip of the Moho towards the north along the northern half of line 2. The seismic data do not give reliable estimates of the amount of dip or the real  $P_n$  velocity. However, the regional gravity gradient of about -0.06 mgals/km northwards is consistent with an increase of crustal thickness from 27 km in the region of shot 26 to about 30 km beneath the Waterford station representing a Moho dip of about one degree.

Fig.35. The stacked record of the line 2 shots at the Waterford station.



T - 4/60 SECS

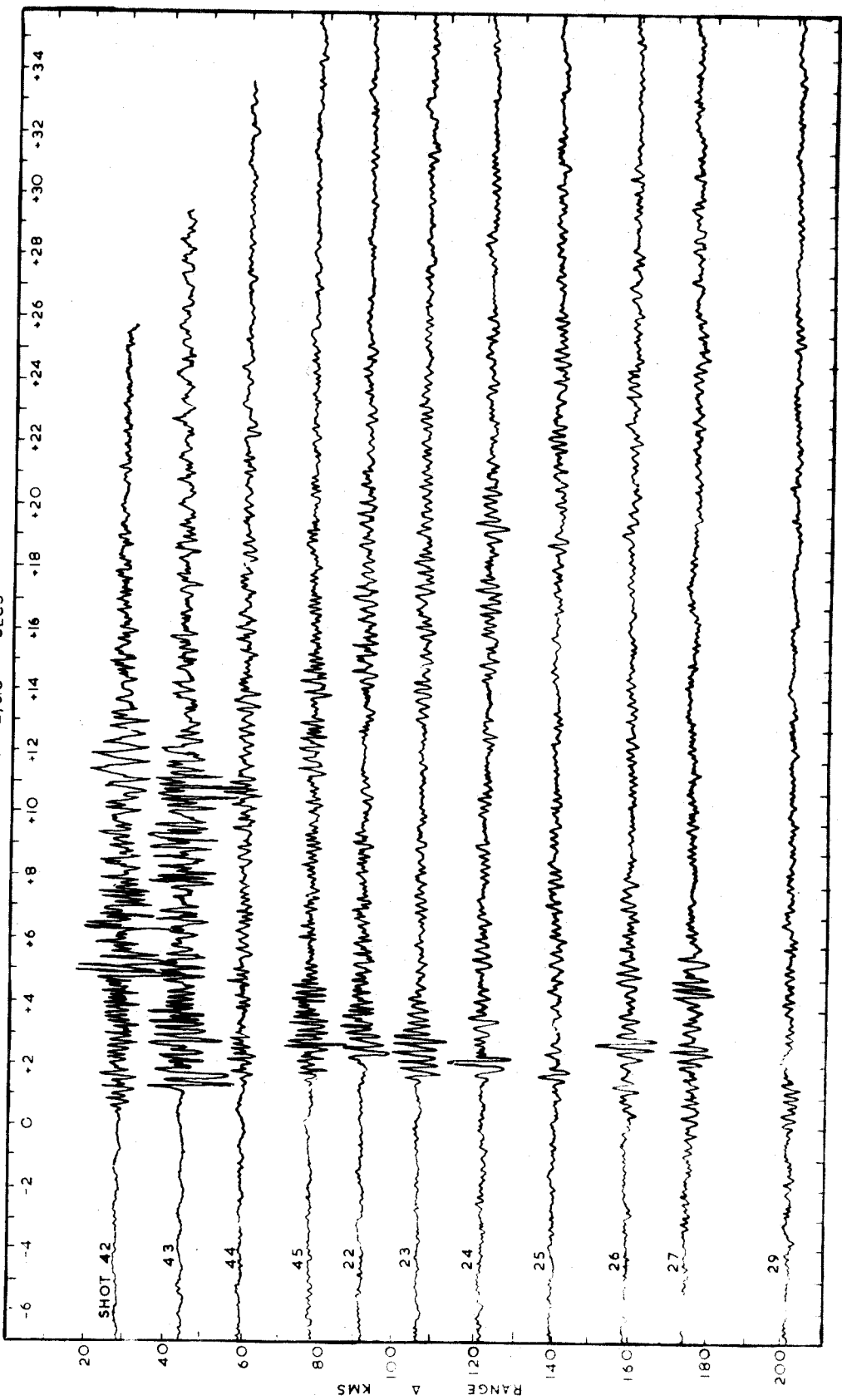
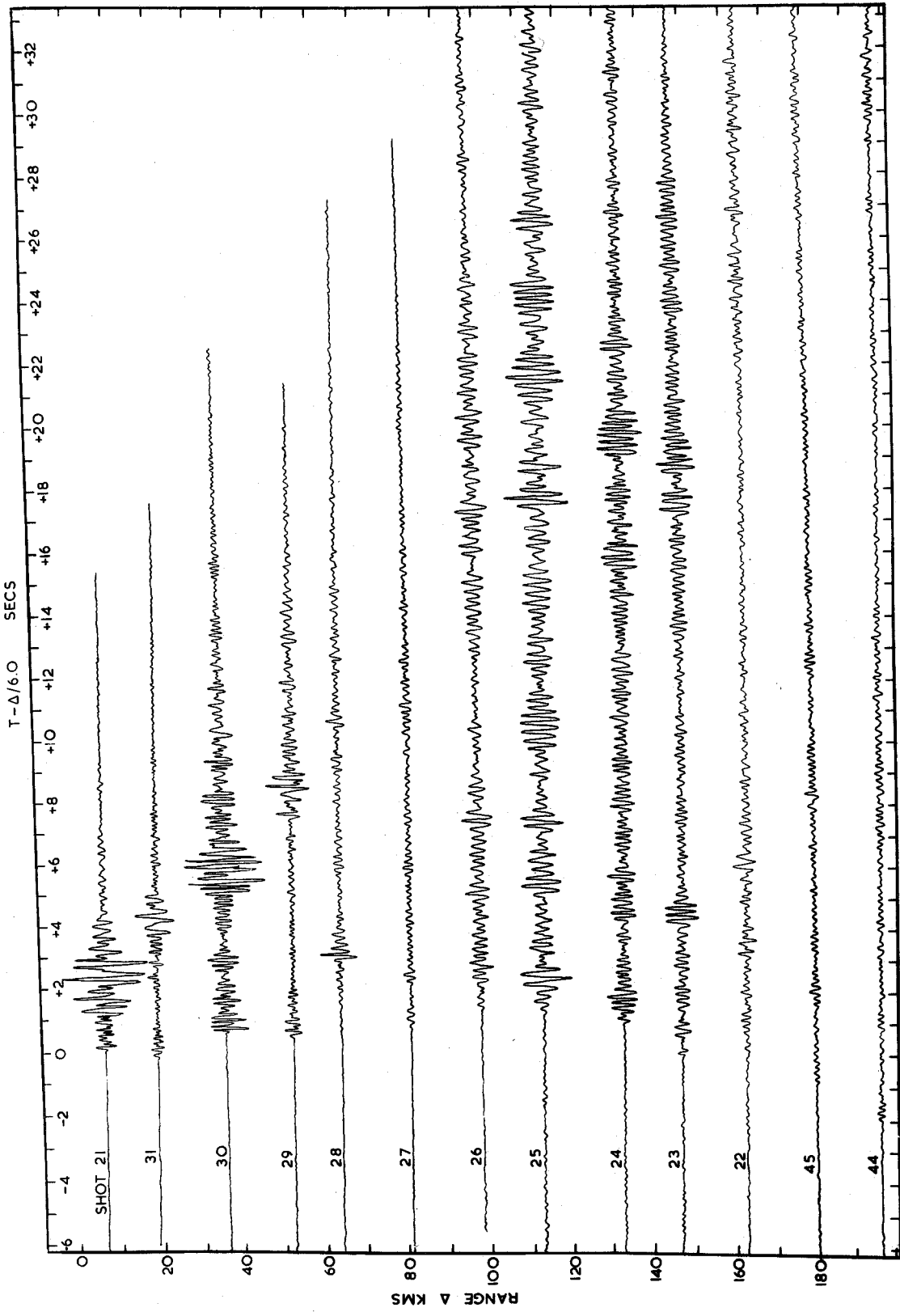


Fig.36. The stacked record of the line 2 shots  
at the Land's End station.



The maximum amplitude distance of PMP at the Land's End station is less than that observed for line 1. It is estimated that the average crustal velocity is about 6.25 km/sec in the southern part of the line and 6.20 km/sec in the northern part. In view of the uncertainties involved, these estimates are not considered to be significantly different from those obtained for line 1.

There is also a possible secondary maximum amplitude of PMP at greater distances (see traces of shot 25 at the Land's End station and shot 24 at the Waterford station). This means that there may be an increase of velocity with depth in the lower part of the crust. However, a persistent  $\bar{P}_g$  phase is difficult to recognise on either record.

There are many other phases on these records especially from the more distant shots on the Land's End record. For example, a phase showing a similar trend to the  $P_n$  arrivals can be seen approximately 3 seconds behind the first arrivals from shots 44 to 24. S phases are also present although their onsets are difficult to pick in most cases. However, in the absence of any reliable methods of analysis of these records no further interpretation of the data from this line has been attempted. A crustal model is presented in fig. 34 but its unreliable nature must be emphasised.

#### 4.4.6 Line 3, results and interpretation

A similar problem regarding the measurement of amplitudes occurs for this line also. However, the overall interpretation of the data is more reliable than that of line 2 because of the availability of a few velocity filtering measurements and the more reliable nature of the first arrival travel time results.

The stacked record for the Land's End station is presented in fig. 37. It is slightly less complicated than the records of line 1 and line 2 at the same station. The PMP phase is prominent on the traces of shots 35 to 38 with its maximum amplitude distance estimated to be about 75 km. Its apparent velocity increases from 7.1 km/sec for shot 38 (109.4 km) to 8.1 km/sec for shot 35 (60.6 km). A secondary amplitude maximum may occur at a distance of 140 km (see trace of shot 40, fig. 37). S phases are visible on all traces but their onsets are mostly difficult to pick with certainty. No other persistent phases are seen on this record.

Some of the stacked records of the French stations are presented by Revoy (1969) but a composite record of the P arrivals only is presented here (fig. 38). The most prominent feature of this record is the presence of the large amplitude secondary P arrivals. The sudden increase in amplitude of the PMP arrival at a distance of about 80 km and the secondary increase in

Fig.37. The stacked record of the line 3 shots  
at the Land's End station.

T-Δ/6.0 SECS

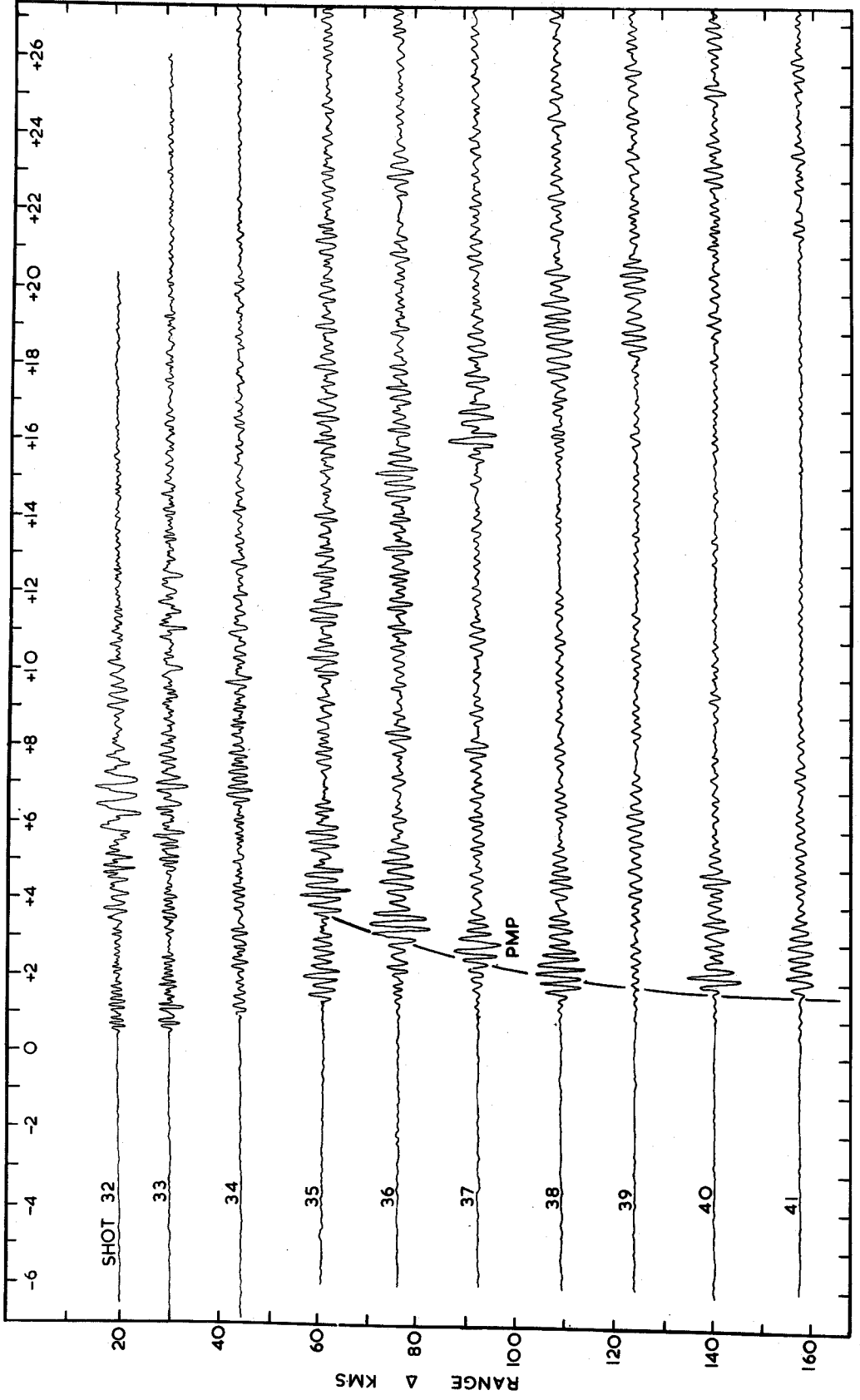
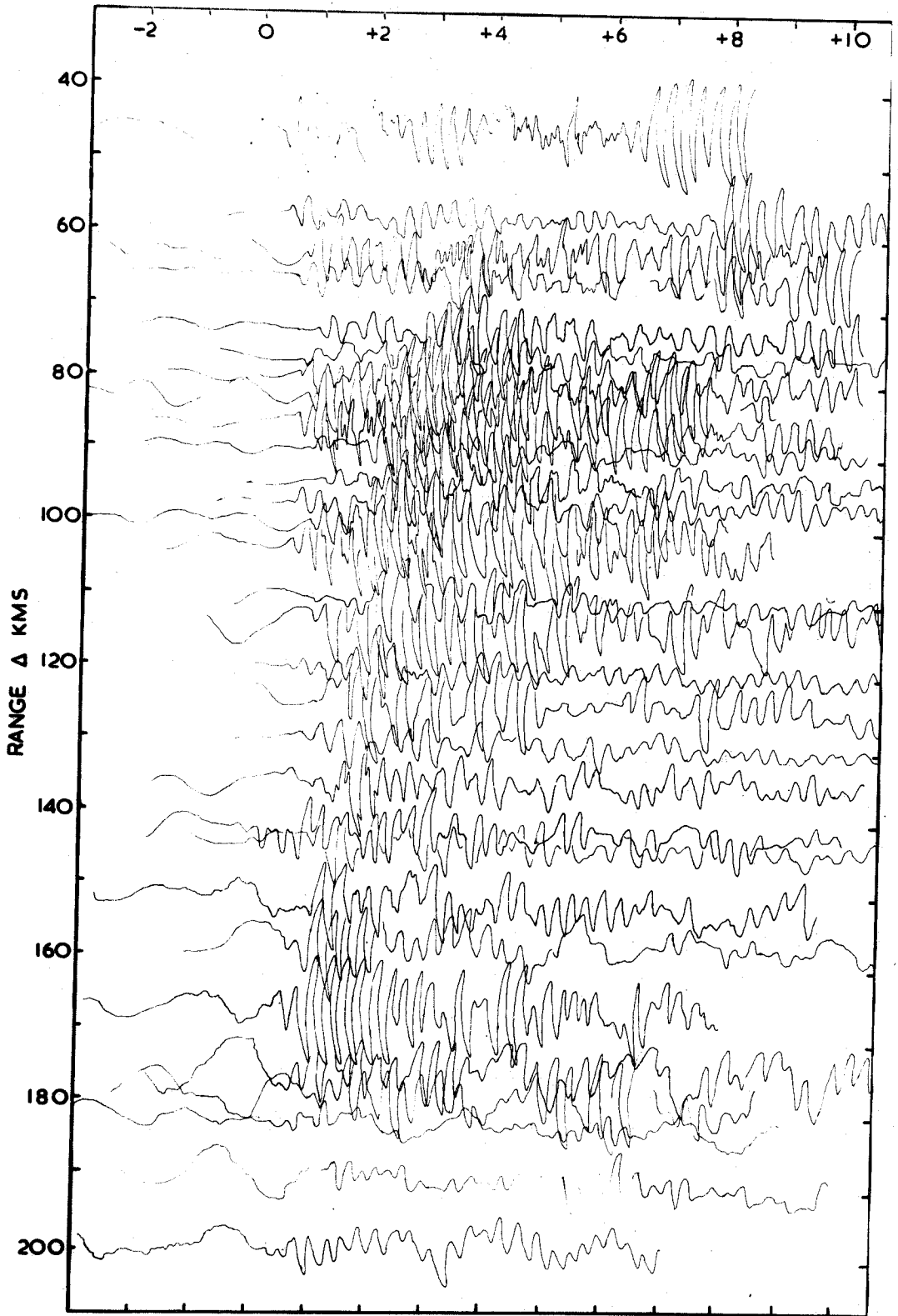


Fig.38. The stacked record of the line 3 shots at  
the French stations.



$T - \Delta/6.0$  SECS



amplitude at a distance of about 160 km are clearly seen. A study of the individual French stations indicates that the frequency content of this phase changes little from shot to shot and that the maximum amplitude distance at each station falls in the range 75 to 85 km. Thus the estimate of  $80 \pm 5$  km is thought to be a reliable estimate of the real maximum amplitude distance.

The observation of this distance has been used in a similar manner to that for line 1. The critical distance is assumed to be  $65 \pm 5$  km using Cervený. The estimate of absolute maximum crustal thickness is  $38.8 \pm 2.5$  km and a better estimate of the maximum crustal thickness is  $31.5 \pm 2.4$  km. The estimate of real crustal thickness is  $28.4 \pm 1.1$  km and the average crustal velocity is  $6.08 \pm .11$  km/sec. For the same reason as that given in section 3.3.6, the above estimate of real crustal thickness includes the varying thicknesses of sediment known to be present in the region of the shots. The estimates of real crustal thickness and average crustal velocity are not significantly different from those along line 1. If there is a difference in the average crustal velocities as seen along both lines, then it is explained by the fact that the effects of the sedimentary low velocity layers have not been completely eliminated in the estimation of the crustal velocity along line 3. The effect is thus to weight the average velocity to a slightly lower value.

Thus the crustal model along the region of the line 3 shots and French stations consists of a horizontal layer about 28 km thick underlain by the Moho with an upper mantle  $P_n$  velocity of 8.07 km/sec. The average crustal velocity is 6.08 km/sec and the upper parts of the crustal layer in the region of the shots consists of up to 3 km of low velocity sediments.

The nature of the increase of velocity within the crust required to give an average crustal velocity of 6.08 km/sec is more difficult to ascertain for this line than it is for line 1. Revoy (1969) indicates a step-like increase of velocity at a depth of 17.5 km with a sub-refractor velocity of 6.57 km/sec and a total crustal thickness of 27.3 km. This gives an average crustal velocity of 6.12 km/sec which, together with that of the estimate of real crustal thickness, agrees closely with the findings of the present author. However, the evidence given by Revoy for such an intermediate refractor is tenuous. Head waves from such a refractor are always secondary arrivals and the line fitted by Revoy indicating this phase is based upon arrivals seen only on two or three traces. On most traces there is no sign of an arrival anywhere near the predicted time. The few velocity filtering results available from the Land's End station provide little evidence of this refractor and thus its presence is doubtful.

More reliable evidence of the nature of this increase is present in the form of the secondary amplitude maximum of the PMP phase on both the French and Land's End records. In a similar manner to that shown for line 1 this secondary amplitude maximum is evidence for a gradual increase of velocity with depth. This is thought to be the most likely situation along this line. However, no estimates of the depth at which the increase may begin can be made without reliable amplitude measurements.

The crustal model thus proposed for line 3 is that given in fig. 34. The model has been assumed in the calculation of travel times of the PMP phase. A line representing this phase has been drawn on the Land's End record (fig. 37). Except for shot 38 the calculated travel times fall within 0.1 sec of the observed travel times. The model also fits the individual French station records reasonably well although the line representing the PMP arrivals is not drawn on fig. 38 because of the large number of seismic traces. Thus the estimates of real crustal thickness and average crustal velocity presented here are thought to be reliable within the error limits given. Apart from the suggestion of a gradual increase of velocity with depth, no further reliable information regarding the structure within the crust along this line has been obtained.

#### 4.5 Conclusion

The interpretation of the south west England experiment data presented here has been based largely upon the use of the PMP arrival. Its presence on these records has been proved almost conclusively by amplitude and velocity filtering measurements and by the goodness of fit of the observed travel times to those calculated for it. More reliable estimates of real crustal thickness and average crustal velocity have been obtained by using it in conjunction with the first arrival travel time results. Its importance has been demonstrated also in the evaluation of structures within the crust especially for media exhibiting suspected gradual increases of velocity with depth.

The presence of this phase is not confined to this experiment. Both Berry and West (1966b) and Roller and Healy (1963) present amplitude measurements with similar characteristics to those described here of a phase which they interpreted to be PMP. In their cases, however, the secondary amplitude maxima are not explained. The stacked records of Fuchs and Landisman (1966) show a similar set of large amplitude secondary arrivals which could equally well be explained by the type of structure envisaged here as that proposed by them. It is the author's opinion that gradual increases of velocity with depth within the crust are probably

more widespread than is usually indicated. Section 4.4.3 has described how such increases can be recognised and how their extent and magnitude can be measured. A more realistic model of crustal structure can thus be obtained which may help in the understanding of the nature of the materials and the processes that occur within the crust.

## CHAPTER 5

The results from the analysis of the data from the south west England experiment have so far been presented in the form of velocity-depth models along the three refraction lines (see fig. 34). The first section of this chapter compares the broad crustal structure obtained here with that in other regions of the British Isles. The second section discusses the geological interpretation of the results especially with regard to the problem of origin of the granite. A final section provides suggestions for the design of future crustal structure experiments around the British Isles in the light of the experience gained from the south west England experiment and the general standard of the data collected from previous seismic experiments in the region.

### 5.1 Comparative crustal structure around the British Isles

The nearest profile to those of the south west England experiment is that of Bunce et al (see fig. 4). They suggest that the Moho is dipping southwards along the line from about 16 km depth at the northern end to about 25 km at the southern end with a  $P_n$  velocity of 7.7 km/sec. The poor weather conditions experienced and the fact that the  $P_n$  arrival would be seen as first arrivals only along a short segment of the

line may mean that this interpretation is considerably in error. This is reflected in the tentative way in which Bunce et al present their model.

Profiles shot off the continental margin south west of the profile of Bunce et al may be more reliable. Most of these profiles show a typical oceanic crust with crustal thicknesses varying from about 14 km near the continental margin to about 10 km in deeper water areas (Ewing and Ewing 1959, Hill and Laughton 1954). Crustal velocities seem to vary considerably but the  $P_n$  velocities are all about 7.8 km/sec which is significantly less than that found in the south west England experiment and in other experiments on the shelf around the British Isles (see below).

One of the more recent crustal structure experiments carried out in the British Isles is that reported by Blundell and Parks (1969). They present the results of a time term analysis of the data collected from a seismic experiment undertaken in the southern Irish Sea in 1965. Although the author would challenge their  $P_g$  solution because they have used  $\bar{P}_g$  data as well as  $P_g$  in the evaluation of the  $P_g$  time terms, the remaining results are probably reliable within the error limits given.

There are significant differences between the crustal structure in the southern Irish sea region and that along lines 1 and 3 of the south west England experiment. The main difference



is that there is reliable evidence for an intracrustal refractor at a depth of about 24 km beneath the Irish sea with a subrefractor velocity of about 7.3 km/sec. The upper crustal velocity was found to be about 6.14 km/sec and thus, for any finite thickness of the lower crustal layer, the average crustal velocity beneath the upper crustal sedimentary layer will be significantly larger in this region than that found in south west England. The depth to which the 7.3 km/sec layer extends, i.e. the depth to the Moho, is difficult to ascertain with certainty because of the unreliabilities of the  $P_n$  time terms.  $P_n$  arrivals were recorded only at the Eskdalemuir and Rookhope stations with the result that control on the velocity was poor. However, their estimate of  $29.9 \pm 2.4$  km is probably reliable within the error limits given. Thus there is evidence of a significant difference in average crustal velocity between the two regions and a possible difference in total crustal thickness.

The average value of the  $P_n$  time terms for the southern Irish sea region given by Blundell and Parks is 3.34 sec. This is significantly larger than that obtained along line 1 of the south west England experiment (2.99 sec) but similar to that found along line 2 (3.44 sec). Most of the difference that is observed can be attributed to the variations in sedimentary thicknesses present at each survey

point but no further comparison is warrantable until the  $P_n$  time terms from the Irish sea are obtained more reliably.

Information about the crustal structure beneath northern Britain is provided by the explosion programme carried out to calibrate the UKAEA seismic array at Eskdalemuir. The results have been interpreted in terms of crustal structure by Agger and Carpenter (1965). A time term analysis was applied to both the  $P_g$  and  $P_n$  data. However, in both cases the requirement for interchange was not fulfilled, thus necessitating the assignment of a value to the arbitrary constant which is present in each solution. Also for the  $P_g$  solution, both  $P_g$  and  $\bar{P}_g$  data were used although the possibility that the secondary P arrivals could be a phase equivalent to  $\bar{P}_g$  was recognised. The reliability of the time terms depends largely upon the reliability of the value chosen for the arbitrary constant. For the  $P_g$  case this value can be assumed reasonably accurately but as Agger and Carpenter point out "the arbitrary constant for the  $P_n$  data is subject to a much wider range, with little geological or other geophysical evidence to guide the choice".

There is considerable variation in the  $P_n$  time term thus obtained. The value obtained for the Eskdalemuir station was 2.87 sec. Those obtained from the Irish sea and south west England experiments were 3.04 and 3.14 sec respectively.

Assuming that the value chosen for the arbitrary constant was a reasonable one then this difference may be explained by the fact that poor velocity control was obtained by both the Irish Sea and south west England experiments whereas fully reversed coverage was obtained in the Eskdalemuir calibrations experiment. This value is thus not significantly different from the typical value found in the region of the stations along the south west England peninsula (cf. 2.72 sec at Land's End, 2.89 sec at Bodmin Moor). The  $P_g$  velocity obtained from the time term solution was  $6.12 \pm .06$  km/sec. This was assumed to extend all the way down to the bottom of the crust in the estimation of crustal thicknesses. These estimates were 27.1 km at the Eskdalemuir station and 25.1 km at the Rookhope station. Estimates of crustal thickness at the shot points ranged from 22.3 km for shot 5W to 34.2 km for shot 1W.

The velocity within the crust is almost certainly higher than  $P_g$ , thus the true crustal thicknesses are probably larger than those given above. It is thus suggested that the crust beneath northern England is significantly thicker than that in the south west England area. The  $P_n$  velocity obtained by Agger and Carpenter ( $7.99 \pm .10$  km/sec) is not significantly different from that found elsewhere in the British Isles. No reliable estimate of the average crustal velocity in the northern England area is available but it is suspected that it is more comparable to that in the southern Irish Sea than to that in south west England.

One further observation given by Agger and Carpenter was that of the possible presence of an intracrustal refractor as revealed by velocity filtering measurements at the Eskdalemuir array. This would agree with the observations of Key et al (1963) who recognised on some local earthquake records an arrival which was interpreted to be a  $P^*$  arrival associated with an intermediate layer. This would be additional evidence of a higher average crustal velocity in this region. However, the presence of such a layer in the vicinity of the Eskdalemuir station was not insisted upon by Agger and Carpenter.

Two measurements of  $P_n$  velocity in the North Sea are given by Collette et al (1967) and Sornes (1968). Collette et al shot two unreversed refraction lines, one of which was across the Dogger Bank. The preliminary analysis of this line gave estimates of the crustal thickness of 30 km and a  $P_n$  velocity of 8.30 km/sec although subsequent examination of the data has revealed that a  $P_n$  velocity of 8.15 km/sec is just as likely. Sornes obtained a velocity of 8.12 km/sec from a line of shots between Norway and Scotland but the crustal velocity is not reliably known and estimates of crustal thickness are not presented. These estimates of  $P_n$  velocity are thus probably not significantly different from those found elsewhere around Britain.

The evidence provided by the Southern Irish and Eskdalemuir calibration experiments suggest that the crust beneath

the more northerly parts of Britain may be significantly thicker than that beneath south west England. Also there is reliable evidence that, at least beneath the southern Irish Sea and probably more widely in northern Britain, the average crustal velocity is significantly larger than that in the south west. The significance of these observations will be discussed in the next section.

## 5.2 Geological interpretation of the results from the south west England experiment

This experiment has not been primarily concerned with the geological nature of the surface layers in the south west England region. However, where certain structures have been found, e.g. the sedimentary basin in the northern half of line 2, brief geological discussions have been presented (see Chapter 3). The main object of the experiment was to elucidate the crustal structure in the region along the granite batholith and in two lines at right angles to it. Parameters such as P-wave velocity have been measured and structures have been sought which may suggest the type of materials present and the processes that have occurred within the crust in this region.

The main feature of the Earth's crust in the area covered by the south west England experiment is that of the remarkable consistency it exhibits along two of the lines of shots.



In the region of lines 1 and 3 the crust is about 27 to 28 km thick bounded by an almost flat-lying Moho. The  $P_n$  velocity is about 8.07 km/sec and the average crustal velocity is about 6.1 to 6.15 km/sec. The results from line 2 of this experiment indicate that the Moho may dip gently towards the north at least along the northern half of the line with the result that the crust may be about 30 km thick beneath southern Ireland.

There is also some indication of a slightly higher  $P_n$  velocity and average crustal velocity along this line when compared to those along lines 1 and 3. However, the results from line 2 are not as reliable as those from lines 1 and 3 and it may be that there is no significant difference in these parameters from all three lines of the experiment.

The southern part of the south west England experiment is located well within that part of the crust dominated by the Hercynian orogeny. As has been indicated in section 5.1, the average crustal velocity in this region seems to be significantly lower than that in the northern parts of Britain. These latter areas are situated in regions of the crust which have been dominated by the Caledonian orogeny and have not subsequently been affected seriously by later orogenies. It is suggested that the difference noted in the average crustal velocities may be related not so much to the different orogenies themselves but to the difference in the type of materials that

were available for formation of 'new' crust in the areas affected by these orogenies. Seismic P-wave velocities within the basement rocks are predominantly lower in the Hercynian regions of the south west England area when compared to those obtained in the Caledonian region of the southern Irish Sea and in northern Britain. This difference at the surface may reflect the situation throughout the whole thickness of the crust in these contrasting regions.

If there are significantly higher average crustal velocities along line 2 of the south west England experiment, an explanation may be found in the fact that this line is close to the front between Caledonian and Hercynian belts. The crustal structure may be considerably complicated by the mixing together of two types of crust. The residual graph for the Land's End  $P_n$  data, after being compensated for the effects of the sedimentary basin (see section 3.3.4), may possibly be explained in terms of complexities at lower levels within the crust in this region.

Most of the early theories of the composition of the Earth's crust divided the crust into two layers, an upper 'granitic' layer and a lower 'basaltic' layer. Several variations of this theme have been suggested. For example, Bott (1961) postulated a crust consisting of an upper metamorphic layer beneath which a granitic layer is present

rising to the surface at the centre of mountain ranges. A layer below the granitic layer is postulated to be 'basaltic'. Recently, experimental and petrologic evidence has shown that the inference that the lower crust is composed of gabbroic and basaltic rocks is almost certainly wrong (Ringwood and Green 1964, Green and Ringwood 1967, Ringwood and Green 1966a).

In a paper discussing all their evidence, Ringwood and Green (1966b) show that gabbroic and basaltic rocks cannot exist at the pressures and temperatures which are presumed to be present in the lower parts of the crust. They suggest that in stable continental regions where the lower crust has usually undergone a complex orogenic, magmatic and metamorphic evolution, conditions are usually dry and the lower crust is probably composed of acid to intermediate rocks in the eclogite facies. However, in regions which have undergone a comparatively simple evolution under wet conditions, according to Ringwood and Green, the lower crust might contain large amounts of amphibolite.

The Caledonian region of northern Britain may be described as having undergone a simple evolution under wet conditions in the context of Ringwood and Green and thus it is possible that the lower crust in this region may consist of large amounts of amphibolite. The P-wave velocities measured in the southern Irish sea region especially are consistent with this hypothesis. On the other hand, the velocities measured in the Hercynian region of south west



England are not wholly explained by the contrasting presence of a lower crust composed of acidic to intermediate rocks in the eclogite facies. The region may have been subject to a more complex orogenic, magmatic and metamorphic evolution but the materials that were available for the formation of the 'new' crust during this evolutionary process must have been different from those available in northern Britain. The types of geological environment known to have been present in the two regions are consistent with this conclusion. Vast thicknesses of relatively high velocity basic volcanic lavas and tuffs are known to have been laid down along with sedimentary material in the Caledonian geosyncline whereas in the regions affected by the Hercynian orogeny in the south relatively little volcanic material was deposited.

The description of the upper crust as 'metamorphic' is reasonable in that the basement in many parts of the world is seen to be composed predominantly of metamorphic rocks. Apart from the presence of the granite batholith, this is true for the area covered by the south west England experiment where metamorphosed Devonian slates are present along the peninsula and metamorphic rocks occupy large areas of the basement in north western France. The presence of a true granitic layer beneath the 'metamorphic' layer, however, is still speculative.

The seismic results from line 1 have confirmed that a homogeneous layer, interpreted as granite, extends to a depth of about 10 to 11 km. Beneath this layer the lower crust has been interpreted to consist of materials exhibiting a gradual increase of velocity with depth to the base of the crust which is at a depth of 27 km. The true granite is thus occupying well over a third of the total crustal volume and it is shown to merge gradually into the lower crust.

A possible sequence of events leading to the origin of the granite batholith can be postulated. During the Hercynian orogeny, the crust was remobilised and the granite was formed by a process of selective fusion within the lower part of the crust. The true granite then migrated upwards towards the Earth's surface. As it did so, the relatively low velocity country rocks were broken up and sank as stoped material through the rising granite material. The lower crust thus consists of a mixture of the residuum left behind from the process of granite formation and the stoped material of the upper crust which the granite has replaced. The relatively low average P-wave velocity may be explained by the presence of large amounts of the low velocity upper crustal material which are present at depth. Those regions off the line of the batholith have probably not contributed to the process of granitisation. They owe their low average crustal

velocities to the low upper crustal velocity and the relatively low velocity in the lower crustal material whose acidic components have not been removed. A geological interpretation of the crustal structure in the region of the granite batholith is shown in fig. 39.

The geological interpretation presented above may be the subject of some difference of opinion but, at least, the aim of the south west England experiment to investigate a granite batholith in relation to the crust as a whole has provided further information which may help in the understanding of the origin of granite and its mode of emplacement.

### 5.3 Suggestions for the design of future crustal structure experiments

In the light of this interpretation of the south west England experiment and of those of other similar experiments around the British Isles, the following suggestions for the design of future crustal structure experiments in the region are proposed.

- 1) The advantage of the optimum shot and station conditions present in the British Isles should be utilised. The large sea areas bounded by the peninsulas of the British Isles provide the best conditions for the firing of large charges of explosive and for reception of the seismic waves

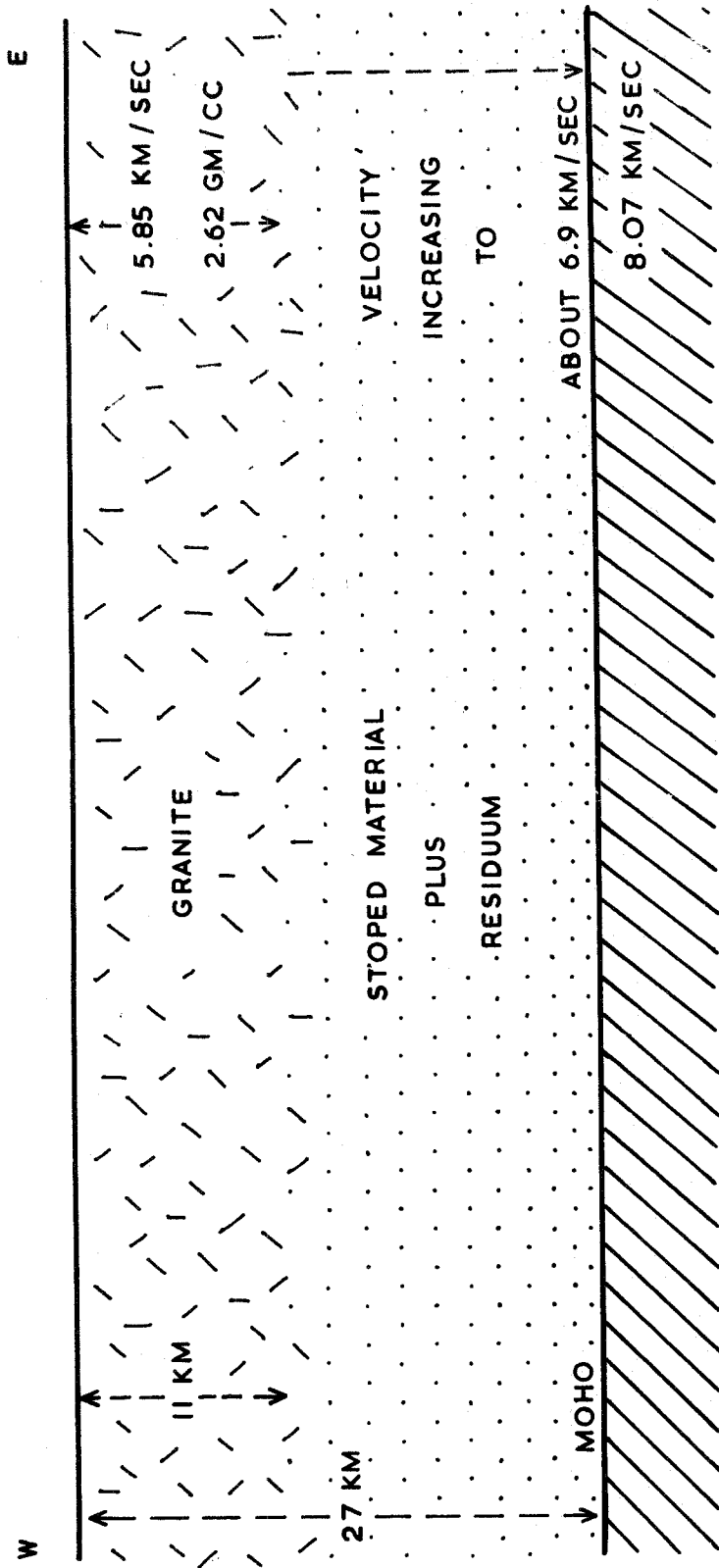


Fig.39. The geological interpretation of the crustal model along line 1.

thus generated at large distances. Navigation by the usual methods (Decca, Loran) is usually good in the sea areas around the British Isles except for a few localities. In addition, the use of satellite navigation is a further advantage which should be used if possible.

2) An experiment should be planned in relation to the known geological and geophysical features of the region. This is exemplified in the south west England experiment where lines of shots were exploded, one along the line of the granite batholith and two others at right angles to the known geological trends.

3) Provision must be made for the measurement of upper crustal variation in the vicinity of each shot point. This usually means the use of one or two ships using the seismic reflection technique (Hersey 1963), a sonobuoy refraction system (Hill 1963) or a two ship refraction system (Shor 1963) in the evaluation of such parameters as the thickness and the seismic velocity of the sediments above the basement. These ships may also be used in the main experiment to record the large shots.

4) In addition to the study of refracted arrivals, adequate provision should be made for the detailed study of the PMP phase and the other important phases described in this thesis. This is probably best achieved by the use of lines of shots between pairs of stations. In this way stacked

records can be obtained which may be used for correlation purposes. The use of arrays of seismometers for at least one of each pair of stations is also suggested for the measurement of phase velocities which aids identification. In addition, the lines of shots can be used to obtain reversed estimates of particular refractor velocities providing that overlapping segments representing the same refractor are present.

The shot spacing along these lines is important. In the regions of interest, e.g. near any suspected cusp point on a travel time graph, the shots should be as closely spaced as possible. A maximum shot spacing of 5 km should be sought if reasonably reliable estimates of, for example, maximum amplitude distances are to be obtained. The size of the shots is also important in this respect. Amplitude measurements are facilitated by the use of standard shot sizes and it is thus suggested that along these lines, at least, the size of the shots should not be altered.

5) The use of the time term approach as a basis for the design of an experiment is suggested although the following points should be considered.

a) It should first be ascertained whether any of the basic assumptions inherent in the time term approach are likely to be violated in the particular area of study. If they are, then the method of analysis should be abandoned and another basis of design adopted.

b) Provision for the interchange requirement must be made.

c)  $P_g$  arrivals are seen only in the range 10 to 120 km and  $P_n$  arrivals at distances greater than 120 km or more. The shot-station configuration must be designed accordingly if reliable time terms for these two refractors and for any intermediate refractor are to be obtained.

d) The shot-station configuration must provide lines of shots for the reason given in item 4 above.

It is hoped that future crustal structure experiments will benefit from these suggestions which are based upon the experience gained from the south west England crustal structure experiment.

APPENDIX A

## South west England experiment - shot data

SHOT NO.	DEPTH (METRES) ±4 METRES	POSITION		ERROR (KM)	TIME
		N	W		8TH NOV. 1966
1	154	49°01.0N	8°33.5W	3	06 01 03.41
2	160	49°09.0N	8°16.0W	2	07 15 56.86
3	154	49°14.5N	8°05.5W	2	07 56 11.80
4	150	49°19.0N	7°54.0W	2	08 37 42.00
5	126	49°24.0N	7°42.0W	2	09 19 50.07
6	142	49°28.0N	7°31.0W	2	09 58 45.72
7	136	49°33.0N	7°19.0W	2	10 44 46.24
8	134	49°38.0N	7°06.0W	1	11 26 47.99
9	128	49°43.0N	6°58.0W	1	12 01 50.68
10	112	49°46.5N	6°46.0W	1	12 37 54.22
11	104	49°50.2N	6°35.1W	1	13 12 48.51
12	72	49°52.1N	6°27.3W	0.5	13 49 30.13
13	80	49°55.9N	6°13.9W	0.5	14 57 37.50
14	80	49°58.0N	6°09.2W	0.5	15 14 56.20
15	78	50°00.1N	6°03.6W	0.5	15 33 56.83
16	72	50°03.2N	5°54.4W	0.5	16 06 23.68
17	64	50°05.1N	5°47.9W	0.5	16 37 03.69
18	60	50°06.1N	5°45.0W	0.5	16 53 52.75
					7TH NOV.
19	60	50°01.2N	5°43.5W	0.5	17 00 05.76



SHOT NO.	DEPTH (METRES) ± 4 METRES	POSITION		ERROR (KM)	TIME
		N	W		8TH NOV. 1966
20	50	50°11.5N	5°44.0W	0.5	17 23 19.13 5TH NOV.
21	44	50°13.2N	5°35.0W	0.5	10 59 19.02 4TH NOV.
22	92	51°28.4N	6°36.1W	1	21 23 48.99
23	104	51°21.0N	6°29.7W	1	22 01 39.49
24	106	51°13.8N	6°25.5W	1	22 44 30.34
25	114	51°04.9N	6°16.8W	1	23 33 05.96 5TH NOV.
26	108	50°57.5N	6°10.2W	1	07 00 58.95
27	108	50°49.5N	6°03.6W	1	07 40 53.13
28	100	50°41.2N	5°57.1W	1	08 23 03.15
29	96	50°35.5N	5°52.9W	1	08 51 55.13
30	82	50°27.9N	5°45.6W	0.5	09 39 57.70
31	60	50°19.8N	5°39.4W	0.5	10 20 10.63
32	58	50°01.1N	5°25.2W	0.5	13 48 31.45
33	68	49°55.6N	5°19.7W	0.5	14 17 58.26
34	94	49°48.9N	5°16.3W	0.5	14 50 06.85
35	100	49°41.4N	5°09.4W	1	15 30 45.45
36	102	49°33.7N	5°03.5W	1	16 08 58.61
37	116	49°26.1N	4°56.9W	1	16 48 01.55
38	108	49°18.2N	4°50.3W	1	17 28 00.75

SHOT NO.	DEPTH	POSITION		ERROR (KM)	TIME
	(METRES) $\pm$ 4 METRES	N	W		5TH NOV. 1966
39	110	49°11.0N	4°44.9W	1	18 06 56.63
40	132	49°02.9N	4°39.5W	1	18 47 07.61
41	112	48°55.1N	4°33.0W	1	19 25 30.11
					4TH NOV.
42	64	51°58.6N	7°00.7W	1	18 45 46.16
43	78	51°50.7N	6°55.2W	1	19 27 51.49
44	82	51°44.1N	6°49.5W	1	20 03 52.98
45	80	51°36.7N	6°43.0W	1	20 40 16.81

Notes on accuracy

1. The shot position errors are the maximum errors as supplied by the Navy.
2. Depth limits also given by the Navy (N.B. all shots exploded on seabed).
3. Because of some difficulty in identifying the water wave arrival for shots, 19, 28, 29, 31, 34, 38, 39, 40, 41, 44 these times are within  $\pm$  0.05sec. All other shot times are estimated to be within  $\pm$  0.02 sec.

APPENDIX B

First arrival travel time data for all stations from  
the south west England experiment

SCHELLY ISLES

SHOT NO.	FIRST ARRIVAL ONSET TIME			RANGE KM	$t_h$ HEIGHT SEC	1ST ARRIVAL TRAVEL TIME SEC
	HRS	MIN	SEC			
1	06	01	33.78	191.8	+0.02	30.40
2	07	16	23.55	165.9	+0.02	26.70
3	07	56	36.30	149.7	+0.02	24.50
4	08	38	04.49	133.4	+0.02	22.50
5	09	20	10.11	116.2	+0.02	20.05
6	09	59	03.01	101.0	+ 0.02	17.30
7	10	45	00.51	83.8	+0.02	14.25
8	11	26	59.30	65.6	+0.02	11.35
9	12	01	59.58	52.8	+0.02	8.90
10	12	38	00.46	37.0	+0.01	6.25
11	13	12	52.30	22.2	+0.01	3.80
12	13	49	32.15	12.3	+0.0	2.05
13	14	57	38.61	5.5	+0.01	1.10
14	15	14	58.39	12.0	+0.01	2.20
15	15	34	00.35	19.7	+0.01	3.55
16	16	06	29.30	32.1	0	5.60
17	16	37	10.67	40.6	0	7.00
18	16	54	00.56	44.6	0	7.70
20	17	23	28.11	50.8	0	9.00

SHOT NO.	FIRST ARRIVAL ONSET TIME			RANGE KM	$t_h$ HEIGHT SEC	1ST ARRIVAL TRAVEL TIME SEC
	HRS	MIN	SEC			
19	17	00	13.14	43.1	0	7.40
21	10	59	29.15	61.4	0	10.15
27	07	41	10.90	101.8	+0.01	17.75
28	08	23	19.0	88.3	+0.01	15.85
29	08	52	8.9	80.3	+0.01	13.75
30	09	40	10.1	71.8	+0.01	12.40
31	10	20	21.54	64.9	0	10.90
32	13	48	42.54	64.5	0	11.10
33	14	18	10.38	70.3	0	12.10
34	14	50	20.15	75.4	+0.01	13.30
35	15	31	00.77	86.8	+0.01	15.30
36	16	09	16.0	98.6	+0.01	17.20
38	17	28	22.61	126.6	+0.01	21.85
40	18	47	33.46	154.1	+0.02	26.85
41	19	25	58.62	169.5	+0.01	28.50

LAND'S END

1	06	01	41.31	252.9	-0.02	37.90
2	07	16	31.20	227.0	-0.02	34.30
3	07	56	43.67	210.8	-0.02	31.85
4	08	38	12.01	194.5	-0.02	30.00
5	09	20	18.03	177.3	-0.02	27.95
6	09	59	11.66	162.1	-0.02	25.90

SHOT NO.	FIRST ARRIVAL ONSET TIME			RANGE KM	$t_h$	1ST ARRIVAL TRAVEL TIME SEC
	HRS	MIN	SEC		HEIGHT SEC	
<u>LANDAS END (Cont.)</u>						
7	10	45	10.04	144.9	-0.02	23.80
8	11	27	09.57	126.7	-0.02	21.55
9	12	02	10.22	113.9	-0.02	19.50
10	12	38	11.13	98.1	-0.03	16.90
11	13	13	02.93	83.3	-0.03	14.40
12	13	49	42.79	73.4	-0.04	12.60
13	14	57	47.16	55.9	-0.03	9.65
14	15	15	04.94	49.1	-0.03	8.70
15	15	34	04.23	41.4	-0.03	7.35
16	16	06	28.87	29.0	-0.04	5.15
17	16	37	7.35	20.5	-0.04	3.60
18	16	53	55.71	16.6	-0.04	2.90
19	17	00	09.62	21.3	-0.04	3.80
20	17	23	21.59	13.5	-0.04	2.40
21	10	59	20.07	5.8	-0.04	1.00
22	21	24	15.73	162.6	-0.03	26.70
23	22	02	03.95	147.0	-0.03	24.45
24	22	44	53.45	132.9	-0.03	23.10
25	23	33	26.14	113.6	-0.03	20.15
26	07	01	16.65	97.9	-0.03	17.65
27	07	41	07.50	81.1	-0.03	14.35

SHOT NO.	FIRST ARRIVAL ONSET TIME			RANGE KM	$t_h$	1ST ARRIVAL TRAVEL TIME SEC
	HRS	MIN	SEC		HEIGHT SEC	

LAND'S END (Cont.)

28	08	23	14.51	63.9	-0.03	11.35
29	08	52	04.30	52.3	-0.03	9.15
30	09	40	04.37	35.8	-0.03	6.65
31	10	20	13.68	19.1	-0.04	3.00
32	13	48	35.04	19.5	-0.04	3.55
33	14	18	04.02	31.6	-0.04	5.70
34	14	50	15.12	44.5	-0.03	8.25
35	15	30	56.74	60.6	-0.03	11.25
36	16	09	02.26	76.6	-0.03	13.60
37	16	48	18.0	92.7	-0.03	16.40
38	17	28	20.43	109.4	-0.03	19.65
39	18	07	19.10	124.3	-0.03	22.45
40	18	48	21.07	140.6	-0.02	24.40
41	19	25	56.88	157.1	-0.03	26.75
44	20	04	23.55	195.6	-0.03	30.55
45	20	40	45.91	179.9	-0.03	28.95

CARNMENELLIS

1	06	01	44.10	273.7	-0.02	40.65
2	07	16	34.16	247.8	-0.02	37.30
3	07	56	46.72	231.7	-0.02	34.90

SHOT NO.	FIRST ARRIVAL ONSET TIME			RANGE KM	$t_h$ HEIGHT SEC	1ST ARRIVAL TRAVEL TIME SEC
	HRS	MIN	SEC			

CARNMENELLIS

5	09	20	20.98	198.3	-0.02	30.90
6	09	59	14.59	183.1	-0.02	28.85
7	10	45	13.20	166.0	-0.02	26.95
8	11	27	12.45	147.9	-0.02	24.45
9	12	02	13.41	135.3	-0.02	22.70
10	12	38	14.82	119.5	-0.03	20.55
11	13	13	6.62	104.7	-0.03	18.10
12	13	49	46.48	94.8	-0.04	16.30
13	14	57	50.95	77.2	-0.03	13.80
14	15	15	8.54	70.6	-0.03	12.30
15	15	34	7.99	62.9	-0.03	11.15
16	16	06	32.64	50.7	-0.04	8.90
17	16	37	11.21	42.2	-0.04	7.50
18	16	53	59.55	38.4	-0.04	6.75
20	17	23	25.70	35.8	-0.04	6.50

BODMIN MOOR

3	07	56	53.58	286.0	-0.03	41.75
5	09	20	27.45	252.5	-0.03	37.45
6	09	59	21.11	237.3	-0.03	35.35
7	10	45	19.70	220.1	-0.03	33.45
8	11	27	19.13	201.9	-0.03	31.10

SHOT NO.	FIRST ARRIVAL ONSET TIME			RANGE KM	$t_h$	1ST ARRIVAL TRAVEL TIME SEC
	HRS	MIN	SEC		HEIGHT SEC	
<u>BODMIN MOOR</u>						
9	12	02	20.00	189.0	-0.03	29.30
10	12	38	21.50	173.2	-0.04	27.25
11	13	13	14.15	158.5	-0.04	25.60
12	13	49	54.38	148.6	-0.05	24.20
13	14	57	59.45	131.1	-0.04	21.90
14	15	15	17.45	124.3	-0.04	21.20
15	15	34	17.00	116.6	-0.04	20.15
16	16	06	41.6	104.2	-0.05	17.85
17	16	37	20.22	95.7	-0.05	16.50
18	16	54	8.60	91.8	-0.05	15.80
19	17	00	22.7	95.1	-0.05	16.70
20	17	23	34.02	86.2	-0.05	14.85
21	10	59	31.80	75.1	-0.05	12.75
22	21	24	17.10	175.8	-0.04	28.05
25	23	33	28.95	133.3	-0.04	22.95
26	07	00	20.05	120.3	-0.04	21.15
27	07	41	11.68	107.6	-0.04	18.50
28	08	22	19.9	96.1	-0.04	16.70
29	08	52	10.50	89.6	-0.04	15.70
30	09	40	11.85	80.7	-0.04	14.10
31	10	20	23.28	75.8	-0.05	12.60



SHOT NO.	FIRST ARRIVAL ONSET TIME			RANGE KM	$t_h$ HEIGHT SEC	1ST ARRIVAL TRAVEL TIME SEC
	HRS	MIN	SEC			
<u>BODMIN MOOR (Cont.)</u>						
32	13	48	45.0	78.3	-0.05	13.50
33	14	18	12.45	81.5	-0.05	14.15
34	14	50	22.50	89.4	-0.04	15.70
41	19	26	00.50	176.4	-0.04	30.35
<u>DARTMOOR</u>						
3	07	56	59.32	335.9	-0.06	47.45
7	10	45	25.25	270.0	-0.06	39.85
8	11	27	25.30	251.8	-0.06	37.25
11	13	13	19.94	208.4	-0.07	31.35
12	13	50	00.41	198.5	-0.08	30.20
13	14	58	5.62	181.1	-0.07	28.05
14	15	15	23.57	174.3	-0.07	27.30
15	15	34	23.34	166.5	-0.07	26.45
16	16	06	49.00	154.1	-0.08	25.10
17	16	37	27.45	145.6	-0.08	23.70
18	16	54	16.06	141.7	-0.08	23.25
19	17	00	29.45	144.9	-0.08	23.60
20	17	23	41.75	136.0	-0.08	22.55
<u>WATERFORD</u>						
22	21	24	05.86	92.3	0	16.85
23	22	01	58.77	107.8	0	19.25
24	22	44	52.08	122.0	0	21.75

SHOT NO.	FIRST ARRIVAL ONSET TIME			RANGE KM	$t_h$	1ST ARRIVAL TRAVEL TIME SEC
	HRS	MIN	SEC		HEIGHT SEC	

WATERFORD (Cont.)

25	23	33	30.40	141.3	0	24.45
26	07	01	25.22	157.0	0	26.25
27	07	41	21.11	173.7	0	28.00
28	08	23	33.32	190.9	0	30.15
29	08	52	26.71	202.5	0	31.60
30	09	40	31.02	219.0	0	33.30
42	18	45	51.44	29.7	-0.01	5.25
43	19	28	00.15	45.6	0	8.65
44	20	04	04.18	59.4	0	11.20
45	20	40	30.72	75.0	0	13.90
31	10	20	47.17	235.7	-0.01	35.40

ESKDALEMUIR

22	21	24	56.2	484.1	-0.04	67.15
23	22	02	47.4	493.3	-0.04	67.85
24	22	45	39.6	503.4	-0.04	69.20
25	23	34	16.4	514.6	-0.04	70.40
26	07	02	10.30	524.5	-0.04	71.30
28	08	24	17.9	547.7	-0.04	74.70
29	08	53	10.8	556.2	-0.04	75.65
30	09	41	14.6	567.1	-0.05	76.85
42	18	46	48.4	449.3	-0.05	62.20
43	19	28	55.0	458.4	-0.04	63.50
44	20	04	57.7	465.7	-0.04	64.70
45	20	41	22.6	474.1	-0.04	65.75

SHOT NO.	FIRST ARRIVAL ONSET TIME			RANGE KM	$t_h$ HEIGHT SEC	1ST ARRIVAL TRAVEL TIME SEC
	HRS	MIN	SEC			
<u>FRENCH 2</u>						
41	19	25	30.11	46.7	0.01	8.10
40	18	47	18.92	63.1	0.02	11.30
39	18	07	10.53	79.5	0.01	13.90
38	17	28	17.36	94.3	0.01	16.60
37	16	48	20.9	111.0	0.01	19.35
36	16	09	20.36	127.2	0.01	21.75
35	15	31	09.33	143.1	0.01	23.85
34	14	50	32.74	159.3	0.01	25.90
33	14	18	25.72	172.2	0	27.45
<u>FRENCH 3</u>						
41	19	25	40.15	57.5	-0.01	10.05
40	18	47	20.87	73.9	0	13.25
39	18	07	12.43	90.3	-0.01	15.80
38	17	28	19.4	105.1	-0.01	18.65
37	16	48	23.0	121.8	-0.01	21.45
36	16	09	21.97	138.0	-0.01	23.15
35	15	31	10.63	153.9	-0.01	25.15
<u>FRENCH 4</u>						
41	19	25	41.82	66.9	0	11.70
40	18	47	22.47	83.4	+0.01	14.75
39	18	07	14.11	99.7	0	17.50
38	17	28	21.01	114.6	0	20.25
37	16	48	24.50	131.3	0	22.95
36	16	09	23.09	147.4	0	24.50
<u>FRENCH 5</u>						
41	19	25	43.78	77.7	-0.02	13.65
40	18	47	24.43	94.2	-0.01	16.80
39	18	07	16.00	110.6	-0.02	19.35
38	17	28	22.71	125.4	-0.02	21.95
37	16	48	25.8	142.1	-0.02	23.25
35	15	31	13.36	174.2	-0.02	27.90

SHOT NO.	FIRST ARRIVAL ONSET TIME			RANGE KM	$t_h$	1ST ARRIVAL TRAVEL TIME SEC
	HRS	MIN	SEC		HEIGHT SEC	
<u>FRENCH 6</u>						
41	19	25	45.17	87.0	0	15.05
40	18	47	25.85	103.5	+0.01	17.85
39	18	07	17.43	119.8	0	20.80
<u>FRENCH 7</u>						
41	19	25	46.9	97.0	-0.02	16.75
40	18	47	27.5	113.5	-0.01	19.90
39	18	07	19.06	129.9	-0.02	22.40
38	17	28	24.88	144.7	-0.02	24.10
35	15	31	15.50	193.5	-0.02	30.05
<u>FRENCH 9</u>						
41	19	25	50.58	119.5	-0.01	20.45
40	18	47	30.63	135.9	0	23.00
36	16	09	29.60	200.0	-0.01	31.00
<u>FRENCH 10</u>						
41	19	25	51.78	128.2	0	21.65
40	18	47	31.69	144.7	+0.01	24.10
38	17	28	28.64	175.9	0	27.90

## APPENDIX C

## Paper tape data input programme

The system developed by Dr. Lucas for the handling of paper tapes had to be scrapped completely when the Elliott 803 computer for which it had been developed was replaced by the IBM 360/67 computer early in 1968. A major problem was encountered in this change which will be described below.

The paper tape code used by Dr. Lucas is shown in fig.40 (see Lucas 1966 for a full description of this code). It can be seen that the second character of a pair constituting a single sample of information could be, in certain circumstances, a column of 8 blank locations. The high speed IBM 360 paper tape reader at Newcastle ignores blank characters with the consequence that vital pieces of information would be lost and the sequential flow of the data interrupted.

A PL/1 computer programme was written with the aid of Mr. R. Oddy of the Durham computer unit staff to read these tapes into the 360. Use was made of the regular pattern of blanks and holes which appears in location eight of each character in an effort to overcome the blank character problem. This pattern is interrupted when the time is written in code at the beginning of each second. The only way to overcome this problem is to punch single holes in location four of each blank character in the vicinity of the time code. This is absolutely necessary if the tape reader on the 360

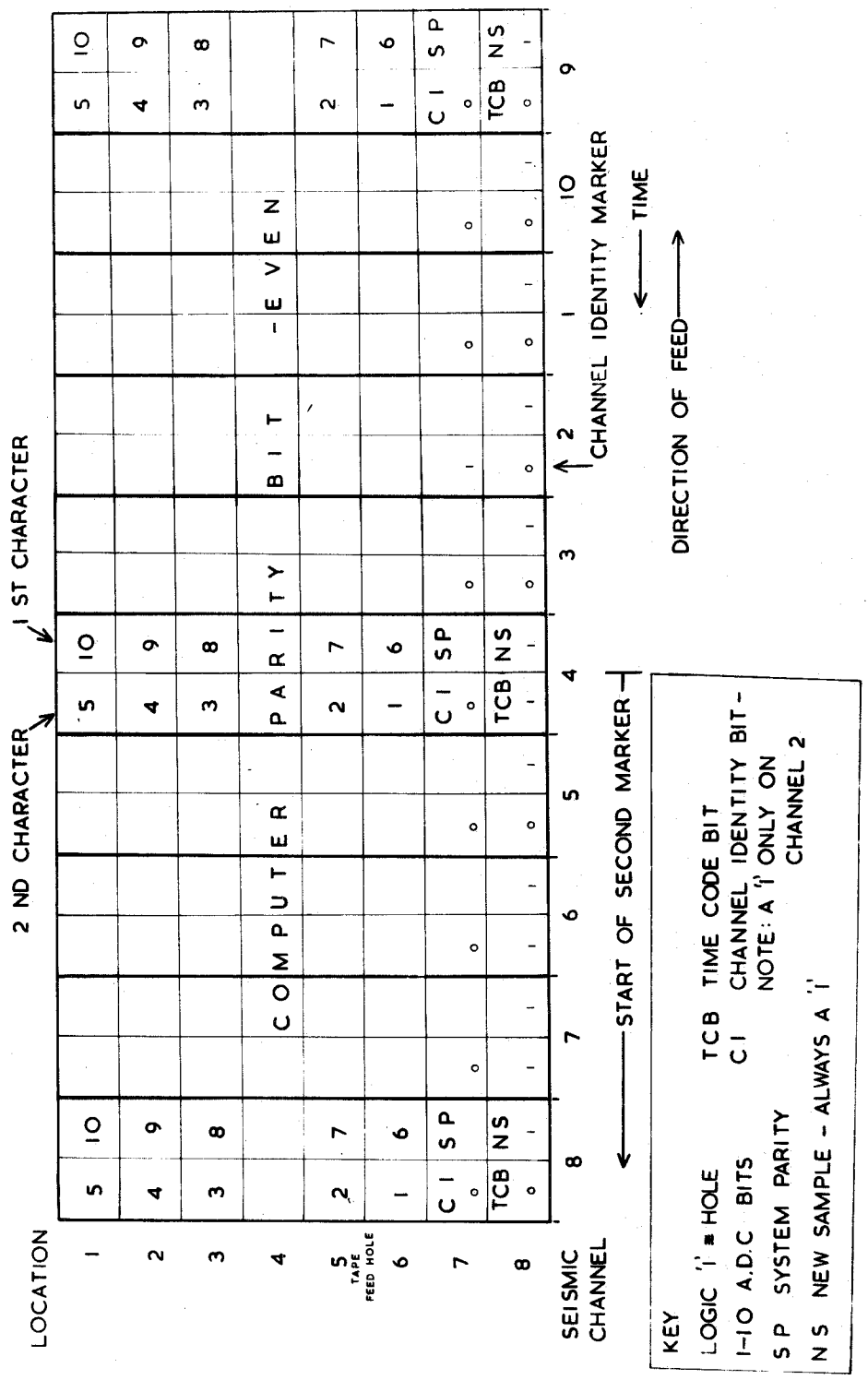


Fig.40. Paper tape format (after Lucas 1966).

in Newcastle is to be used.

There is a tape reader on the 1130 computer in Durham but it is sixteen times slower than the 360 reader. A tape containing 20 recorded seconds of seismic data takes 2.5 minutes to read and store on magnetic tape using the 360 reader. The 1130 reader is more difficult to programme for this sort of problem, the time involved is almost prohibitive and there is the added problem that the data must be transmitted to Newcastle via the G.P.O. telephone link for storage. The large amounts of data which result from a seismic survey such as the south west England experiment are far too much to store on the 1130 itself.

A further complication has arisen with the presence of what appears to be a random malfunctioning of the 360 paper tape reader in the reading of single hole characters. The overall effect of these problems is that less than half of the data recorded by the Land's End station is stored properly on the computer magnetic tape ready for processing.

The best way to overcome these problems would be to go back to the digital recording apparatus and modify the electronics such that no blank character was possible. It is possible, however, that a faster paper tape reader will soon be installed in Durham and it may be that this will provide an alternative solution to a most frustrating problem.

A print-out of the programme which is used to read in the paper tapes after they have been modified in the manner

described above is given below. The main programme steps are as follows.

- 1) A block of 1000 samples, each sample composed of two characters, is read into the computer. Each sample is unscrambled by stringing the relevant 'bits' together to form bit strings. These bit strings are then converted to decimal numbers by the subroutine STON which is written in Assembler and permanently stored in the computer. This operation is carried out in the double loop labelled LOOP.
- 2) Each individual channel sample is depedestalled by subtracting the mean of the first 100 samples of the particular seismic channel.
- 3) The computer space occupied by each sample is then halved by using the subroutine ECON which strings together one recorded second of data consisting of 100 samples of each seismic channel occupying a total of 2000 bytes of storage space. The subroutine NTOS, written in Assembler and permanently stored in the computer, is used here.
- 4) The recorded second of data, identified as REC, is then written on to computer magnetic tape in a physical sequential manner.
- 5) The next block of data is then read and processed in the manner described above.

The mean of the first 100



The means of the first 100 samples of each seismic channel are printed on the line-printer. Also the value of the variable LBTCH is increased by 1 and printed on the line-printer each time a block of 1000 samples is written successfully on to the magnetic tape. A final LBTCH number and a variable TOTAL indicating the total number of samples which have been successfully processed are printed at the top of a new page. This indicates where the programme has stopped reading the tape and thus tape errors can be found easily.

There are several built-in safeguards to make sure that the data stored on computer magnetic tape is correct. The programme will go to exit for the following reasons :

- a) There are more than 3 consecutive (alternate) blank characters. (Note, the programme could be modified, in the subroutine PAIR, to accept any number of alternate blank characters.)
- b) If, for any reason, the first character in a pair does not have a hole punched in location eight.
- c) If the number two seismic channel does not have a hole punched in location seven of the second character of a pair.
- d) If two consecutive characters with single holes punched in location four are detected. This is used to signify the end of the tape.

The programme is itself stored on disc and the whole operation is controlled by a simple 'calling' programme fed into the Newcastle card reader terminal.

Each paper tape from the south west England experiment was edited into lengths of 20 to 30 recorded seconds. The tapes were read into the computer as separate data sets identified by a dataset name and an SL number. Of the tapes that were successfully read into the computer some were read completely but others only partly so. A list of the dataset names and SL numbers and also the TOTAL numbers is given after the programme listing. Any programme requiring to use any one of these data sets needs to specify the dataset name and SL number in the job control cards.

```

/*          PAPER TAPE DATA INPUT PROGRAMME          */
PAPER:PROC OPTIONS(MAIN);
    DCL TOTAL FIXED BIN;
    DCL(ONE FIXED BIN INITIAL(1), ZERO FIXED BIN INITIAL(0))STATIC;
    DCL(LP FIXED BIN, ERRORS FLOAT)STATIC;
    DCL(T1,T2)CHAR(1), (B1,B2,B22,B23,B24,B25)BIT(8), (REC)CHAR(2000);
    DCL V BIT(32)ALIGNED, SEISMO(100,10)FIXED BIN;
    DCL(STON,NTOS)ENTRY EXTERNAL;
    DCL(MEAN(10))FIXED BIN, HALF FLOAT INITIAL(0.5);
    DCL SISYN FILE STREAM INPUT;
    DCL SEISM FILE STREAM OUTPUT;
    DCL PAIR ENTRY RETURNS(FIXED BIN);
    B22=(8)'0'B; B23=(8)'0'B; B24=(8)'0'B; B25=(8)'0'B;
    TOTAL=0; ERRORS=0; NN=0;

/**/
/**/
/**/
GET FILE(SISYN) LIST(LEATCH);
LBATCH=LBATCH-1;

/**/
LCCP: DO J=1 TO 100;
    DO K=1 TO 10;
        TOTAL=TOTAL+1;
        IF (TOTAL>1000*NN+990) THEN NN=NN+1;
        LQ=PAIR;
        IF LQ=ONE THEN GO TO FINISH;
        IF K=2 THEN EC;
        IF SUBSTR(B2,7,1)=0 THEN CC;
        GO TO FINISH; END; END;
        CALL PARITY(B1); IF B2=-'00010000'B THEN CALL PARITY(B2);

/**/
        W=(22)'0'B||SUBSTR(B1,1,3)||SUBSTR(B1,5,2)
           ||SUBSTR(B2,1,3)||SUBSTR(B2,5,2);

/**/
        CALL STON(W,M); SEISMO(J,K)=M;
        END; END;

/**/
/**/
IF LBATCH=0 THEN DO K=1 TO 10;
    MEAN(K)=FLOOR(SUM(SEISMO(*,K))/100+HALF);
    PUT SKIP DATA (MEAN(K)); END;

/**/
DO K=1 TO 10;
    SEISMO(*,K)=SEISMO(*,K)-MEAN(K); END;

/**/
CALL ECCN;
LBATCH=LBATCH+1;
PUT DATA (LBATCH);

/**/
PLT FILE (SEISM) EDIT (REC)(A(2000));

/**/
GO TO LCCP;

/**/
FINISH:PLT PAGE DATA (LBATCH);
PUT DATA (TOTAL);

/**/

```

```

PAIR: PRCC FIXEL BIN;
IF B22=(8)'0'B THEN DC;
B1=B22; B22=(8)'0'B;
GET EDIT (T2)(A(1)); P23=UNSPEC(T2);
IF SUBSTR(B23,8,1)=0 THEN DC;
B2=B23; B23=(8)'0'B; GO TO P1; END;
P2=(8)'0'B; GO TO P1; END;

/**/
IF B23=(8)'0'B THEN DC;
B1=B23; B23=(8)'0'B;
GET EDIT (T2)(A(1)); B24=UNSPEC(T2);
IF SUBSTR(B24,8,1)=0 THEN DC;
B2=B24; B24=(8)'0'B; GO TO P1; END;
P2=(8)'0'B; GO TO P1; END;

/**/
IF B24=(8)'0'B THEN DC;
B1=B24; B24=(8)'0'B;
GET EDIT (T2)(A(1)); P25=UNSPEC(T2);
IF SUBSTR(B25,8,1)=0 THEN DC;
B2=B25; B25=(8)'0'B; GO TO P1; END;
PUT LIST('MORE THAN 3 CONSECUTIVE BLANKS. LBATCH=',LBATCH);
PUT DATA (TCTAL);
STOP; END;

/**/
GET EDIT (T1,T2)(A(1));
IF (TCTAL>1000*NN-10) & (TCTAL<1000*NN+30) THEN DC;
B1=UNSPEC(T1); B2=UNSPEC(T2); GO TO P1; END;
P1=UNSPEC(T1); P22=UNSPEC(T2);
IF SUBSTR(B22,8,1)=0 THEN DC;
B2=B22; B22=(8)'0'B; GO TO P1; END;
P2=(8)'0'B;
P1: IF SUBSTR(B1,8,1)=0 THEN RETURN(CNE);
RETURN(ZERO);
END PAIR;

/**/
PARITY: PRCC(B);
DCL B BIT(8);
NCCOUNT=0;
DO N=1 TO 8;
NCCOUNT=NCCOUNT+SUBSTR(B,N,1); END;
IF (MOD(NCCOUNT,2)-=0) & (SUBSTR(B,5,1)=1) THEN DC;
SUBSTR(B,5,1)=0; END;
END PARITY;

/**/
ECCN: PRCC;
DCL (CCMP) CHAR(4);
DO J=1 TO 100;
DO K=1 TO 17;
M=SEISM(J,K); CALL NTCS(CCMP,M);
SUBSTR(REC,20*J+2*K-21,2)=SUBSTR(CCMP,3,2);
END; END; END ECCN;
END PAFFER;

```

Data from the Land's End station successfully recorded on  
computer magnetic tape

Magnetic tape            VOLUME = SER = DGPO4SO

Shot number	Dataset name	SL	Length of tape in secs	Value of TOTAL
20	DGPO420	1	12	12111
21	DGPO421	2	12	12091
30	DGPO430	3	22	22091
31	DGPO431	6	12	12091
34	DGPO434	7	22	22071
8 (1st part)	DGPO48A	9	20	20001
11	DGPO411	10	32	16999
12	DGPO412	11	33	33091
13	DGPO413	12	23	23091
44 (1st part)	DGPO444A	13	25	13046
16	DGPO416	14	22	19028
26 (2nd part)	DGPO426B	15	21	6996
3 (2nd part)	DGPO43B	16	24	23101
42 (2nd part)	DGPO442B	17	20	20001
9 (1st part)	DGPO49A	18	21	21001
1 (1st part)	DGPO41A	19	20	17028
1 (3rd part)	DGPO41C	20	20	20001
1 (2nd part)	DGPO41B	21	20	18028
1 (4th part)	DGPO41D	22	22	18799
2 (1st part)	DGPO42A	23	28	16042
14	DGPO414	24	23	23091
15	DGPO415	25	22	22091
18	DGPO418	26	22	22081
38 (1st part)	DGPO438A	28	20	11705
4 (1st part)	DGPO44A	29	27	15994
40 (1st part)	DGPO440A	30	20	20001
33 33	DGPO433	31	22	10002
35	DGPO435	32	32	32091
36	DGPO436	33	22	11995
27	DGPO427	34	33	18994

Magnetic tape            VOLUME = SER = DGPO4TO

26 (1st part)	DGPO426A	2	20	9608
45 (1st part)	DGPO445A	3	25	7962
22 (1st part)	DGPO422A	4	25	25001
5 (1st part)	DGPO45A	5	17	16992

```

C  LEAST SQUARES STRAIGHT LINE FIT PROGRAMME.
C  COMPUTES BEST STRAIGHT LINE TO FIT A SET OF
C  N PAIRS OF COORDINATES. GIVES GRADIENT OF LINE,
C  INVERSE OF GRADIENT, I.E. VELOCITY AND TIME
C  INTERCEPT. ALSO COMPUTES STANDARD ERRORS ON
C  THESE VALUES AND TIME RESIDUALS (OBSERVED-
C  CALCULATED) FOR EACH OBSERVATION
C  DATA CARDS REQUIRED ARE AS FOLLOWS
C    1. CARD BEARING TITLE OR IDENTIFYING MESSAGE.
C      FORMAT AS IN STATEMENT LABELLED 1
C    2. N WHERE N=NO.OF PAIRS OF COORDINATES TO
C      BE USED TO FIT THE STRAIGHT LINE
C      CODE WHERE 'CODE' IS AN IDENTIFIER FOR
C      THE PARTICULAR SET OF N PAIRS OF
C      COORDINATES
C      FORMAT AS IN STATEMENT LABELLED 2
C    NEXT N CARDS.  X  DISTANCE (ABSCISSA)
C                  Y  TRAVEL TIME (ORDINATE)
C      FORMAT AS IN STATEMENT LABELLED 3
C  THE PROGRAMME THEN RETURNS TO READ THE NEXT CARD
C  BEARING 'N' AND 'CODE' FOR THE NEXT SET OF DATA.
C  ANY NO. OF SETS OF DATA CAN BE PROCESSED IN THIS
C  WAY
C  A FINAL BLANK DATA CARD IN PLACE OF AN 'N, CODE'
C  CARD IS USED TO STOP THE PROGRAMME.

```

```

C      DIMENSION X1(100),Y1(100),AY(100),R(100)
10  READ(5,1)
1   FORMAT(72H
1       )
1   WRITE(6,1)
C
20  READ(5,2) N, CODE
2   FORMAT(14,2X,A4)
   WRITE(6,22) CODE
22  FORMAT(2X,A4)
   WRITE(6,5)
5   FORMAT(1H0 20X 'GRADIENT'5X,'INTERCEPT'5X,
1   'VELOCITY'5X,'SUM ERRORS'5X,'SE GRADIENT'5X,
2   'SE INTERCEPT'5X,'SE VELOCITY')
   IF (N.EQ.0) GO TO 50
C
   SX=0.
   SY=0.
   SX2=0.
   SY2=0.
   SXY=0.
   I=1
30  READ(5,3) X,Y
3   FORMAT(2F10.5)
   X1(I)=X
   Y1(I)=Y

```

```

C
      SX=SX+X
      SY=SY+Y
      SX2=SX2+X**2
      SY2=SY2+Y**2
      SXY=SXY+X*Y
      I=I+1
C
      IF (I.LE.N) GO TO 30
C
      XN=N
C
      A=(XN*SXY-SX*SY)/(XN*SX2-SX*SX)
      B=(SY*SX2-SX*SXY)/(XN*SX2-SX*SX)
      V=1./A
      RES=SY2+A*A*SX2+B*B*XN-2.*A*SXY-2.*B*SY
1+2.*A*B*SX
      C=RES/(XN-2.)
C
      SAS=XN*C/(XN*SX2-SX*SX)
      SBS=C*SX2/(XN*SX2-SX*SX)
      SA=SQRT(SAS)
      SB=SQRT(SBS)
C
      PERCA=100.*SA/A
C
      SV=V*PERCA/100.
C
      WRITE(6,4)A,B,V,C,SA,SB,SV
4  FORMAT(17X,F11.5,F14.5,F13.5,F15.5,F16.5,F18.5,
1F16.5)
      DO 40 I=1,N
      AY(I)=X1(I)*A+B
40  R(I)=Y1(I)-AY(I)
      WRITE(6,6)(AY(I),Y1(I),R(I),I=1,N)
6  FORMAT(1H0,20X,'CALCULATED'5X,'OBSERVED'5X,
1'RESIDUAL'//(20X,F10.5,2F13.5))
C
      GO TO 20
C
C
50 CALL EXIT
      END

```

## APPENDIX E

C TIME TERM ANALYSIS PROGRAMME.  
 C USES METHOD OF LEAST SQUARES TO SOLVE A NUMBER OF  
 C EQUATIONS GIVING TIME TERMS FOR N SHOTS AND  
 C STATIONS AND WITH THE OPTION OF CALCULATING THE  
 C SUB-REFRACTOR VELOCITY (ALSO BY LEAST SQUARES) OR  
 C CONSTRAINING THIS VELOCITY TO 10 SEPARATE VALUES.  
 C DATA CARDS REQUIRED ARE AS FOLLOWS

C 1. N WHERE N IS THE TOTAL NUMBER OF SHOTS  
 C AND STATIONS.

C FORMAT AS IN STATEMENT LABELLED 10

C THE NEXT SET OF DATA CARDS BEAR ALL THE TRAVEL  
 C TIME-DISTANCE OBSERVATIONS USED IN THE LEAST  
 C SQUARES PROCESS. EACH PAIR OF OBSERVATIONS IS  
 C RECORDED ON A SEPARATE CARD THUS

C I WHERE 'I' IS THE STATION CODE NUMBER  
 C J WHERE 'J' IS THE SHOT CODE NUMBER  
 C T(I,J) WHERE T(I,J) IS THE TRAVEL TIME  
 C OBSERVATION OF THE J'TH SHOT AT  
 C THE I'TH STATION.

C DELTA(I,J) WHERE DELTA(I,J) IS THE  
 C DISTANCE BETWEEN THE I'TH  
 C STATION AND J'TH SHOT.

C A BLANK CARD INDICATES THE END OF A  
 C PARTICULAR SET OF OBSERVATIONS

C FORMAT AS IN STATEMENT LABELLED 20

C NEXT CARD. VEL(II), II=1,10 WHERE VEL(II)  
 C ARE 10 CONSTRAINED VELOCITY VALUES  
 C IF THIS CARD IS LEFT BLANK THEN  
 C PROGRAMME COMPUTES LEAST SQUARES  
 C VELOCITY.

C FORMAT AS IN STATEMENT LABELLED 30

C NEXT CARD IS THAT BEARING THE TOTAL NUMBER OF  
 C SHOTS AND STATIONS FOR A DIFFERENT SET OF  
 C OBSERVATIONS. IT IS FOLLOWED BY THE SAME  
 C SEQUENCE OF DATA CARDS AS THAT DESCRIBED  
 C ABOVE. IF IT IS LEFT BLANK THEN THE PROGRAMME  
 C STOPS.

C NOTE THE SHOTS AND STATIONS MUST BE ASSIGNED  
 C CODE NUMBERS WHICH ARE LESS THAN OR EQUAL TO  
 C N AND THERE MUST BE NO OMISSIONS.

C NOTE ONLY A TOTAL OF 60 SHOTS AND STATIONS CAN  
 C BE USED WITH THE PROGRAMME AS IT IS. IF THERE  
 C ARE MORE SHOTS AND STATIONS THAN THIS THEN THE  
 C DIMENSION STATEMENTS MUST BE ALTERED ACCORDINGLY.



C  
 C NOTE SCIENTIFIC SUBROUTINES 'ARRAY', 'MINV' AND  
 C 'GMPRD' ARE USED BY THIS PROGRAMME. THUS THE JOB  
 C CONTROL CARDS MUST INDICATE THE USE OF THE  
 C SCIENTIFIC SUBROUTINE PACKAGE  
 C  
 C

```

      DIMENSION T(60,60),DELTA(60,60),EA(60),FA(60),
      1E(60),F(60),VEL(10),LK(60),MK(60)
      COMMON GAMMA(60,60),C(60,60),A(60),N
      REAL NUM
84 READ(5,10) N
      IF(N) 82,83,82
82 CONTINUE
      DO 100 I=1,N
      DO 100 J=1,N
      GAMMA(I,J)=0.
      C(I,J)=0.
      T(I,J)=0.
      DELTA(I,J)=0.
100 CONTINUE
25 READ(5,20) I,J,T(I,J),DELTA(I,J)
      WRITE(6,20) I,J,T(I,J),DELTA(I,J)
      IF(I) 5,15,5
5 DELTA(J,I)=DELTA(I,J)
      GAMMA(I,J)=1.
      GO TO 25
15 DO 1 I=1,N
      DO 2 J=1,N
      IF(I.NE.J) GO TO 4
      GO TO 50
4 C(I,J)=GAMMA(I,J)+GAMMA(J,I)
      GO TO 2
50 C(I,I)=0.
      DO 6 K=1,N
      C(I,I)=C(I,I)+GAMMA(I,K)+GAMMA(K,I)
6 CONTINUE
2 CONTINUE
1 CONTINUE
      WRITE(6,81)((C(I,J),I=1,6),J=1,6)
45 DO 500 I=1,N
      EA(I)=0
      FA(I)=0
      DO 600 J=1,N
      EA(I)=EA(I)+T(I,J)*GAMMA(I,J)+T(J,I)*GAMMA(J,I)
      FA(I)=FA(I)+DELTA(I,J)*(GAMMA(I,J)+GAMMA(J,I))
600 CONTINUE
500 CONTINUE
      CALL ARRAY(2,N,N,60,60,C,C)
      CALL MINV(C,N,D,LK,MK)
      WRITE(6,81)((C(I,J),I=1,6),J=1,6)
      CALL GMPRD(C,EA,E,N,N,1)
      CALL GMPRD(C,FA,F,N,N,1)
      READ(5,30)(VEL(II),II=1,10)
      IF(VEL(1))55,65,55

```

```

65 NUM=0
   DEN=0
   DO 700 I=1,N
   DO 800 J=1,N
   NUM=NUM+GAMMA(I,J)*(DELTA(I,J)-F(I)-F(J))**2
   DEN=DEN+GAMMA(I,J)*(DELTA(I,J)-F(I)-F(J))*
1(T(I,J)-E(I)-E(J))
800 CONTINUE
700 CONTINUE
   V=NUM/DEN
   DO 900 J=1,N
   A(J)=E(J)-F(J)/V
900 CONTINUE
   NUM=0
   DEN=0
   DO 1000 I=1,N
   DO 1100 J=1,N
   C(I,J)=T(I,J)-DELTA(I,J)/V-A(I)-A(J)
   NUM=NUM+(C(I,J)**2)*GAMMA(I,J)
   DEN=DEN+GAMMA(I,J)
1100 CONTINUE
1000 CONTINUE
   DEN=DEN-N
   IF(DEN.LE.0.5) GO TO 445
   SIGMAV=SQRT(NUM/DEN)
   WRITE(6,40)
   WRITE(6,51) V,SIGMAV
   GO TO 11
445 WRITE(6,54) V
11 CALL ERRORS
   GO TO 2000
55 WRITE(6,60)
   DO 1200 II=1,10
   WRITE(6,70) VEL(II)
   DO 1300 J=1,N
   A(J)=E(J)-F(J)/VEL(II)
1300 CONTINUE
   BURT=0
   FRED=0
   DO 1400 I=1,N
   DO 1500 J=1,N
   C(I,J)=T(I,J)-DELTA(I,J)/VEL(II)-A(I)-A(J)
   FRED=FRED+(C(I,J)**2)*GAMMA(I,J)
   BURT=BURT+GAMMA(I,J)
1500 CONTINUE
1400 CONTINUE
   BURT=BURT-N
   FITMOD=SQRT(FRED/BURT)
   WRITE(6,3) FITMOD
3 FORMAT(//F10.5)
   CALL ERRORS
1200 CONTINUE
10 FORMAT(I6)
20 FORMAT(2I6,4X,F5.2,4X,F6.2)

```

```
30 FORMAT(10F8.2)
40 FORMAT(2X 'CALCULATED VELOCITY'5X,'STD DEV OF
1VELOCITY')
51 FORMAT(10X,F6.3,15X,F8.6)
54 FORMAT(10X,F6.2)
60 FORMAT(22H CONSTRAINED VELOCITY)
70 FORMAT(F10.2)
81 FORMAT(6F10.2)
2000 CONTINUE
GO TO 84
83 CONTINUE
END
```

```
      SUBROUTINE ERRORS
C     SUBROUTINE OF TIME TERM ANALYSIS PROGRAMME
C     CALCULATES STANDARD DEVIATIONS AND STANDARD
C     ERRORS OF THE TIME TERMS.
      COMMON GAMMA(60,60),C(60,60),A(60),N
      REAL NUM
      WRITE(6,80)
      DO 3000 K=1,N
      NUM=0
      DEN=0
      DO 4000 I=1,N
      NUM=NUM+(C(I,K)**2)*GAMMA(I,K)+(C(K,I)**2)
      I*GAMMA(K,I)
      DEN=DEN+GAMMA(I,K)+GAMMA(K,I)
4000  CONTINUE
      DEN=DEN-1
      IF(DEN.LE.0.5) GO TO 8000
      SIGMA=SQRT(NUM/DEN)
      SIGMAS=SIGMA/SQRT(DEN+1)
      WRITE(6,90) K,A(K),SIGMA,SIGMAS
      GO TO 3000
8000  WRITE(6,95) K,A(K)
3000  CONTINUE
      80  FORMAT(2X 'SHOT/STAT NO'3X,'TIME TERM'2X,
      1'STD DEV'2X,'STD ERR')
      90  FORMAT(I9,9X,F6.2,4X,F8.5,F10.5)
      95  FORMAT(I9,9X,F6.2)
      END
```

## APPENDIX F

## Velocity filtering programme and results.

The listing of the programme given below is self-explanatory as far as the data and the main programme steps are concerned. However, the following points should be noted.

- 1) The programme has been written specifically for the Land's End array. Certain statements should be changed for any other array configuration. These statements are indicated in the listing.
- 2) It has been written assuming a fixed sampling interval of 0.01 second.
- 3) It works within a field of 11 seconds of recorded data but the first half-second and last second are lost in the process of obtaining the smoothed output. In addition, the second half-second is also lost when the smoothed output is plotted in graph form.
- 4) It assumes plane wave fronts.
- 5) The azimuth and distance of the event from the station are calculated using formula 5 given by Bullen (1963).
- 6) The output of the programme consists of line-printer output and punched cards. The first 10 samples of each seismic channel, the azimuth and distance of the event from the station and the delay distances are printed on the

line-printer. The delay times and smoothed output for each velocity value used in the velocity filtering process are also printed on the line-printer. The smoothed output for alternate velocity values and the 900 samples of a single seismic channel (channel 8) covering the 9 seconds of smoothed output are punched on cards. These cards are then used by the programme listed in Appendix G to plot records of the type given as a pull-out supplement in the back of this thesis.

The programme was tested with a plane sine wave which was presumed to have originated somewhere along line 2, travelling with a velocity of 5km/sec across the array. The maximum amplitude of the smoothed output and cross-correlation output for each 0.1km/sec increment of velocity from 4.0km/sec to 6.0km/sec are plotted in fig. 41. Both functions peak sharply at a velocity of 5.05km/sec. Thus for a discrete phase travelling across the array the programme may be assumed to give velocities which are reliable within  $\pm 0.1$ km/sec. The smoothed output is used to obtain estimates of phase velocity because it gives the same result as the cross-correlation output but with the amount of output reduced by a factor of 20.

The results obtained from this programme are presented after the programme listing below. It should be noted that not all the shots have been velocity filtered and usually only the first 11 seconds covering the onsets of the P-wave phases have

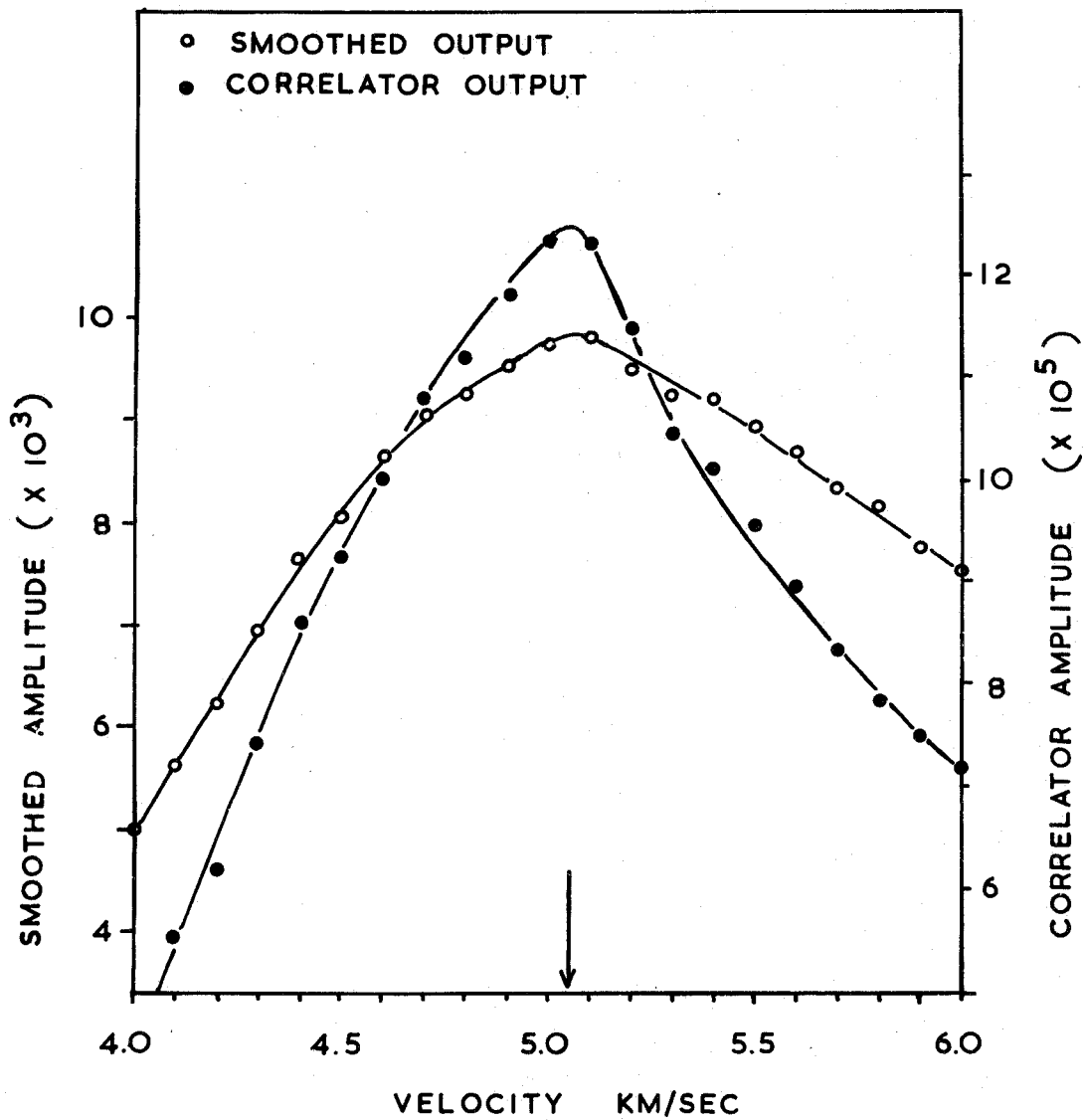


Fig.41. Smoothed and correlator outputs for an arrival travelling across the Land's End array at a velocity of 5 km/sec.

been processed. For a limited number of shots, however, the 11 second record including the onsets of the S phases have also been processed.

The array unit rectilinear coordinates as used for the velocity filtering process are as follows.

seismic channel	X (metres)	Y (metres)
1	73.21	73.21
2	669.40	-428.86
3	115.06	376.56
4	721.60	1098.3
5	-449.78	449.78
6	-868.18	805.42
7	-774.04	-606.68
8	-1014.62	-868.18
9	-1774.82	303.34
10	-282.42	156.90

It should be noted that channels 4 and 6 were permanently interchanged in the recording sequence after the firing of shot 19. Therefore, for shots 1 to 20, excluding shot 19, the recording sequence is : seismic channels 1, 2, 3, 6, 5, 4, 7, 8, 9 and 10.



C VELOCITY FILTERING PROGRAMME  
 C AFTER FIRST COMPUTING THE RANGE AND AZIMUTH OF  
 C AN EVENT FROM THE STATION THE PROGRAMME VELOCITY  
 C FILTERS OVER RECORDS OF 11 SECONDS LENGTH. IT  
 C DOES THIS AT VELOCITY INTERVALS OF 0.1 KM/SEC  
 C SUMMING TWO SETS OF SEISMOMETERS AND MULTIPLYING  
 C THE SUMS TOGETHER. IT SMOOTHS THE OUTPUT OVER A  
 C SQUARE WINDOW OF 0.2 SECONDS.  
 C FIRSTLY THE ARRAY SEISMIC DATA IS CALLED DOWN  
 C FROM THE EXTERNAL STORAGE DEVICE, IN THIS CASE A  
 C MAGNETIC TAPE, AND STORES IT THE COMPUTER MAIN  
 C STORAGE AREAS. THIS IS DONE IN STATEMENTS 7 TO 13  
 C THE FOLLOWING DATA CARDS ARE REQUIRED

- C 1. TITLE OR IDENTIFYING MESSAGE  
 C       FORMAT AS IN STATEMENT LABELLED 1
- C 2. W    THE EASTWARD DEVIATION OF THE Y AXIS  
 C        IN MINUTES.  
 C        DEG    REPRESENTING THE LATITUDE OF THE  
 C        MIN    REFERENCE POINT OF THE ARRAY IN  
 C        DEGREES AND MINUTES  
 C        FORMAT AS IN STATEMENT LABELLED 1 OF THE  
 C        SUBROUTINE 'ADELAY'
- C 3. DEG   REPRESENTING THE LONGITUDE OF THE  
 C        MIN    REFERENCE POINT OF THE ARRAY IN  
 C        DEGREES AND MINUTES  
 C        FORMAT AS IN STATEMENT LABELLED 2 OF THE  
 C        SUBROUTINE 'ADELAY'
- C 4. XD    THE X COORDINATE OF THE ARRAY  
 C        REFERENCE POINT.  
 C        YD    THE Y COORDINATE OF THE ARRAY  
 C        REFERENCE POINT.  
 C        FORMAT AS IN STATEMENT LABELLED 3 OF THE  
 C        SUBROUTINE 'ADELAY'
- C 5. N     THE NUMBER OF UNITS IN THE ARRAY  
 C        FORMAT AS IN STATEMENT LABELLED 4 OF THE  
 C        SUBROUTINE 'ADELAY'
- C 6,6+N. AX(I),AY(I),I=1,N   THE X AND Y  
 C        COORDINATES OF EACH ARRAY UNIT.  
 C        FORMAT AS IN STATEMENT LABELLED 3 OF THE  
 C        SUBROUTINE 'ADELAY'
- C 6+N+1. DEG    REPRESENTING THE LATITUDE OF THE  
 C        MIN    EVENT IN DEGREES AND MINUTES  
 C        FORMAT AS IN STATEMENT LABELLED 2 OF THE  
 C        SUBROUTINE 'ADELAY'
- C 6+N+2. DEG    REPRESENTING THE LONGITUDE OF THE  
 C        MIN    EVENT IN DEGREES AND MINUTES

```

C          FORMAT AS IN STATEMENT LABELLED 2 OF THE
C          SUBROUTINE 'ADELAY'
C
C          6+N+3  NVMIN  THE MINIMUM VELOCITY*10 TO BE
C                   USED
C          NVMAX  THE MAXIMUM VELOCITY*10 TO BE
C                   USED.
C          NDATFD WHERE NDATFD=1 IF SAMPLING OF
C                   ALL CHANNELS IS INSTANTANEOUS,
C                   =5 IF SAMPLING IS CYCLIC.
C          FORMAT AS IN STATEMENT LABELLED 2
C
C          6+N+4. G(I),I=1,N THE GAIN FACTORS INCLUDING
C                   POLARITY OF EACH ARRAY UNIT
C          FORMAT AS IN STATEMENT LABELLED 4
C
C  NOTE  PROGRAMME IS WRITTEN FOR A FIXED SAMPLING
C        INTERVAL PER CHANNEL OF .01 SECOND.
C        NORTH AND EAST ARE TAKEN TO BE POSITIVE
C
C
C        COMMON DEL(20),N,YD(20),IYY(20),BBXRR(3000),
C        1IINTEG(300)
C        COMMON SEISMO(1200,10)
C        INTEGER*2 SEISMO
C        DIMENSION TDEL(20),YO(20),G(20),SUMBB(3000),
C        1SUMRR(3000)
C        INTEGER SUMBB,SUMRR,G
C        INTEGER BBXRR
C
C        DO 1000 KK=1,1001,100
C        N1=KK+99
C        READ(1,400)((SEISMO(I,J),J=1,10),I=KK,N1)
C 1000 CONTINUE
C        400 FORMAT(200A2,200A2,200A2,200A2,200A2)
C        WRITE(6,401)((SEISMO(I,J),J=1,10),I=1,10)
C        401 FORMAT(10I10)
C
C        READ(5,1)
C        WRITE(6,1)
C
C        CALL ADELAY
C        WRITE(6,3)
C
C        READ(5,2) NVMIN,NVMAX,NDATFD
C        READ(5,4) (G(I),I=1,N)
C
C        DO 10 NV=NVMIN,NVMAX
C        V=NV
C        RV=V/10
C        WRITE(6,6) RV
C

```

C 20 LOOP COMPUTES FIRST DATA LOCATIONS TO BE USED  
C IN VELOCITY FILTERING CALCULATION  
C

```
DO 20 I=1,N
TDEL(I)=DEL(I)/V
IF(NDATFO.EQ.1) GO TO 100
YO(I)=51-(I-1)/N
GO TO 200
100 YO(I)=51
200 CONTINUE
YD(I)=YO(I)+TDEL(I)
YD(I)=YD(I)-1
20 CONTINUE
WRITE(6,59)(YD(I),I=1,N)
59 FORMAT(10F10.2)
```

C  
C  
C 30 LOOP CYCLES THROUGH K SETS OF DATA SUMMING  
C AND MULTIPLYING WITHIN EACH SET  
C

```
DO 30 K=1,1010
```

C  
C 40 LOOP CYCLES THROUGH EACH CHANNEL COMPUTING  
C DATA VALUES TO BE USED IN 30 LOOP  
C

```
DO 40 I=1,N
40 YD(I)=YD(I)+1
```

CALL INTERP

```
DO 41 I=1,N
41 IYY(I)=IYY(I)*G(I)
```

C  
C SUMMATION. THESE CARDS NEED TO BE CHANGED TO SUIT  
C PARTICULAR ARRAY CONFIGURATIONS.  
C

```
SUMBB(K)=IYY(6)+IYY(7)+IYY(8)+IYY(10)
SUMRR(K)=IYY(2)+IYY(5)+IYY(4)+IYY(9)
BBXRR(K)=SUMBB(K)*SUMRR(K)
```

30 CONTINUE

CALL INTEG

```
WRITE(6,5)(IINTEG(I),I=1,7)
WRITE(6,7)(IINTEG(I),I=8,187)
IF(AMOD(V,2.).GT.0.2) GO TO 55
WRITE(7,7)(IINTEG(I),I=8,187)
```

55 CONTINUE  
10 CONTINUE

```
WRITE(7,7)(SEISMO(I,8),I=101,1000)
```

1 FORMAT(72H  
1 )  
2 FORMAT(3I3)

```
3 FORMAT(///' VELOCITY')
4 FORMAT(10I3)
5 FORMAT(///7I7)
6 FORMAT(F10.2)
7 FORMAT(10I7)
```

C

```
GO TO 300
300 CALL EXIT
END
```

## SUBROUTINE ADELAY

C SUBROUTINE OF VELOCITY FILTERING PROGRAMME  
 C COMPUTES RANGE AND AZIMUTH OF EVENT FROM  
 C REFERENCE POINT OF A SEISMIC ARRAY, THE UNITS  
 C OF WHICH ARE REPRESENTED AS COORDINATES ON A  
 C LOCAL RECTILINEAR GRID AND FINDS DELAY DISTANCES  
 C OF EACH UNIT RELATIVE TO THE REFERENCE POINT  
 C ASSUMING A PLANE WAVE.

COMMON DEL(20),N,YD(20),IYY(20),BBXRR(3000),  
 LIINTEG(300)

COMMON SEISMO(1200,10)

INTEGER BBXRR

INTEGER\*2 SEISMO

DIMENSION AX(20),AY(20)

REAL LAT, LONG, K, M, MIN

INTEGER DEG

C  
 C READ EASTWARD DEVIATION OF Y-AXIS IN MINUTES  
 C AND LATITUDE OF REFERENCE POINT.

READ(5,1) W, DEG, MIN

PI=4\*ATAN(1.0)

RTOD=180/PI

LAT=(DEG+MIN/60)/RTOD

LAT=ATAN(.993277\*TAN(LAT))

C  
 C READ LONGITUDE OF REFERENCE POINT OF ARRAY

READ(5,2) DEG, MIN

LONG=(DEG+MIN/60)/RTOD

A=COS(LAT)\*COS(LONG)

B=COS(LAT)\*SIN(LONG)

C=SIN(LAT)

D=SIN(LONG)

E=-COS(LONG)

G=SIN(LAT)\*COS(LONG)

H=SIN(LAT)\*SIN(LONG)

K=-COS(LAT)

C  
 C READ X AND Y COORDINATES OF REFERENCE POINT

READ(5,3) XO, YO

C  
 C READ NUMBER OF ARRAY UNITS

READ(5,4) N

C  
 C READ X, Y COORDINATES OF ARRAY UNITS

READ(5,3){AX(I),AY(I),I=1,N}

```

C      READ LATITUDE OF EVENT
C
      READ(5,2) DEG,MIN
      LAT=(DEG+MIN/60)/RTOD
      LAT=ATAN(.993277*TAN(LAT))
C
C      READ LONGITUDE OF EVENT
C
      READ(5,2) DEG,MIN
      LONG=(DEG+MIN/60)/RTOD
      AD=COS(LAT)*COS(LONG)
      BD=COS(LAT)*SIN(LONG)
      CD=SIN(LAT)
      CANGLE=A*AD+B*BD+C*CD
      ANGLE=ARCOS(CANGLE)
      R=ANGLE*6371.024
      SANGLE=SIN(ANGLE)
      ANGLE=ANGLE*RTOD
      SZ=((AD-D)**2+(BD-E)**2+CD**2-2)/(2*SANGLE)
      CZ=((AD-G)**2+(BD-H)**2+(CD-K)**2-2)/
1      (2*SANGLE)
      Z=ARSIN(SZ)
C
      IF((SZ.GE.0).AND.(CZ.GE.0)) GO TO 40
      IF((SZ.GE.0).AND.(CZ.LT.0)) GO TO 50
      IF((SZ.LT.0).AND.(CZ.LT.0)) GO TO 50
      IF((SZ.LT.0).AND.(CZ.GE.0)) GO TO 60
C
40      Z=Z
      GO TO 120
50      Z=PI-Z
      GO TO 120
60      Z=2*PI+Z
C
120     T=Z*RTOD
C
      WRITE(6,6)
      WRITE(6,7) ANGLE,R,T
C
C      CALCULATION OF ARRAY DELAY DISTANCES FOR
C      AZIMUTH T(Z)
C
      M=3*PI/2-Z+W/(RTOD*60)
      IF((ABS(M).LT.5E-5).OR.(ABS(PI-M).LT.5E-5))
1GO TO 10
      IF((ABS(M-PI/2).LT.5E-5).OR.(ABS(M+PI/2).LT.
15E-5).OR.(ABS(3*PI/2-M).LT.5E-5)) GO TO 20
C
      M=TAN(M)
      K=M+1/M
      SZ=SIN(Z-W/(RTOD*60))
C

```

```

DO 30 I=1,N
C
      XB=(M*XO+AX(I)/M+AY(I)-YO)/K
      YB=(M*AY(I)+YO/M+AX(I)-XO)/K
C
      DELAY=SQRT((XO-XB)**2+(YO-YB)**2)
C
      IF(ABS(SZ-(XB-XO)/DELAY).LT.1E-5) GO TO 70
C
110 DEL(I)=DELAY
      GO TO 30
C
70 DELAY=-DELAY
      GO TO 110
30 CONTINUE
      WRITE(6,1000)(DEL(I),I=1,N)
C
      GO TO 100
10 DO 80 I=1,N
      DELAY=SZ*(XO-AX(I))
      DEL(I)=DELAY
80 CONTINUE
      WRITE(6,1000)(DEL(I),I=1,N)
      GO TO 100
C
20 DO 90 I=1,N
      DELAY=CZ*(YO-AY(I))
      DEL(I)=DELAY
90 CONTINUE
      WRITE(6,1000)(DEL(I),I=1,N)
      GO TO 100
C
C
1 FORMAT(F9.2,5X,I4,5X,F6.2)
2 FORMAT(I4,5X,F6.2)
3 FORMAT(F9.2,5X,F9.2)
4 FORMAT(I3)
6 FORMAT(///' ANGLE      RANGE      AZIMUTH')
7 FORMAT(F6.2,4X,F7.2,4X,F6.2)
1000 FORMAT(10F10.2)
C
100 RETURN
      END

```

## SUBROUTINE INTERP

```
C
C SUBROUTINE OF VELOCITY FILTERING PROGRAMME.
C INTERPOLATES BETWEEN TWO VALUES BY THE METHOD
C OF FORWARD DIFFERENCES.
C
```

```
COMMON DEL(20),N,T(20),IYY(20),BBXRR(3000),
IIINTEG(300)
```

```
COMMON SEISMO(1200,10)
```

```
INTEGER*2 SEISMO
```

```
INTEGER DY0,DY1,DY2,D2Y0,D2Y1,D3Y0
```

```
INTEGER BBXRR
```

```
C
DO 10 I=1,N
    IT=T(I)
    XXO=T(I)-(IT-1)
```

```
C
C CALCULATES 1ST,2ND AND 3RD FORWARD DIFFERENCES
C
```

```
DY0=SEISMO(IT,I)-SEISMO(IT-1,I)
```

```
DY1=SEISMO(IT+1,I)-SEISMO(IT,I)
```

```
DY2=SEISMO(IT+2,I)-SEISMO(IT+1,I)
```

```
D2Y0=DY1-DY0
```

```
D2Y1=DY2-DY1
```

```
D3Y0=D2Y1-D2Y0
```

```
C
    IYY(I)=SEISMO(IT-1,I)+XXO*DY0+(XXO*(XXO-1)
10 CONTINUE
    *D2Y0)/2+(XXO*(XXO-1)*(XXO-2)*D3Y0)/(3*2)
```

```
C
    RETURN
    END
```



```
SUBROUTINE INTEG
C SUBROUTINE OF VELOCITY FILTERING PROGRAMME.
C SMOOTHS M+1 VALUES OF BBXRR WHERE M=FIFTH OF
C THE CHANNEL SAMPLING RATE PER SECOND BY THE
C TRAPEZOIDAL METHOD
COMMON DEL(20),N,YD(20),IYY(20),BBXRR(3000),
1IINTEG(300)
COMMON SEISMO(1200,10)
INTEGER*2 SEISMO
INTEGER BBXRR
C
      I=1
      L=2
      M=20
10 MOSTY=0
   DO 20 K=L,M
20 MOSTY=MOSTY+BBXRR(K)
   MOSTY=2*MOSTY
C
   IINTEG(I)=(BBXRR(L-1)+BBXRR(M+1)+MOSTY)/2000
C
      L=L+5
      M=M+5
      I=I+1
   IF(M.GE.1001) GO TO 30
   GO TO 10
30 CONTINUE
RETURN
END
```

## Results from the velocity filtering programme.

Shot no.	Phase	Phase Velocity km/sec	Approximate Onset time		
			hrs	mins	secs
1	P <sub>n</sub> (1)	7.9	06	01	41.3
1	P <sub>n</sub> (2)	7.9	"	"	42.0
1	P <sub>g</sub>	5.6	"	"	46.5
1	?	5.6	"	"	47.7
2	P <sub>n</sub> (1)	7.9	07	16	31.2
2	P <sub>n</sub> (2)	7.8	"	"	31.4
2	P <sub>g</sub>	5.8	"	"	35.9
2	?	6.0	"	"	37.3
2	?	6.4	"	"	38.8
4	P <sub>n</sub> (1)	8.0 (8.5)	08	38	12.6
4	P <sub>n</sub> (2)	8.0	"	"	12.9
4	?	5.2	"	"	16.2
4	P <sub>g</sub>	5.7	"	"	16.6
4	?	5.9	"	"	17.6
4	?	6.2	"	"	19.6
8	P <sub>n</sub>	7.7	11	27	09.6
8	P <sub>g</sub> or PMP	5.6	"	"	10.2
8	?	6.8	"	"	11.4
8	?	5.7	"	"	13.1
9	P <sub>g</sub>	5.3	12	02	11.9
9	PMP	6.1	12	02	12.1
9	?	5.3	"	"	17.0
9	S <sub>g</sub>	3.4	"	"	23.4
9	SMS	4.1	"	"	25.4
11	P <sub>g</sub>	5.6	13	13	02.9
11	?	6.0	"	"	03.6
11	PMP	7.1	"	"	04.9
11	S <sub>g</sub>	3.4	"	"	15.8
11	SMS	4.3	"	"	17.5

Shot No.	Phase	Phase Velocity km/sec	Approximate Onset time		
			hrs	mins	secs
12	P <sub>g</sub>	5.6	13	49	42.8
12	?	5.9	"	"	44.6
12	PMP	8.4	"	"	46.2
12	S <sub>g</sub>	3.4	"	"	53.9
12	?	3.7	"	"	55.4
13	P <sub>g</sub> (1)	5.4	14	57	47.2
13	P <sub>g</sub> (2)	5.4	"	"	47.5
14	P <sub>g</sub> (1)	5.4	15	15	04.9
14	P <sub>g</sub> (2)	5.3	"	"	05.2
15	P <sub>g</sub> (1)	5.1	15	34	04.2
15	P <sub>g</sub> (2)	5.3	"	"	04.5
15	S <sub>g</sub> (1)	3.1	15	34	10.1
15	S <sub>g</sub> (2)	3.0	"	"	10.8
16	P <sub>g</sub> (1)	5.4	16	06	28.9
16	P <sub>g</sub> (2)	5.6	"	"	29.8
18	P <sub>g</sub> (1)	5.2	16	53	55.7
18	P <sub>g</sub> (2)	5.0	"	"	56.1
18	S <sub>g</sub>	3.1	"	"	57.5
21	P <sub>g</sub> (1)	5.0	10	59	20.1
21	P <sub>g</sub> (2)	5.1	"	"	20.4
21	S <sub>g</sub>	2.9	"	"	20.7
21	Surface waves	2.5	"	"	21.7
30	P <sub>g</sub>	5.3	09	40	04.4
30	?	5.9	"	"	04.8
30	S <sub>g</sub> (1)	4.0	"	"	08.9
30	S <sub>g</sub> (2)	4.0	"	"	09.4
35	P <sub>g</sub> (1)	6.4	15	30	56.7
35	P <sub>g</sub> (2)	6.4	"	"	57.2
35	PMP	8.1	"	"	59.4
36	P <sub>g</sub>	5.3	16	09	02.3
36	?	6.8	"	"	02.5

Shot no.	Phase	Phase Velocity km/sec	Approximate onset time		
			hrs	mins	secs
36	PMP	7.9	16	09	04.2
38	P <sub>g</sub>	6.5	16	48	18.0
38	PMP	7.1	"	"	18.4
40	P <sub>n</sub> (1)	7.7	18	48	21.1
40	P <sub>n</sub> (2) ?	8.3	"	"	21.3

## APPENDIX G

```

C          PLOT OF VELOCITY FILTERED RECORDS
C THIS PROGRAMME TAKES THE PUNCHED CARD OUTPUT FROM THE
C VELOCITY FILTERING PROGRAMME AND PLOTS THE SMOOTHED
C OUTPUT FOR EACH INCREMENT OF VELOCITY AND THE UNPROCESSED
C SINGLE CHANNEL SEISMIC DATA ON THE GRAPH PLOTTER WITH THE
C AID OF THE PLOTTING SUBROUTINES PROVIDED WITH THE 1130
C COMPUTER.
C THE DATA CARDS REQUIRED ARE AS FOLLOWS
C   1. CARD BEARING TITLE TO BE WRITTEN ON THE GRAPH
C      FORMAT AS IN STATEMENT LABELLED 52
C   2. NOPRO  NUMBER OF PROFILES TO BE PLOTTED
C      PRINT   INTERVAL BETWEEN PROFILES IN INCHES
C      VEINT   VELOCITY INTERVAL IN KM/SEC
C      VEMAX   MAXIMUM VELOCITY VALUE
C      NOBS   NUMBER OF VALUES TO BE PLOTTED FOR EACH
C             PROFILE
C      YSCAL   SCALE FACTOR FOR AMPLITUDES OF PROFILES
C      FORMAT AS IN STATEMENT LABELLED 51
C NEXT SET OF CARDS BEARS THE SMOOTHED OUTPUT FOR NOPRO
C PROFILES, 10 VALUES PER CARD
C      FORMAT AS IN STATEMENT LABELLED 14
C NEXT 90 CARDS BEAR THE UNPROCESSED SINGLE CHANNEL SEISMIC
C DATA VALUES, 10 TO A CARD
C      FORMAT AS IN STATEMENT LABELLED 14
C DIMENSION IAMPL(200),AMPL(200)
C CALL SCALE(1.,1.,0.,0.)
C YAX=-1.78
C ITIME=11
C PI=3.14159
C
C 1 LOOP WRITES TIMES FROM 10 TO 1 AT 1 INCH INTERVALS
C*****
C DO 1 I=1,10
C   YAX=YAX+1.
C   CALL ECHAR(-0.35,YAX,0.15,0.2,-PI/2)
C   ITIME=ITIME-1
C   WRITE(7,4)ITIME
C 4  FORMAT(I2)
C 1  CONTINUE
C*****
C X AXIS IS DRAWN AND LABELLED
C
C CALL EGRID(3,0.,8.,1.,9)
C CALL ECHAR(-0.7,4.8,0.16,0.2,-PI/2)
C WRITE(7,5)
C 5  FORMAT('TIME (SECS)')
C READ(2,52)
C 52 FORMAT(43H
C WRITE(5,52)
C READ(2,51)NOPRO,PRINT,VEINT,VEMAX,NOBS,YSCAL
C 51 FORMAT(12,3F4.1,I3,E10.2)

```

```

C HEADINGS AND DATA PRINTED ON LINEPRINTER
  WRITE(5,53)
53 FORMAT(3X 'NOPRO'5X, 'PRINT'5X, 'VEINT'5X, 'VEMAX'5X,
  1'NOBS'4X, 'YSCAL')
  WRITE(5,54) NOPRO, PRINT, VEINT, VEMAX, NOBS, YSCAL
54 FORMAT(//I6, 3F10.1, I10, E13.2)
C DRAW Y-AXIS, WRITE VELs AT CHOSEN PROFILE INTERVALS
C AND LABEL AXIS.
C
  CALL EGRID(0,0.,8.,PRINT,NOPRO)
  A=NOPRO+1
  XAX=A*PRINT
  VEMAX=VEMAX+VEINT
C*****
  DO 6 I=1,NOPRO
  XAX=XAX-PRINT
  CALL ECHAR(XAX,8.7,0.15,0.2,-PI/2)
  VEMAX=VEMAX-VEINT
  WRITE(7,8)VEMAX
  8 FORMAT(F4.1)
  6 CONTINUE
C*****
  YUNIT=A*PRINT/2-1
  CALL ECHAR(YUNIT,8.75,0.15,0.2,0)
  WRITE(7,11)
  11 FORMAT('VELOCITY KM/S')
C
C DOUBLE LOOP READS AMPLITUDES, IAMPL, AND PLOTS PROFILE.
C PEN RETURNS TO NEW ORIGIN AND PLOTS NEXT PROFILE
C
  CALL EPLLOT(1,0.,8.)
  PORIG=0.
  PORIG=PORIG+PRINT/YSCAL
C*****
  DO 12 J=1,NOPRO
  CALL SCALE(YSCAL,1.,-PORIG,0.)
  CALL EPLLOT(1,0.,0.)
  CALL EPLLOT(2,0.,0.)
  CALL POINT(1)
  TINT=0.05
C
  *****
  READ(2,14)(IAMPL(I),I=1,NOBS)
  14 FORMAT(10I7)
  DO 13 I=1,NOBS
  AMPL(I)=IAMPL(I)
  TINT=TINT-0.05
  CALL EPLLOT(2,AMPL(I),TINT)
  13 CONTINUE
C
  *****
  CALL EPLLOT(1,0.,0.)
  12 CONTINUE
C
C FOR LAND'S END DATA IF YSCAL=0.50E-02 THEN NEXT CARD IS
C CORRECT. IF YSCAL=0.50E-03 THEN NEXT CARD SHOULD READ
C
  CALL SCALE(YSCAL*10.,1.,-2.*PORIG/10.,0.)
  CALL SCALE(YSCAL,1.,-2*PORIG,0.)
  CALL EPLLOT(1,0.,0.)

```

```
TINT=0.01
DO 16 J=1,9
READ(2,14)(IAMPL(I),I=1,100)
DO 15 I=1,100
TINT=TINT-0.01
AMPL(I)=IAMPL(I)
CALL EPLOT(2,AMPL(I),TINT)
15 CONTINUE
16 CONTINUE
CALL EPLOT(1,0.,0.)
C*****
CALL SCALE(1.,1.,0.,0.)
B=PRINT+1
CALL ECHAR(B,0.,0.2,0.2,-PI/2)
WRITE(7,52)
CALL EXIT
END
```

## APPENDIX H

The theory behind the use of the critical distance ( $C_1$ ) and the grazing incidence distance ( $C_2$ ) in the evaluation of the depth at which a linear increase of velocity with depth begins.

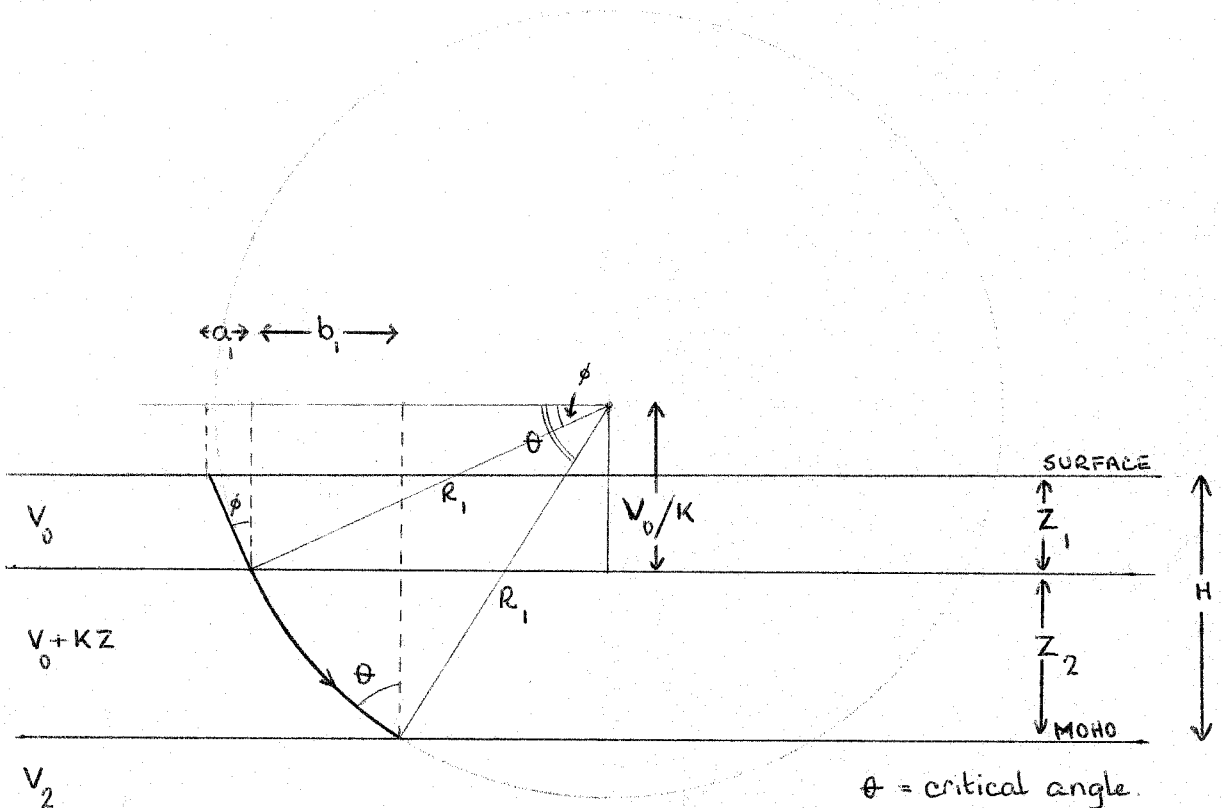


Diagram 1. The crustal model and critical distance ray path.

Consider a model of the crust, total thickness  $H$ , consisting of an upper homogeneous layer with velocity  $V_0$  and thickness  $Z_1$  and a lower layer, thickness  $Z_2$ , exhibiting a linear increase of velocity with depth given by the relationship  $V_0 + KZ$ , overlying a half-space with velocity  $V_2 > V_0 + KZ_2$ .



Assuming this model and the critical ray path of a P-wave travelling through this structure then, from a consideration of diagram 1, the critical distance ( $C_1$ ) can be obtained in terms of the constant of velocity ( $K$ ) and the thickness of the upper layer ( $Z_1$ ) thus :-

$$C_1 = 2 (a_1 + b_1).$$

$$\frac{C_1}{2} = Z_1 \tan \phi + \frac{V_0}{K \tan \phi} - \frac{(V_0 + KZ_2)}{K \tan \theta}.$$

Substituting for  $\tan \phi$  and  $\tan \theta$  we have

$$\frac{C_1}{2} = \frac{Z_1 V_0}{\sqrt{K^2 R_1^2 - V_0^2}} + \frac{\sqrt{K^2 R_1^2 - V_0^2}}{K} - \frac{\sqrt{K^2 R_1^2 - (V_0 + KZ_2)^2}}{K}.$$

We have from Snell's law,

$$\sin \theta = \frac{V_0 + KZ_2}{V_2}.$$

Therefore

$$\frac{V_0 + KZ_2}{R_1 K} = \frac{V_0 + KZ_2}{V_2}.$$

Therefore

$$R_1 = \frac{V_2}{K}.$$

Therefore

$$\frac{C_1}{2} = \frac{Z_1 V_0}{\sqrt{V_2^2 - V_0^2}} + \frac{\sqrt{V_2^2 - V_0^2}}{K} - \frac{\sqrt{V_2^2 - (V_0 + KZ_2)^2}}{K}, \quad (1)$$

where  $Z_2 = H - Z_1$ .

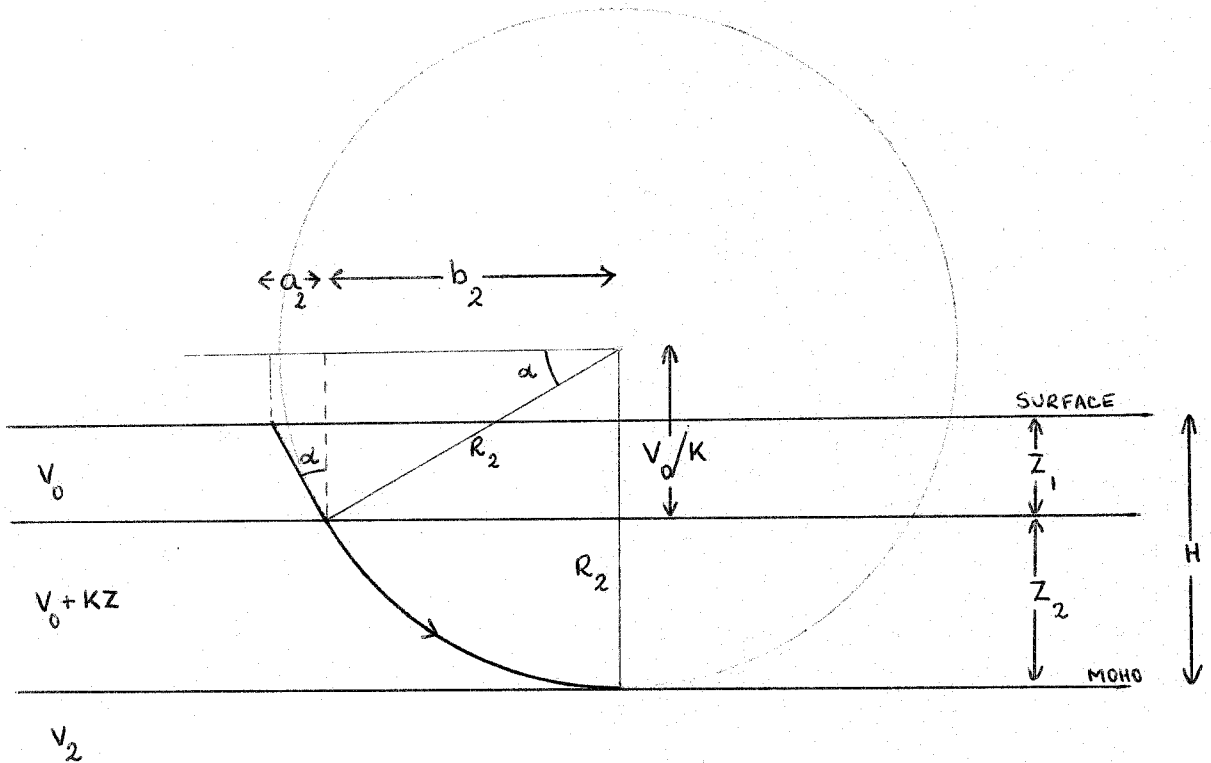


Diagram 2. The crustal model and grazing incidence ray path.

Assuming the same model of the crust but the grazing incidence ray path of a P-wave travelling through the structure then, from a consideration of diagram 2, the grazing incidence distance ( $C_2$ ) can be obtained in terms of  $K$  and  $Z_1$  thus :-

$$C_2 = 2(a_2 + b_2),$$

$$\text{where } a_2 = Z_1 \tan \alpha$$

$$\text{and } b_2 = \frac{V_0}{K \tan \alpha}.$$

Therefore, substituting for  $\tan \alpha$ ,

$$\frac{C_2}{2} = \frac{Z_1 V_0}{\sqrt{K^2 R_2^2 - V_0^2}} + \frac{V_0 \sqrt{K^2 R_2^2 - V_0^2}}{V_0 K}$$

$$R_2 = \frac{V_0 + K Z_2}{K}$$

Therefore

$$\frac{C_2}{2} = \frac{Z_1 V_0}{\sqrt{\frac{(V_0 + K Z_2)^2 K^2}{K^2} - V_0^2}} + \frac{\sqrt{\frac{K^2 (V_0 + K Z_2)^2}{K^2} - V_0^2}}{K}$$

$$\frac{C_2}{2} = \frac{Z_1 V_0}{\sqrt{(V_0 + K Z_2)^2 - V_0^2}} + \frac{\sqrt{(V_0 + K Z_2)^2 - V_0^2}}{K}, \quad (2)$$

where  $Z_2 = H - Z_1$ .

We thus have two non-linear simultaneous equations, (1) and (2), with the two unknowns,  $K$  and  $Z_1$ .

## BIBLIOGRAPHY

- Agger, H.E. and Carpenter, E.W., 1965. A crustal study in the vicinity of the Eskdalemuir seismological array station. *Geophys. J.R. astr. Soc.*, 9, 69-83.
- Allerton, H.A., 1968. An interpretation of the gravity of the north Minch, Scotland. Unpublished M.Sc. thesis, University of Durham.
- Al-Sadi, H.N., 1967. A gravity investigation of the Pickwell Down Sandstone, north Devon. *Geol. Mag.*, 104, 63-72.
- Berry, M.J. and West, G.F., 1966a. A time term interpretation of the first arrival data of the 1963 Lake Superior Experiment, in "The Earth beneath the continents." American Geophysical Union, Geophysical Monograph 10, Washington, D.C.
- Berry, M.J. and West, G.F., 1966b. Reflected and head wave amplitudes in a medium of several layers, in "The Earth beneath the Continents." American Geophysical Union, Geophysical Monograph 10, Washington, D.C.
- Birch, F., 1958. Interpretation of the seismic structure of the crust in the light of experimental studies of wave velocities in rocks, in "Contributions to Geophysics in Honor of Beno Gutenberg." Pergamon Press, New York.
- Birch, F., 1960. The velocity of compressional waves in rocks to 10 kilobars, part 1. *J. Geophys. Res.*, 65, 1083-1102.

- Birtill, J.W. and Whiteway, F.E., 1965. The application of phased arrays to the analysis of seismic body waves. Phil. Trans. roy. Soc., 258A, 421-494.
- Blundell, D.J., Davey, F.J. and Graves, L.J., 1968. A sedimentary basin in the south Irish Sea. Nature, Lond., 219, 55.
- Blundell, D.J. and Parks, R., 1969. A study of the crustal structure beneath the Irish Sea. Geophys. J.R. astr. Soc., 17, 45-62.
- Bott, M.H.P., 1956. A geophysical study of the granite problem. Quart. J. Geol. Soc. Lond., 112, 45-68.
- Bott, M.H.P., Day, A.A. and Masson-Smith, D., 1958. The geological interpretation of gravity and magnetic surveys in Devon and Cornwall. Phil. Trans. roy. Soc., 251A, 161-191.
- Bott, M.H.P., 1961. The granitic layer. Geophys. J.R. astr. Soc., 5, 207-216.
- Bott, M.H.P. and Scott, P., 1964. Recent geophysical studies in south-west England, in "Present views of some aspects of the geology of Cornwall and Devon." Ed. K.F.G. Hosking and G.J. Shrimpton. Royal Geological Society of Cornwall, Penzance.
- Browne, B.C. and Cooper, R.I.B., 1952. Gravity measurements in the English Channel. Proc. roy. Soc., 139B, 426-447.
- Bullard, E.C. and Gaskell, T.F., 1941. Submarine seismic investigations. Proc. roy. Soc., 177A, 476-499.

- Bullen, K.E., 1963. An introduction to the theory of seismology.  
Cambridge.
- Bunce, E.T., Crampin, S., Hersey, J.B. and Hill, M.N., 1964.  
Seismic refraction observations on the continental  
boundary west of Britain. J. Geophys. Res., 69,  
3853-3863.
- Gerveny, V., 1966. On dynamic properties of reflected and head  
waves in the n-layered Earth's crust. Geophys. J.R.  
astr. Soc., 11, 139-147.
- Collette, B.J., Lagaay, R.A., Ritsemà, A.R. and Schouten, J.A., 1967.  
Seismic investigations in the North Sea - I and II.  
Geophys. J.R. astr. Soc., 12, 363-373.
- Day, A.A., Hill, M.N., Laughton, A.S. and Swallow, J.C., 1956.  
Seismic prospecting in the Western Approaches to the  
English Channel. With an appendix on the results at  
two additional seismic stations, by R.D. Adams and A.A. Day.  
Quart. J. geol. Soc. Lond., 112, 15-44.
- Dewey, H., 1948. British regional geology (second edition).  
South-west England. London : H.M. Stationery Office.
- Dodson, M.H., 1961. Isotopic ages from the Lizard peninsula,  
south Cornwall. Proc. geol. Soc. Lond., No. 1591,  
133-136.
- Donovan, D.H., 1968. Geology of the Continental shelf around Britain,  
in "Geology of Shelf Seas." Ed. D.T. Donovan. Edinburgh.

- Ewing, J. and Ewing, M., 1969. Seismic refraction measurements in the Atlantic Ocean basins, in the Mediterranean Sea, on the mid-Atlantic ridge and in the Norwegian Sea. Bull. geol. Soc. Am., 70, 291-317.
- Exley, C.S. and Stone, M., 1964. The granite rocks of south-west England, in "Present views of some aspects of the geology of Cornwall and Devon." Ed. K.F.G. Hosking and G.J. Shrimpton. Royal Geological Society of Cornwall, Penzance.
- Flett, J.S. and Hill, J.B., 1946. Geology of the Lizard and Meneage (second edition). Mem. Geol. Surv. U.K., 359, 1-208.
- Fuchs, K. and Landisman, M., 1966. Detailed crustal investigation along a north-south section through the central part of Western Germany, in "The Earth beneath the Continents." American Geophysical Union, Geophysical Monograph 10, Washington, D.C.
- Green, D.H. and Ringwood, A.E., 1967. An experimental investigation of the gabbro to eclogite transformation and its petrological applications. Geochim. Cosmochim. Acta, 31, 767-833.
- Gutenberg, B., 1950. Structure of the Earth's crust in the continents. Science, III, 29.
- Gutenberg, B., 1951. Crustal layers of the continents and oceans. Bull. geol. Soc. Am., 62, 427-439.

- Gutenberg, B., 1954. Effects of low velocity layers. *Geophys. pura appl.*, 28, 1-10.
- Gutenberg, B., 1955. Channel waves in the Earth's crust. *Geophysics*, 20, 283-294.
- Hersey, J.B., 1963. Continuous reflection profiling, in "The Sea" vol. 3. Ed. M.N. Hill, London.
- Hill, M.N. and Laughton, A.S., 1954. Seismic observations in the eastern Atlantic. *Proc. roy. Soc.*, 222A, 348-355.
- Hill, M.N., 1963. Single-ship seismic refraction shooting, in "The Sea." Vol. 3. Ed. M.N. Hill, London.
- Hill, M.N. and Vine, F.J., 1965. A preliminary magnetic survey of the Western approaches to the English Channel. *Quart. J. Geol. Soc. Lond.*, 121, 463-475.
- Hughes, D.A. and Maurette, C., 1956. Variation of elastic wave velocities in granites with pressure and temperature. *Geophysics*, 21, 277-284.
- Iyer, H.M., 1968. Determination of frequency-wave number spectra using seismic arrays. *Geophys. J.R. astr. Soc.*, 16, 97-117.
- James, D.E. and Steinhart, J.S., 1966. Structure beneath Continents : A critical review of explosion studies 1960-1965, in "The Earth beneath the Continents." American Geophysical Union, Geophysical Monograph 10, Washington, D.C.



- Key, F.A., Marshall, P.D. and McDowall, A.J., 1964. Two recent British earthquakes recorded at the UKAEA seismometer array at Eskdalemuir. *Nature, Lond.*, 201, 484-485.
- Key, F.A., 1967. Signal-generated noise recorded at the Eskdalemuir seismometer array station. *Bull. seism. Soc. Am.*, 57, 27-37.
- Key, F.A., 1968. Some observations and analyses of signal generated noise. *Geophys. J.R. astr. Soc.*, 15, 377-392.
- Landisman, M. and Mueller, S., 1966. Seismic studies of the Earth's crust in continents, 2, Analysis of wave propagation in continents and adjacent shelf areas. *Geophys. J.R. astr. Soc.*, 10, 539-548.
- Long, L.E., 1962. Some isotopic ages from south west England, in "Some aspects of the Variscan fold belt." Manchester.
- Long, R.E., 1968. Temporary seismic array stations. *Geophys. J.R. astr. Soc.*, 16, 37-45.
- Lucas, A.L., 1966. A system for the acquisition and processing of seismic data for refraction studies of the Earth's crust. Unpublished Ph.D. thesis, University of Durham.
- Merriweather, A.S., 1958. A seismic refraction - shooting survey off the north coast of Cornwall. *Geophys. J.R. astr. Soc.*, 1, 73-91.
- Midford, R.L., 1966. A surface marine gravity and magnetic reconnaissance traverse from the Shetland Isles to Land's End. Unpublished M.Sc. thesis, University of Durham.

- Miller, J.A. and Green, D.H., 1961a. Preliminary age-determinations in the Lizard area. *Nature*, 191, 159-160.
- Miller, J.A. and Green, D.H., 1961b. Age determinations of rocks in the Lizard (Cornwall) area. *Nature*, 192, 1175-1176.
- Miller, J.A. and Mohr, P.A., 1964. Potassium - Argon measurements on the granites and some associated rocks from south-west, England. *Geol. J.*, 4, 105-126.
- Mueller, S. and Landisman, M., 1966. Seismic studies of the Earth's crust in continents, I, Evidence for a low-velocity zone in the upper part of the lithosphere. *Geophys. J.R. astr. Soc.*, 10, 525-538.
- O'Brien, P.N.S., 1968. Lake Superior crustal structure - a re-interpretation of the 1963 seismic experiment. *J. Geophys. Res.*, 73, 2669-2690.
- Parks, R., 1967. Seismic refraction networks in the study of the Earth's crust. Unpublished Ph.D. thesis, University of Edinburgh.
- Rastall, R.H., 1931. The Tertiary igneous geology of the British Isles : an essay-review. *Geol. Mag.*, 68, 121-126.
- Read, H.H., 1957. The granite controversy. London (Murby).
- Revoy, M., 1969. Etude d'un profil de sismique - refraction en Bretagne. Unpublished thesis, University of Paris.
- Reynolds, D.L., 1947. The granite controversy. *Geol. Mag.*, 84, 209-223.

- Richards, T.C., 1960. Wide angle reflections and their application to finding limestone structures in the foothills of western Canada. *Geophysics*, 25, 385-407.
- Ringwood, A.E. and Green, D.H. 1964. Experimental investigations bearing on the nature of the Mohorovicic Discontinuity. *Nature, Lond.*, 201, 566-567.
- Ringwood, A.E. and Green, D.H., 1966a. An experimental investigation of the gabbro to eclogite transformation and some geophysical implications. *Tectonophysics*, 3.
- Ringwood, A.E. and Green, D.H., 1966b. Petrological nature of the stable continental crust, in "The Earth beneath the continents." American Geophysical Union. *Geophysical Monograph 10*. Washington, D.C.
- Roller, J.C. and Healy, J.H., 1963. Seismic-refraction measurements of crustal structure between Santa Monica Bay and Lake Mead. *J. Geophys. Res.*, 68, 5837-5849.
- Roller, J.C., 1965. Crustal structure in the eastern Colorado plateaus province - seismic refraction measurements. *Bull. seism. Soc. Am.*, 55, 107-120.
- Ryall, A. and Stuart, D.J., 1963. Travel times and amplitudes from nuclear explosions, Nevada Test Site to Ordway, Colorado. *J. Geophys. Res.*, 68, 5821-5835.
- Ryall, A., 1964. Improvement of array seismic recordings by digital processing. *Bull. seism. Soc. Am.*, 54, 277-294.

- Sabine, P.A. and Snelling, N.J., 1969. The Seven Stones Granite, between Land's End and the Scilly Isles. Proc.geol. Soc. Lond., no. 1654, 47-50.
- Schiedegger, A.E. and Willmore, P.L., 1957. The use of the least squares method for the interpretation of data from seismic surveys. Geophysics, 22, 9-22.
- Shor, G.G., 1963. Refraction and reflection techniques and procedure, in "The Sea." vol.3. Ed. M.N. Hill, London.
- Shurbet, D.H., 1960. The P phase transmitted by crustal rocks to intermediate distances. J. Geophys. Res., 65, 1809-1814.
- Sornes, A., 1968. P<sub>n</sub> time term survey Norway - Scotland 1967. A.R.P.A. Supplementary Scientific Report No. 612 - 1.
- Smith, T.J., Steinhart, J.S. and Aldrich, L.T., 1966. Lake Superior crustal structure. J. Geophys. Res., 71, 1141-1172.
- Steinhart, J.S. and Meyer, R.P., 1961. Explosion studies of continental structure. Carnegie Inst. Wash. Publ. 622.
- Tilley, C.E., 1923. The petrology of the metamorphosed rocks of the Start area (south Devon). Quart. J. Geol. Soc. Lond., 79, 172-204.
- Truscott, J.R., 1965. The Eskdalemuir seismological station. Geophys. J.R. astr. Soc., 9, 59-68.
- UKAEA, 1965. The detection and recognition of underground explosions. A special report of the United Kingdom Atomic Energy Authority. London.

- Werth, G.C., Herbst, R.F. and Springer, D.L., 1962. Amplitudes of seismic arrivals from the M. discontinuity. J. Geophys. Res., 67, 1587-1610.
- Whitmarsh, R.B., 1967. Explosion seismology on the sea bed. Unpublished Ph.D. thesis, University of Cambridge.
- Whittard, W.F., 1962. Geology of the Western Approaches of the English Channel : a progress report. Proc. roy. Soc., 265A, 395-406.
- Willmore, P.L. and Bancroft, A.M., 1960. The time term approach to refraction seismology. Geophys. J.R. astr. Soc., 3, 419-432.



VELOCITY FILTERED RECORD OF SHOT 2

SINGLE CHANNEL

